

Effects of sensory experience on early stages of
olfactory processing in the fruit fly

Thesis by

Zhannetta V. Gugel

In Partial Fulfillment of the Requirements for

the degree of

Doctor of Philosophy

The logo for the California Institute of Technology (Caltech), featuring the word "Caltech" in a bold, orange, sans-serif font.

CALIFORNIA INSTITUTE OF TECHNOLOGY

Pasadena, CA

2020

(Defended 09 December, 2019)

© 2020

Zhannetta V. Gugel
ORCID: 0000-0003-1082-3281

All rights reserved except where otherwise noted

To my parents

Acknowledgements

I thank my committee for being supportive throughout my time at Caltech and helping push my project and career forward. Michael, Markus, and Henry: I enjoyed your different perspectives and expertise in Neuroscience. I could always turn to you for help. I enjoyed working with John Allman in the lab and as a TA in the classroom. I will never forget the interesting collection of brains you have in your lab fridge.

I felt very lucky to be Betty Hong's first student. I remember watching the lab space being built during my rotations before Betty arrived. I experienced the lab grow from its roots, and learned patch-clamp physiology by her side. I thank Betty for being an open-minded and supportive advisor.

I thank the Hong lab. Only you know the ins and outs of lab life, and we could always genuinely bond over our experiments, achievements and gripes. Kristina Dylla, you made lab so much more enjoyable. I could always talk to you, and I loved our discussions. They always turned into at least an hour of talking about what first was experiments, then goals, then jobs, then life. You have a very kind heart, and you are a great friend inside and outside the lab. I know I will see you at this next stage in life, and I look forward to it. Dhruv, we were both part of the first cohort of Caltech's Neurobiology program. I think you were really the only person on campus who could truly relate to me. It was helpful to vent to you about ongoing things, and I would have felt much more isolated without you. Annisa, you were a burst of positivity and youth that I felt like we had lost in the lab. I miss lab without you. Meike, it was unique setting up the lab with you and watching it grow. I honestly don't know what I would have done without you in those early days. Remy, I enjoy talking to you both inside and outside the lab. You have a sense of humor that lightens any environment and a sense of excitement about experiments that is infectious. Tom, I feel as if I have watched you grow in the lab. I

remember when you were interviewing, and now you are this independent and tech-savvy grad student we all ask for help. I enjoyed our honest conversations about lab and life. I hope to see all members of the Hong lab in the coming years. You know where to find me.

I thank Alysha de Souza for always being there for me. Although we did not consistently hang out, you were always so positive and uplifting every time I ran into you. I will never forget that time we happened to run into each other in Florence, Italy in 2015. What are the chances that I happened to visit the same country, same city, walk down the same street, and pass the store in which you were trying on jackets?

I thank Zeynep Turan for being supportive, motivating and inspiring. We are almost family, right? (It's actually true). I admire your strength, work ethic, and athleticism. Maybe I can get the courage to run a marathon with you someday. You are the original Neurobiology mama bird and always will be. I'm sure I will see you and Hoang in the next stage of our lives. I look forward to it.

I thank Bin Yang for being a great friend I could talk to about anything. When times were difficult, we were always there for each other.

I thank Sandy Wong and Cynthia Chai for being great first-year roommates and fellow Neurobiology classmates. I thank Ken Chan for being a great mentor and crutch during my first year. I thank Chanpreet and Dan from the Prober lab for your mentorship early on. Chanpreet, I am really glad we kept in contact throughout my grad school career. I enjoyed our long walks and gossip sessions around campus.

I thank my former mentors from the University of Pittsburgh, particularly TK and Tracy Cui. You helped shape my curiosity and drive to pursue science, and I am grateful. TK, you have taught me what it means to be a good researcher, from proposal writing, to planning manuscripts. I don't deny that I miss the Pitt neural engineering community.

I greatly enjoyed living in Southern California for this part of my life. I remained happy and healthy by finding things I love to do outside of the lab. Running, yoga, hiking and just plain walking around Pasadena were so enjoyable. Although she will probably never look at this thesis, I want to acknowledge Antoinella. She is an amazing yoga instructor and all-around great person. I aspire to be as serene and strong as you. I also thank Wendy and Tara for teaching me how yoga can build strength and positivity. It was comforting to learn from you in such a safe space.

I thank my family for your support. You are always there for me, and I gain strength and encouragement after speaking and spending time with you. There were times when experiments just would not work until I stepped away and had an unexpected phone call with you. Sometimes I even patched while talking to you. I felt reenergized after my visits home, and I wish I could see you more frequently. Caroline, you hold a special place in my heart. The amount of support you provided me during my grad school days is surreal. Heck, you spent two summers living and working with me. I am thankful for all the time we spent together, such as camping in Yosemite, experiencing the weird silence in Murphy's, traveling to Seattle, going on day-hikes, and working in the lab. I would do it all again. I am so lucky to have you in my life. I thank my grandparents for their endless support. I wish бабука Аня were still here. I miss your calls and questions about my life. You'd be happy to see how my life is shaping up, I'm sure. Дедушка Игорь, you are a constant inspiration to me. I ask you to stay strong, loving, humorous, and positive. Дора, Лара, бабушка Аля, мама: I am so lucky to have such strong female role models

in my life. Папа, you are endlessly caring and supportive. You taught me so much about life, perseverance, and compassion. You are always there for me. I thank the Dminov family: Dima, Lena, Allie and Maya. You have been supportive of me throughout this journey, and I thank you. Dima and Lena, I look up to you and hope to be half as cool as you guys are.

I would not be the same without my little California-based family consisting of me and Dima. Dima, I thank you for your enormous support during grad school. You were there for me from day -10, literally. We met while back-packing pre-orientation, and we have been by each other's side ever since. Grad school and life would have been so much harder and less enjoyable without you. I look forward to moving and beginning the next stage of our lives.

Abstract

Plasticity is widely studied across different sensory systems and behavioral paradigms, but the underlying mechanisms are varied and incompletely understood. Previous work in the fruit fly *Drosophila melanogaster* reported changes in odor preference and walking behavior after chronic odor exposure during early adulthood. Here, we investigated the hypothesis that changes in behavior reflect changes in how odors are encoded in the first two layers of the fly olfactory circuit. We chronically exposed flies to naturalistic odor stimuli that selectively and robustly activate a single olfactory receptor neuron (ORN) class. We then performed targeted intracellular recordings from genetically identified second-order olfactory projection neurons (PNs) that either receive direct input from the activated ORN class, or receive indirect activity (via local lateral circuitry), during chronic odor exposure. In addition, we used existing reagents to create a novel optical method to characterize ORN-PN synaptic strength. We find that the fly antennal lobe is resistant to plasticity, with a few exceptions. Of the odors we tested, we find that rearing in trans-2-hexenal, a leaf aldehyde that selectively activates ab4a ORNs, weakly enhanced odor responses in some PNs. The effects of rearing on PNs were not explained by ORN odor responses or changes in ORN-PN synaptic strength. We find evidence that lateral excitation may increase across glomeruli following rearing, suggesting that some odors may alter PN responses globally. We discuss possible reasons for differences between our observations and prior work on olfactory plasticity in this circuit, which has been conducted primarily in the context of exposures to much higher, non-naturalistic concentrations of odor. Our results point to the stability of insect sensory circuits in the face of large perturbations in the sensory environment.

During our optical stimulation experiments, we find that driving Chrimson expression may abolish odor responses in some ORNs. We include sample data highlighting this observation in a population of pb1a olfactory neurons. Lastly, we include antennal local

field potential recordings in response to a variety of odor concentrations to help guide future experiments seeking isointense odor panels.

Published Content and Contributions

Gugel, Z.V., Maurais, E., and Hong, E.J., *Chronic exposure to odors at naturally occurring concentrations triggers limited plasticity at early stages of fly olfactory processing*. Manuscript in preparation.

Z.V.G. contributed: conception, experimental design, data collection, data analysis, writing, editing.

Table of Contents

List of figures	xiii
Nomenclature	xv
Chapter 1: Introduction	1
The Drosophila olfactory circuit.....	1
Prior work in sensory plasticity	8
Overview of our approach and results	19
References.....	23
Chapter 2: Effect of odor rearing on antennal lobe PNs.....	28
Abstract.....	28
Introduction	29
Design of a constant odor exposure paradigm	29
Chronic activation of direct ORN input can modestly increase PN responses to weak odors	32
Chronic elevation of indirect activity perturbs PN response properties	40
Discussion.....	43
Methods	47
References.....	53
Chapter 3: Effect of odor rearing on ORNs and ORN-PN synapses	55
Abstract.....	55
Introduction	55
ORN response properties are unaffected by their chronic, persistent activation	56
The role of central mechanisms in olfactory plasticity.....	62
ORN-PN transforms after direct odor rearing using known models.....	68
Discussion.....	70
Methods	72
References.....	76
Chapter 4: Network-level effects after rearing	78
Abstract.....	78
Introduction	79
Chronic odor exposure can elicit global perturbation in glomerular volume	80
PN coding of odor mixtures is unaffected by chronic odor exposure.....	85
Indirect odor rearing may increase lateral excitation globally	89
Methods	91
Discussion	92

References.....	95
Chapter 5: Expressing Chrimson in ORNs.....	97
Introduction	97
Methods	99
Results	101
References.....	116
Chapter 6 : Antennal LFP responses to odors	117
Introduction	117
Methods	118
Results	119
References.....	125
Appendix	126

List of figures

Figure 1.1: Peripheral olfactory system of <i>Drosophila melanogaster</i>	2
Figure 1.2: Spatial map of sensillar subtypes on the antennae and palp	3
Figure 1.3: ORNs target individual antennal lobe glomeruli	5
Figure 1.4: Organization of the <i>Drosophila</i> olfactory system	6
Figure 1.5: Effects of CO ₂ odor exposure on PNs	12
Figure 1.6: Effects of CO ₂ odor exposure on LNs.....	13
Figure 1.7: Effects of CO ₂ exposure on fruit fly walking behavior	15
Figure 2.1: Chronic stimulation of olfactory neurons in a controlled odor environment ...	31
Figure 2.2: Effects of direct odor rearing on PN responses.....	36
Figure 2.3: Statistical analysis of direct rearing results in PNs	38
Figure 2.4: PN concentration curves following direct odor rearing	40
Figure 2.5: Effect of indirect rearing on PN responses	42
Figure 3.1: ORN responses do not explain the effects of rearing on PNs.....	58
Figure 3.2: Statistical analysis of ORN spiking responses in direct and indirect rearing conditions.....	60
Figure 3.3: Baseline calcium fluorescence of Or7a>opGCaMP6 terminals in DL5	61
Figure 3.4: Cellular and synaptic effects following direct rearing.....	64
Figure 3.5: Supplement to Cellular and synaptic mechanisms following rearing.....	66
Figure 3.6: Raw uEPSCs and exponential model fit overlay	67
Figure 3.7: ORN-PN transforms in direct and indirect rearing conditions.....	69
Figure 4.1: Anatomical characterization of rearing effects in the antennal lobe	82
Figure 4.2: Additional data on antennal lobe anatomy.....	84
Figure 4.3: Odor exposure does not affect PN responses to mixtures	87
Figure 4.4: Lateral excitatory inputs may be increased after trans-2-hexenal exposure .	90
Figure 5.1: Odor-evoked response in ab4 sensilla of a control fly.....	102
Figure 5.2: Light-evoked response in ab4 sensilla in Or7a>Chrimson fly.....	104

Figure 5.3: Odor-evoked responses in ab4 sensilla in Or7a>Chrimson fly	106
Figure 5.4: Odor-evoked responses in Or42a (pb1a) in a control fly	108
Figure 5.5: Light-evoked responses in Or42a>Chrimson (pb1a) ORNs.	109
Figure 5.6: Odor-evoked responses are gone in Or42a>Chrimson (pb1a) ORNs	111
Figure 5.7: Odor-evoked responses in Or71a (pb1b) neuron in a control fly	112
Figure 5.8: Odor-evoked responses are intact in Or71a (pb1b) ORNs in an Or42a>Chrimson fly	114
Figure 6.1: Antennal LFP recordings averaged across locations	120
Figure 6.2: Peak LFP vs. odor concentration across different recording locations.....	122
Figure 6.3: Isointense odor tuning curves averaged across locations.....	124
Figure A.1: LED barrel circuit diagram.....	127
Figure A.2: Photos of LED barrel for rearing and behavior.....	129
Figure A.3: MATLAB GUI interface for physiological data acquisition	130
Figure A.4: ORN spike quantification and recording setup	131
Figure A.5: Sample ab4 spike quantification with trans-2-hexenal stimulation	132
Figure A.6: Sample ab4 spike quantification with geosmin stimulation	133
Figure A.7: Sample antennal lobe dissection and view of patch-clamp recording on a GFP+ PN	134
Figure A.8: Sample recording from a DL5 PN	135
Figure A.9: Validating PN identity using biocytin.....	136
Figure A.10: Quantifying odor-evoked spikes in PNs	137

Nomenclature

OR: olfactory receptor

ORN: olfactory receptor neuron, olfactory sensory neuron

PN: projection neuron

vPN: ventral projection neuron

LN: local neuron

iLN: inhibitory local neuron

eLN: excitatory local neuron

MBON: mushroom body output neuron

MB: mushroom body

LH: lateral horn

EAG: electroantennogram

SSR: single-sensillar recording

LFP: local field potential

EPSC: excitatory post-synaptic current

uEPSC: unitary excitatory post-synaptic current

t2h: trans-2-hexenal

2but: 2-butanone

ga: geranyl acetate

pa: pentyl acetate

iba: iso-butyl acetate

eb: ethyl butyrate

p-cres: *p*-cresol (4-methylphenol)

Chapter 1: Introduction

The olfactory system is an ancient modality used to detect chemical compounds in the external environment. On land and in water, various organisms have adapted to recognize chemical ligands, integrate sensory cues, and produce a behavioral response. Historically, the field of chemosensation has used a rich diversity of species to study neuroanatomy, physiology and behavior such as cockroaches and locusts (Martin, J.P., et al., 2011). As the field has evolved and adopted cutting-edge genetic tools, mice and *Drosophila* have been the focus of most modern experiments and have elucidated interesting insights into the olfactory system. While the general structure of mammalian and insect olfactory system are conserved, the insect olfactory circuit is smaller and relatively less complex than mammalian systems. As such, studying olfaction in insects allows a relatively simpler viewpoint of a similar functional unit.

*The *Drosophila* olfactory circuit*

The olfactory system consists of multiple neuronal layers that are optimized for odorant detection, processing and multimodal integration. Odorant detection begins when chemical ligands interact with olfactory receptor neurons (ORNs) on the fly antennae and maxillary palp (Figure 1.1, 1.2). In the fly, there are ~1000 ORNs which express one of 50 genetically unique odorant receptor (OR) subtypes (Couto, A., et al., 2005; de Bruyne, M., et al., 2001; Hallem, E.A. et al., 2004). Odorant response properties of individual ORNs are shaped by the type of OR expressed. ORs respond to a breadth of chemicals including ketones, aldehydes, alcohols, esters and acetates. While most odorants activate many different ORs, some have been found to activate specific OR types. In addition to odorant tuning, ORN responses can vary in intensity as odorant concentration changes (Hallem, E.A. et al., 2004; Hallem, E.A. and Carlson J.R., 2006; de Bruyne, M., et al., 2001). ORN spike rates are quantified in response to odorant

stimulation and are measured using single-sensillar recordings. ORN spiking responses closely follow a logarithmic function of odor concentration, and this appears to be a feature of all ORNs investigated (Si, G.W., *et al.* 2019).

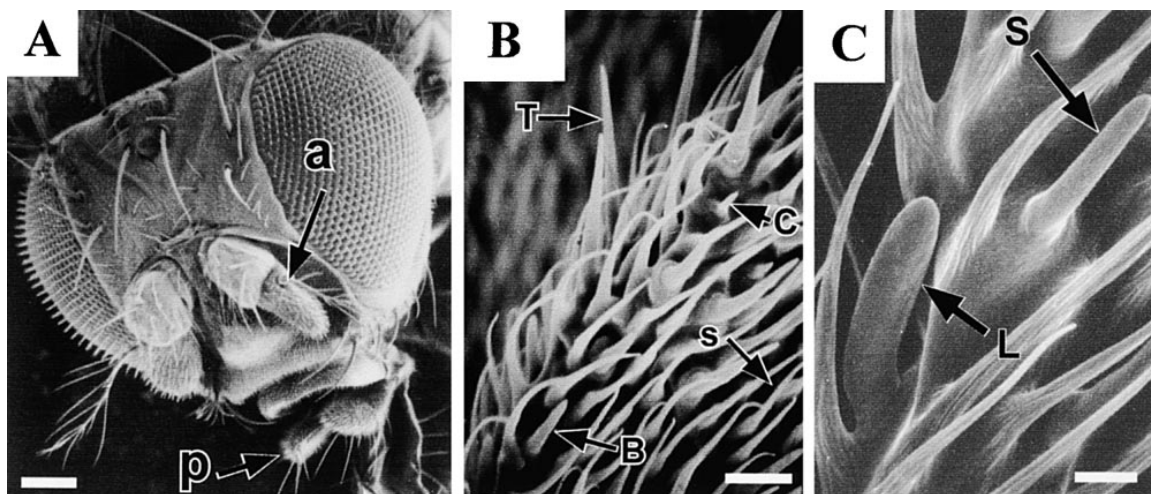


Figure 1.1: Peripheral olfactory system of *Drosophila melanogaster*¹

A) Image of a *Drosophila* head showing the peripheral olfactory organs including the antennae (a) and proboscis (p). Scale bar 100 μ m. **B)** Image of the third antennal segment (arrow a in panel A) showing diversity of sensillar morphology. T: trichoid, C: coeloconic, B: basiconic, and s: spinules. Note that T, C, and B are sensillar subtypes while s sensilla represent uninnervated hairs. Scale bar 5 μ m. **C)** Example of two types of basiconic sensilla, S: small and L: large. Scale bar 2 μ m. (de Bruyne, M., *et al.*, 2001).

The antennae contain the majority of the ORNs, accounting for nearly 90% of all olfactory responses with the palp mediating the remaining 10%. ORNs are found within sensilla, or hair-like processes, that are identified by their morphology and location on

¹ Reprinted from *Neuron*, Vol. 30, de Bruyne, M., Foster, K., and Carlson, J.R., Odor Coding in the *Drosophila* antenna, 537-552, © 2001, with permission from Elsevier.

the olfactory appendages (Figure 1.2). Within each sensillum are typically 1-4 different ORNs, the pairing of which does not appear to have any significance.

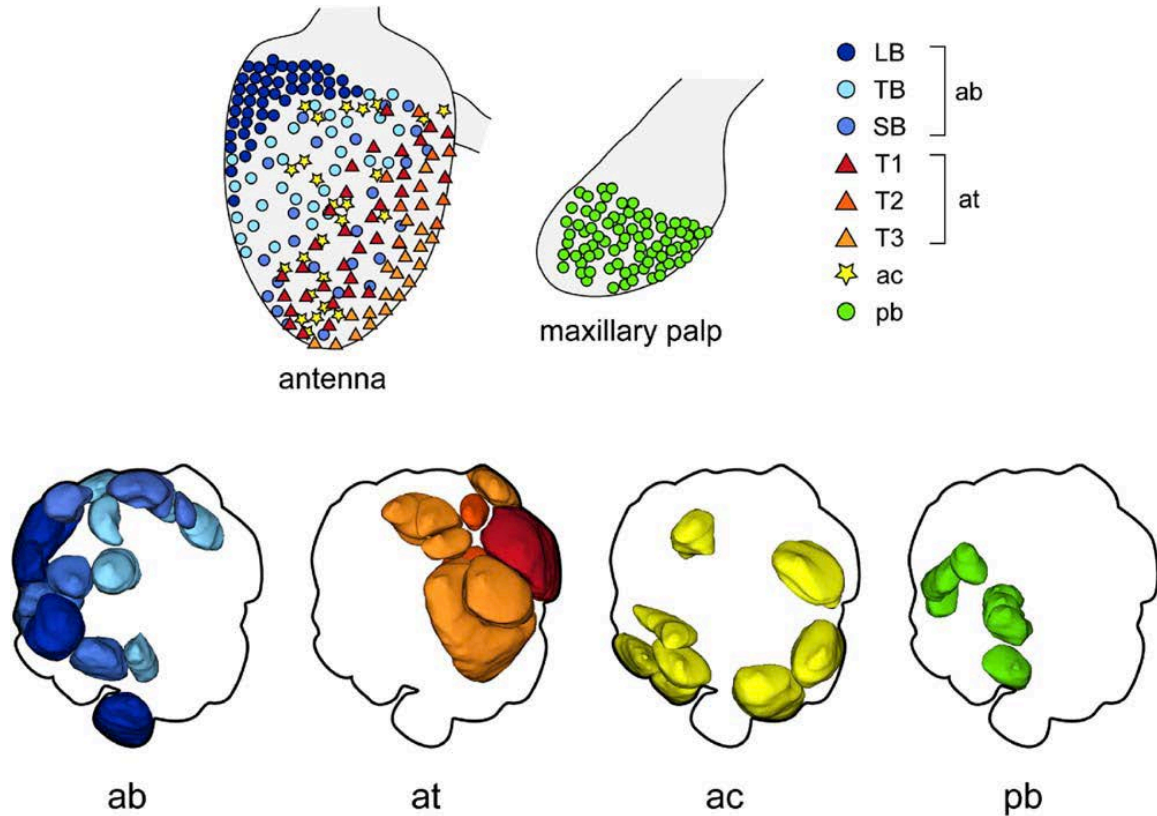


Figure 1.2: Spatial map of sensillar subtypes on the antennae and palp²

Top: Map of spatial arrangement of sensillar types on the *Drosophila* antenna and palp. LB: large basiconic, TB: thin basiconic, SB: small basiconic, T1-3: antennal tricoid, ac: antennal coelconic, pb: palp basiconic. *Bottom:* Glomerular identification of olfactory receptor neuron projections labeled by sensillar type using key used above. (Couto, A., et al., 2005).

² Reprinted from Current Biology, Vol. 15., Couto, A., Alenius, M., and Dickson, B.J., Molecular, Anatomical, and Functional Organization of the *Drosophila* olfactory system, 1535-1547, © 2005, with permission from Elsevier.

ORNs expressing the same OR converge into a single antennal lobe glomerulus in the brain (Figure 1.3; Dobritsa, A.A, et al., 2003; Couto, A., et al., 2005). There, ORNs make synapses with projection neurons (PNs), local neurons (LNs) and neuromodulatory neurons before sending outputs to the mushroom body (Figure 1.4; Wilson, R.I. 2013; Keene, A.C., Waddell, S., 2007). The first stage of olfactory processing occurs between cholinergic ORN-PN synapses. PNs amplify ORN inputs and display broader tuning profiles than presynaptic ORNs (Wilson, R.I., 2013; Olsen, S.R., et al., 2010; Olsen, S.R. and Wilson, R.I., 2008). Previous work has characterized ORN odorant tuning and identified odorants that selectively activate a single ORN type (Hallem, E.A. and Carlson, J.R., 2006; Olsen, S.R., et al., 2010; de Bruyne, M., et al., 2001). This allows a single olfactory glomerulus to be activated with an odorant.

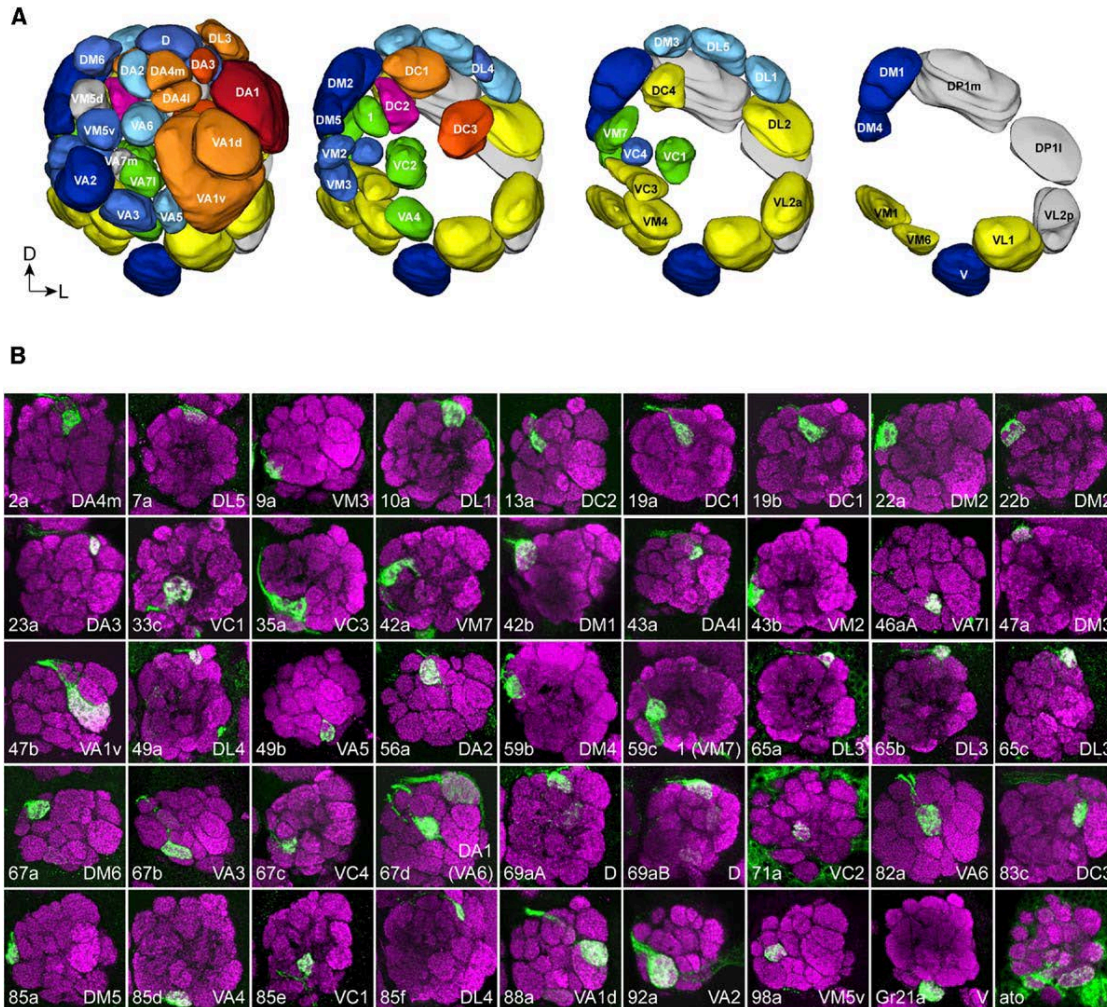


Figure 1.3: ORNs target individual antennal lobe glomeruli³

A) 3D spatial map of *Drosophila* antennal lobe glomeruli. Maps represent increasing antennal lobe depth from left to right. This map, along with other published maps, serve as a reference atlas for ongoing work in *Drosophila* olfaction. **B)** Single-plane confocal images of GFP expression in ORN axon terminals in individual antennal lobe neuropil, termed glomeruli. GFP expression was targeted to genetically identical ORNs, highlighting that ORNs converge into a single glomerulus. The targeted ORN and the innervated glomerulus are written in each panel at the bottom left and right corners, respectively. (Couto, A., et al., 2005).

³ Reprinted from Current Biology, Vol. 15., Couto, A., Alenius, M., and Dickson, B.J., Molecular, Anatomical, and Functional Organization of the *Drosophila* olfactory system, 1535-1547, © 2005, with permission from Elsevier.

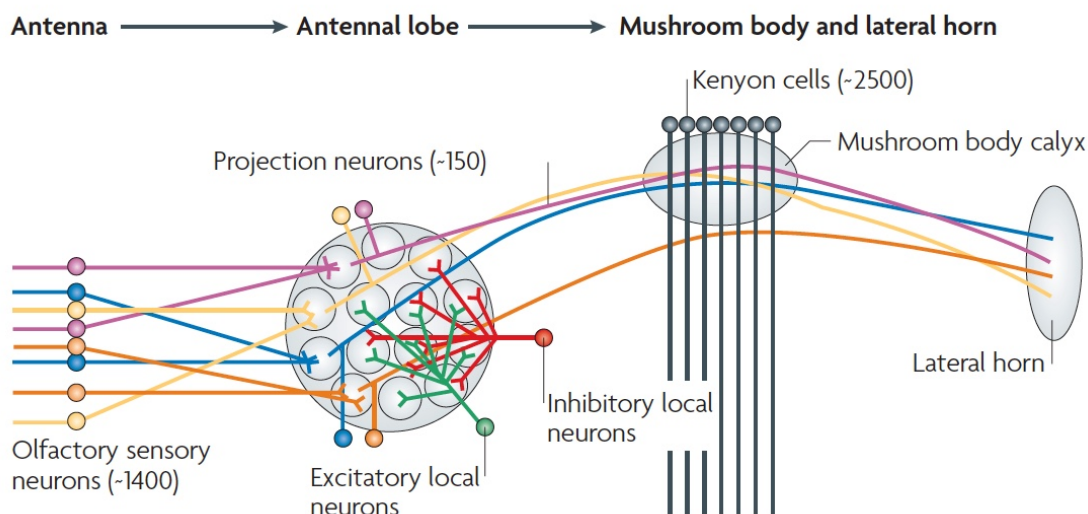


Figure 1.4: Organization of the *Drosophila* olfactory system⁴

About 1400 olfactory receptor neurons (ORNs; referred to as *olfactory sensory neurons* above) project from the periphery into regions of neuropil in the brain, called glomeruli, in the antennal lobe. While there are 1400 total ORNs, there are about 50 different ORN types that are characterized by the type of olfactory receptor expressed on the cell. ORNs expressing the same olfactory receptor converge into one of 50 antennal lobe glomeruli in the brain. There, ORNs make synapses with projection neurons (PNs), of which there are ~150. PNs typically innervate individual glomeruli, and form excitatory cholinergic synapses with ORNs. Excitatory local neurons are another source of excitation across the antennal lobe, and they broadly innervate different glomeruli. Inhibitory neurons are the main source of GABAergic inhibition in the antennal lobe, and these cells also broadly innervate the glomeruli. Both excitatory and inhibitory local neurons only signal within the antennal lobe. PNs receive both excitation and inhibition from all cell types to form the final output signal. PNs project out of the antennal lobe into the mushroom body and lateral horn. About 2500 Kenyon cells form synapses with PNs

⁴ Adapted by permission from Springer Nature Customer Service Centre GmbH: Nature Publishing Group, Nature Reviews Neuroscience, *Drosophila* olfactory memory: single genes to complex neural circuits, Alex C. Keene et al., © 2007

in the mushroom body calyx. The mushroom body is the main region of multimodal learning, memory and behavior in insects. The lateral horn is thought to mediate innate and sexually dimorphic behaviors. (Keene, A.C. and Waddell, S., 2007).

Computational methods have been used to model PN responses to ORN inputs. Olsen et al. use a hyperbolic ratio function (Eq. 1) to describe the ORN-PN spiking transform across different glomeruli (Olsen, S.R., et al., 2010). In Eq. 1, σ represents the PN spike rate at the half maximal ORN spike rate, R_{max} is a fitted constant that represents the maximum PN spike rate, and ORN represents the measured ORN spike rates in response to odor.

$$PN = R_{max} \left(\frac{ORN^{1.5}}{ORN^{1.5} + \sigma^{1.5}} \right) \quad \text{Equation 1}$$

Olsen et al. add lateral inhibition into Eq. 1 by scaling the ORN input (Eq. 2; *input gain control*) or by scaling the output (Eq. 3; *response gain control*) with the parameter, s . In both equations below, s is a fitted parameter that can scale with odor concentration and may be unique to each glomerulus (Olsen, S.R., et al., 2010).

$$PN = R_{max} \left(\frac{ORN^{1.5}}{ORN^{1.5} + s^{1.5} + \sigma^{1.5}} \right) \quad \text{Equation 2}$$

$$PN = \left(\frac{1}{s^{1.5} + 1} \right) R_{max} \left(\frac{ORN^{1.5}}{ORN^{1.5} + \sigma^{1.5}} \right) \quad \text{Equation 3}$$

In addition to PNs, inhibitory local neurons (iLNs) are an essential feature of olfactory circuits. iLNs broadly innervated the antennal lobe, and are broadly tuned to a panel of

odorants (Hong, E.J. and Wilson, R.I., 2015). The majority of glomerular inhibition occurs presynaptically on ORN dendrites, but previous work identified that PN dendrites also receive weak lateral inhibitory inputs (Olsen, S.R. and Wilson, R.I., 2008). In *Drosophila*, LNs form GABAergic synapses that contain both GABA_A and GABA_B receptors and are thus sensitive to the pharmacological reagents picrotoxin, bicuculline, and CGP. LN inputs into glomeruli increase as the total antennal local field potential (LFP) increases (Hong, E.J. and Wilson, R.I., 2015; Olsen, S.R. and Wilson, R.I., 2008; Nagel, K.I., et al., 2015). Another, albeit weak, source of excitation is lateral excitation through excitatory LNs (eLNs) and multiglomerular ventral PNs (vPNs) (Yaksi, E. and Wilson, R.I., 2010; Shimizu, K. and Stopfer, A., 2017). eLNs form electrical synapses within the antennal lobe and provide subthreshold excitation into PNs. The strength of lateral excitation varies among glomeruli and the total depolarization amplitude has some variation across odors. Less work has been done to investigate vPNs, but these are thought to be predominately GABAergic and recruited by broad odors.

Prior work in sensory plasticity

Olfactory cues guide insects towards nutritive food sources, viable oviposition sites, and potential mates (Linz et al., 2013; Keeseey et al., 2015). Adaptive behavior is important for the success of populations and allows animals to succeed in new or unexpected environments. An animal's sensory experience can shape how the external environment is encoded within the brain, as shown in work by Blakemore and Cooper in 1970 and other recent works (Hensch, T.K., 2005; Turrigiano, G., 2011; Geramita, M., and Urban, N.N., 2016). But a cellular- and synaptic-level understanding of how sensory experience changes layers of a sensory circuit is not well described. In the context of an olfactory system, how are persistent odorants encoded? What computations are required by the early olfactory circuit, and which cell types are responsible for plasticity? Prior work has attempted to address this question, but results across studies are contradictory. In the

field of olfactory plasticity, there are several dimensions in which experiments tend to vary, including the stimuli used for exposure, the design of the exposure paradigm and the methods used to assess plasticity. Below, details of a few studies of importance are discussed.

Early work in sensory neuroscience has demonstrated that neural circuits are capable of undergoing plasticity. Many such early studies characterized behavioral and neurophysiological effects of visual experience because of the well-characterized circuits and stimuli involved. In a hallmark experiment performed by Blakemore and Cooper in 1970, kittens were placed in barrels that restricted their visual experiences during early life (Blakemore, C. and Cooper, G.F., 1970). The kittens were housed in complete darkness from birth to two weeks of age. Afterwards, the kittens were placed in barrels containing only black and white vertical stripes or horizontal stripes for five hours each day until an age of five months. Behaviorally, the kittens did not any responses to stripes perpendicular to the orientation they experienced, suggesting that the kittens were virtually blind to a particular orientation. The authors then wanted to determine if there is a neurophysiological basis for this difference in behavior between kittens reared in vertical versus horizontal stripes. To do this, recording electrodes were placed into the visual cortex in anesthetized kittens and bars of different orientations were presented. Nearly 125 neurons were recorded from two kittens that were exposed to either vertical or horizontal stripes during the study. Interestingly, the authors found that neurons fired only to the stripe orientation the kitten was exposed to during early life, and zero neurons responded to the perpendicular orientation. The data suggests that the behavioral data may be explained by the physiological recordings in the visual cortex (Blakemore, C. and Cooper, G.F., 1970). The study leaves a critical open question: at which stage in the visual circuit is the plasticity occurring? Is the primary visual cortex inheriting tuning properties from upstream neurons?

An elegant study from 2003 demonstrated that experience-dependent plasticity can occur in the retina in retinal ganglion cells (RGCs) (Tian, N. and Copenhagen, D. R., 2003). In young mice, 77% of all RGCs have ON-OFF responses. As the mice mature and experience normal light conditions, the percentage of RGCs exhibiting ON-OFF tuning drops to 40%. The cells then develop strong ON or OFF responses. To determine whether normal visual experience may explain this reduction in ON-OFF tuning in RGCs, the authors dark-reared mice from 0 to 29 days of age and recorded RGC single-unit responses to light stimulation. They found that dark-reared mice had more ON-OFF RGCs than similarly aged control mice. The finding that ON-OFF RGCs remain elevated comparable to young mice aged 10-12 days suggests that visual experience can affect RGC tuning (Tian, N. and Copenhagen, D. R., 2003). All in all, work from the mammalian visual cortex suggest that sensory plasticity occurs as early as in the second synapse in the visual circuit.

More recent work in fruit-fly suggests that olfactory circuits can undergo experience-dependent plasticity. A study from 2007 raised flies in a constant CO₂ environment to see whether the V glomerulus, narrowly tuned to CO₂, could change anatomically and physiologically (Sachse et al., 2007). To expose flies to CO₂, the group placed standard fly food vials containing groups of flies into a 5% CO₂ incubator for 2-5 days. The incubator maintained a constant CO₂ concentration. Control flies were raised in ambient conditions consisting of 0.25% CO₂. Anatomical analysis revealed that the size of the V glomerulus increased selectively after CO₂ rearing (Sachse, S. et al., 2007). Fluorescence imaging of GCaMP revealed that odor-evoked projection neuron (PN) responses were decreased while a subpopulation of local neuron (LN) responses were increased (Figure 1.5). The group proposed that greater LN innervation within the glomerulus may have contributed to the greater glomerular volume in CO₂ reared flies. The increase in glomerular volume was only observed within a critical window and could not be induced in flies that were exposed to CO₂ beginning at 7 days post-eclosion.

Changes in glomerular volume due to CO₂ rearing were also reversible when flies were placed back in ambient conditions for 5 days post-exposure. Exposure paradigms lasting longer than 5 days did not produce greater changes in glomerular volume suggesting that the effect saturates within a critical window of around 5 days. Interestingly, the group performed exposure paradigms in other odors including ethyl butyrate, to target DM2. While they did not perform physiological measurements, constant exposure to 1% ethyl butyrate significantly increased DM2 volume selectively. To further confirm that the effect of odor exposure is selective to the targeted glomerulus, animals were reared in 10⁻² cyclohexanol and Or43a was ectopically expressed in Gr21a-expressing ORNs which are responsive to CO₂. Interestingly, they found that after rearing in cyclohexanol, flies with ectopic expression of Or43a in Gr21a ORNs showed an increase in the V glomerulus volume, whereas control flies without ectopic expression showed no effect. This experiment suggests that the effects of odor rearing on glomerular volume are selective.

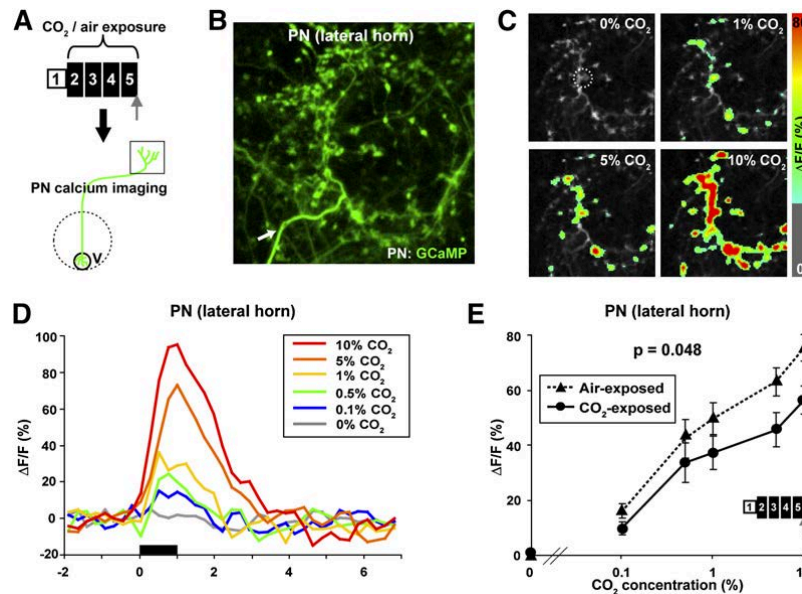


Figure 1.5: Effects of CO₂ odor exposure on PNs⁵

A) CO₂ exposure paradigm. Flies were placed in CO₂ incubator from 2-5 days post-eclosion. Imaging was performed on day 5 post-eclosion. **B)** Representative imaging plane of PN terminals in the lateral horn. PNs projecting into the V glomerulus were labeled with the fluorescent calcium indicator, GCaMP. **C)** Odor responses were imaged to increasing CO₂ concentrations. **D)** Average PN fluorescence vs. time (seconds) to increasing CO₂ concentrations. **E)** Average PN fluorescence response for CO₂-exposed (solid line) and air-exposed (dotted line) flies. A concentration series of CO₂ was presented to the fly. On average, PNs in CO₂-exposed flies show a decrease in fluorescence responses to high concentrations of CO₂. (Sachse, S., et al., 2007).

⁵ Reprinted from Neuron, Vol. 56, Sachse, S., Rueckert, E., Keller, A., Okada, R., Tanaka, N.K., Ito, K., Vosshall, L.B., Activity-Dependent Plasticity in an Olfactory Circuit, 838-850, © 2007, with permission from Elsevier.

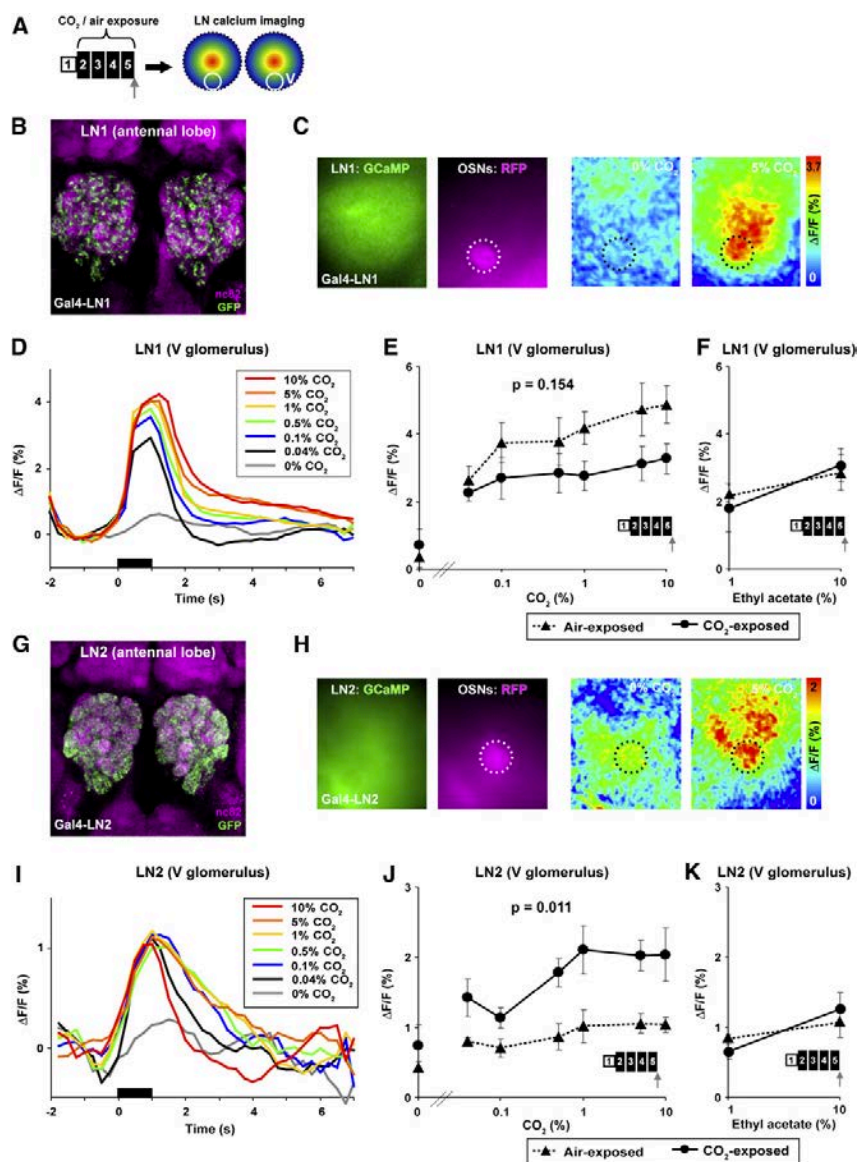


Figure 1.6: Effects of CO₂ odor exposure on LNs⁶

A) CO₂ exposure paradigm. Flies were placed in CO₂ incubator from 2-5 days post-eclosion. Imaging was performed on day 5 post-eclosion. LN fluorescence was measured in the V glomerulus. **B, G)** Confocal image of (b) LN1 neurites (GFP; green), (g) LN2 neurites (GFP; green), and glomeruli (nc82; magenta). **C, H)** Left to right: 2-photon image of GCaMP expression in (c) LN1 and (h) LN2; olfactory sensory neurons

⁶ Reprinted from Neuron, Vol. 56, Sachse, S., Rueckert, E., Keller, A., Okada, R., Tanaka, N.K., Ito, K., Vosshall, L.B., Activity-Dependent Plasticity in an Olfactory Circuit, 838-850, © 2007, with permission from Elsevier.

(OSNs) in V glomerulus via RFP; heatmaps of LN1 fluorescence to 0% and 5% CO₂, respectively. **D, I**) Fluorescence vs. time (seconds) to increasing CO₂ concentrations in (d) LN1 and (i) LN2. **E, J**) Average fluorescence in air- vs. CO₂-exposed conditions to the test odor, CO₂, in LN1 (e) and LN2 (j). **F, K**) Average fluorescence in air- vs. CO₂-exposed conditions to the control odor, ethyl acetate in LN1 (f) and LN2 (k). (Sachse, S., et al., 2007).

Why might odor exposure alter glomerular volume and selectively tune PN and LN responses? The study further assessed walking distance to a CO₂ odor source to determine if the changes they observed translated into noticeable behavioral differences. Flies that were reared in CO₂ walked less than control flies when exposed to high concentrations of CO₂ (Figure 1.6). The authors suggest that CO₂ walking behavior could be a proxy of CO₂-mediated search behavior. It could be that CO₂ exposure induces flies behavioral response by decreasing central sensitivity via an increase in LN inhibition.

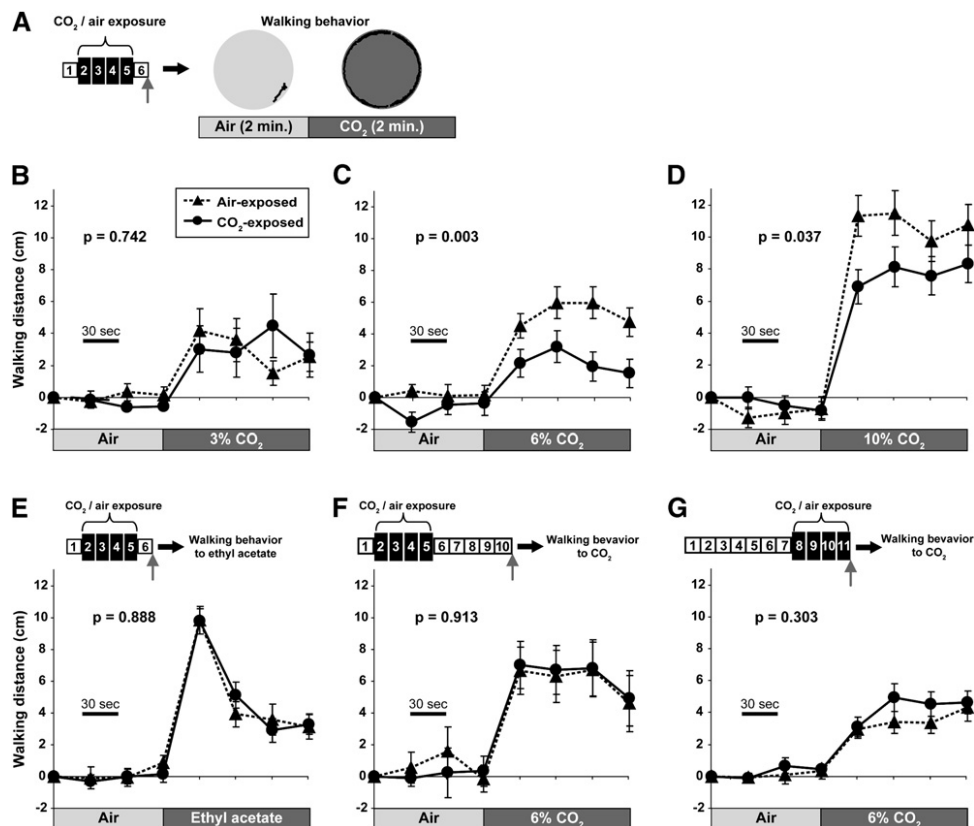


Figure 1.7: Effects of CO₂ exposure on fruit fly walking behavior⁷

A) Schematic of odor exposure paradigm. Flies are placed in a CO₂ incubator from 2-5 days post-eclosion. Flies are kept in ambient conditions and behavior is assessed on day 6 post-eclosion. **B-G)** Walking behavior of flies after CO₂ exposure (solid line) or air exposure (dotted line) assayed on day 6 to a (b) 3% CO₂, (c) 6% CO₂ (d) 10% CO₂ or (e) control odor ethyl acetate. (f) Fly walking behavior to 6% CO₂ on day 10 and (g) late adulthood exposure and behavioral assay on day 11. (Sachse, S., et al., 2007).

⁷ Reprinted from Neuron, Vol. 56, Sachse, S., Rueckert, E., Keller, A., Okada, R., Tanaka, N.K., Ito, K., Vosshall, L.B., Activity-Dependent Plasticity in an Olfactory Circuit, 838-850, © 2007, with permission from Elsevier.

A more recent study using a different odor, geranyl acetate, selective for the VA6 glomerulus, finds that odor exposure increases PN responses (Kidd, S., et al., 2015). This result is in direct contrast to the Sachse et al. study discussed above. The odor exposure paradigm used by this group was similar to the previous study with some key distinctions. Flies were reared on food and placed in an incubator. A microcentrifuge tube containing the odorant used for exposure was placed in proximity to the fly vials within an incubator. Geranyl acetate was diluted to 1% in paraffin oil for the odor exposure group and to just the paraffin oil solvent for the control group. Flies were housed within the incubator for 4 days before dissection, staining and imaging experiments were conducted. This exposure paradigm did not guarantee that the strength of the stimulus remained consistent throughout the course of odor exposure.

Similarly to CO₂ rearing, Kidd et al. found that geranyl acetate exposure selectively increases the VA6 glomerular volume but this effect was reversible as early as 2 days after odor exposure. Kidd et al. found that PN responses were selectively increased after chronic exposure (Kidd et al., 2015). Interestingly, the effects of PN enhancement were seen during calcium influx and efflux, meaning the maximum GCaMP fluorescence was increased and the magnitude of the minimum peak was also enhanced relative to control flies. There were no differences in ORN responses, suggesting that the enhancement in PN responses are not inherited by the cognate ORNs. It is unclear whether differences between the two studies arise because of the odorants used (CO₂ is suggested to be aversive in lab conditions while geranyl acetate is innately appetitive) or if there are confounds in the experimental techniques used.

A recent study from the Brodie lab reared flies in ethyl butyrate to target the VM7 glomerulus. This odor was chosen for its selectivity for VM7 (Golovin, R.M., et al., 2019). The group reared flies by attaching a mesh-covered vial containing 15% and 25% ethyl butyrate (EB) to the top of a standard *Drosophila* food vial. Individual food vials were stored in an airtight glass container to prevent background odors from interfering

with their exposure paradigm. Similarly, their control group consisted of flies raised in identical conditions, but a paraffin oil control vial used for rearing in replacement of the odor vial. Surprisingly, while the studies mentioned above observed an increase in glomerular volume after rearing, this group observed a significant decrease in VM7 glomerular volume. Odor-evoked changes were seen in flies that were reared 0-2 days post-eclosion for 2-4 days, and was not observed in older flies that were reared starting at 7-9 days post-eclosion. This suggests that odor-evoked plasticity occurs within a critical window in early adulthood. The decrease in VM7 glomerular volume was stronger following exposure to 25% EB than to 15%, suggesting that the effect can be modulated in a concentration dependent-manner. Because a stronger effect was observed with 25% EB, this concentration was used throughout the remainder of the study. The decrease in glomerular volume was abolished when the Or42a ORNs, the cells that project into the VM7 glomerulus, were mutated. This suggests that Or42a is necessary for the effect to occur. Further, the group explored what might be the cause of the decrease in glomerular volume. To investigate whether a change in ORN synaptic innervation might explain the decrease in glomerular volume following rearing, the group expressed a *Drosophila* pre-synaptic marker, bruchpilot (*brp*), in Or42a ORNs. Interestingly, rearing in EB caused a significant decrease in ORN pre-synapses, suggesting that the decrease in glomerular volume may be a result of a decrease in synapses made with downstream neurons within the VM7 glomerulus.

Older work done on *Drosophila* olfactory plasticity by Devaud et al. reared flies in benzaldehyde and isoamyl acetate diluted to 10^{-1} in paraffin oil (Devaud, J.M., et al., 2001; Devaud, J.M., et al., 2003). In these experiments, odorants were placed in eppendorf tubes and attached to the cap of fly vials for four days. Surprisingly, the group found that odor exposure decreased the volume of certain olfactory glomeruli, notably DM2 and V after exposure to benzaldehyde. It is likely that the odor concentrations used by this group were toxic to the animal and comprised ORN function. Overall, odor

exposure seemed to reduce flies behavioral responses to odors. It is unclear how ethologically relevant using such high concentrations of odor is and whether there is damage done to the physiology of flies.

Recent work in mice from the Urban lab observed olfactory bulb plasticity after mice were exposed to methyl salicylate, a mint-like odor (Geramita, M. and Urban, N.N., 2016; Liu, A. and Urban, N.N., 2017; Geramita, M. and Urban, N.N., 2017). Here, methyl salicylate was added to standard mouse food, and mice were exposed to odor during food consumption throughout development. The group found that exposure to mint increased the number of excitatory projection neurons within a single olfactory glomerulus. The effect of mint-scented food consumption appeared to increase calcium responses of individual mitral cells. When the group exposed mice to hexenal and acetylaldehyde, they identified an increase in interglomerular lateral inhibition. Overall, the results summarized in this section highlight the uncertainty and confounds within the field of olfactory plasticity. Each study attempted to understand sensory plasticity using physiological and anatomical methods, but did not develop a general theory of olfactory plasticity. It is possible that there are several factors governing olfactory plasticity, and it might depend on the rearing odor, concentration, as well as specific plasticity rules within different glomeruli. In general, the previous studies highlight that the effects of odor exposure are indeed unique, and cannot be explained by a single plasticity rule.

In summary, the first and second layers of the olfactory circuit are thought to be hard-wired. Previous work investigated the effect of long-term odor exposure on PN odorant responses after exposing flies to high concentrations of CO₂ (Sachse, S., et al., 2007). Imaging revealed that PN responses decreased as a result of an increase in LN responses after rearing, but it was unclear if this finding is a general feature of olfactory plasticity following odorant rearing. Another group reared flies in geranyl acetate and imaged PN terminals from the VA6 glomerulus. This group observed the opposite effect, and instead saw a slight increase in PN calcium fluorescence after rearing (Kidd., S., et

al., 2015). In all of these studies, earlier generations of calcium indicators were used and the rearing environments were poorly controlled. We aimed to investigate whether chronic odor rearing invokes plasticity in olfactory PNs and identify the underlying cellular and synaptic mechanisms. Unlike previous studies that utilized low resolution calcium imaging, we performed patch-clamp electrophysiology to measure single-cell spiking in response to odor stimulation. We designed an odorant rearing paradigm to precisely control the odorant environment during rearing and validated the stability of the rearing stimulus over long time-scales.

Overview of our approach and results

We took advantage of the well-characterized olfactory system by selecting odors that are known to activate a single ORN type. We chose odorant concentrations that activate PNs near saturation, and we avoided PN habituation to odorant stimulation by pulsing the odorant into the rearing chamber. Unlike prior studies which only rear in a specific odor, we test the effects of rearing in three different odors. Odors were chosen to specifically activate a single olfactory glomerulus, which we term “direct rearing” throughout the text. In a complementary set of experiments, we performed physiological recordings from PNs that do not receive direct excitation by the rearing odorants, which we term “indirect rearing”. We find that there isn’t a general rule for experience-dependent plasticity in the antennal lobe, and the effects of odor exposure are small. We saw the strongest effect of rearing after directly and indirectly rearing flies in trans-2-hexenal. The direct glomerulus had increased odor responses to low concentrations of odor. Surprisingly, indirectly rearing in this same odor tended to increase excitation across other glomeruli as well. This effect has been previously reported by the Urban lab (Liu, A. and Urban, N.N., 2017), which may suggest that certain odorants may be better at evoking changes in olfactory coding than others. Overall, we found that other glomeruli maintain stable odor-evoked firing rates after direct rearing, suggesting that the

early stages of olfactory processing may indeed be hard-wired to encode a set odorant response. Any behavioral changes that have previously been shown to occur as a result of olfactory exposure are likely not a result of changes in ORNs and PNs but instead by neurons in the mushroom bodies such as KC and MBONs.

We perform an in-depth analysis of PN and ORN odor responses following chronic odor exposure to selective monomolecular ligands. PN responses are measured using whole-cell patch-clamp physiology using genetically labeled GFP⁺ PNs in publicly available fly lines. The odors we use for rearing include trans-2-hexenal, 2-butanone, and geranyl acetate at concentrations that allow the PN to fire at saturating levels. Trans-2-hexenal is a known selective ligand for the Or7a receptor (in ab4a ORNs located on the antennae) and directly activates DL5 PNs. This odorant naturally occurs as a leaf aldehyde and is also used as a defensive odorant by stink bugs (Staples, J.K., et al., 2002). 2-butanone activates the Or42a receptor (in pb1a ORNs located on the maxillary palp) and directly activates VM7 PNs. This odorant is widely used by olfactory papers in *Drosophila* as a selective odor ligand (Olsen, S.R., et al., 2010), and we chose this odor because of its known specificity towards the Or42a receptor. Lastly, we use geranyl acetate to activate Or82a (in antennal ab5a ORNs) which directly innervate the VA6 glomerulus (Couto, A., et al., 2005). This odor was used to chronically rear flies in prior works, and we were interested to see if our use of naturalistic rearing concentrations would generalize across published findings (Kidd, S, et al., 2015).

In general, we find that the effects of chronic odor exposure on the early olfactory circuit are most prominent in PN responses to dilute monomolecular odorants. Trans-2-hexenal direct exposure increased DL5 responses to low odor concentrations. Interestingly, trans-2-hexenal exposure changed PN odor responses in off-target channels as well. VM7 PNs had an increased afterhyperpolarization amplitude whereas VA6 PNs showed a small change in odor-evoked membrane depolarization. This observation suggests that chronic odor exposure does not only change the directly

stimulated channel, but can alter unstimulated PNs across different antennal lobe glomeruli as well. It will be interesting to determine whether the effects of rearing generalize across more glomeruli or odorants spanning chemical classes. While we found effects from trans-2-hexenal exposure on different PNs, we only saw weak effects of direct 2-butanone rearing on VM7 odor-evoked membrane potential. The effects of rearing appeared significantly different in responses to a subset of dilute odor presentations of 2-butanone. In contrast, direct odor rearing in geranyl acetate did not have any effects on VA6 PNs. Our findings suggest that the effects of odor rearing are complex and likely depend on glomerular identity and rearing odor. We also performed patch-clamp measurements of PN odor responses to mixtures and found that broad odors suppress any effects of rearing. In effect, enhancements in feedforward excitation were likely counteracted by an increase in inhibition into a subset of glomeruli.

We wanted to determine whether the effects of rearing on PNs could be explained by a change in presynaptic input arising from the ORNs. To do this, we repeated our rearing experiments and measured ORN spike rates to a concentration series of monomolecular odorants. We confirmed that ORN activity is not changed following odor rearing. In addition to measuring responses at the ORN, we used a genetic strategy to recruit unitary excitatory postsynaptic currents (uEPSCs) in PNs using light stimulation. We compared the peak current amplitude and decay rate between odor exposed and control flies and concluded that there was no effect on the EPSC features. This suggests that rearing does not alter the synaptic strength between ORNs and PNs.

Given that we saw effects of trans-2-hexenal rearing on PN odor responses that are not explained by changes in the inputs, we reasoned that central circuits may be mediating the effects. We focused our final analyses on inhibitory local neurons (iLNs) and quantified fluorescence expression across antennal lobe glomeruli. Trans-2-hexenal odor exposure lead to a reduction of glomerular volume across our samples, and this

lead to a decrease in total iLN innervation density. In contrast, 2-butanone exposure did not have any effects on iLN density. These findings suggest that trans-2-hexenal rearing may nonspecifically alter local neuron circuitry across the antennal lobe.

The magnitude of the effects of trans-2-hexenal rearing on VA6 PNs were not large enough to cause changes in spiking. Prior work suggests that a population of excitatory local neurons (eLNs) provide small depolarization through gap junctions across the antennal lobe (Yaksi, E., and Wilson, R.I., 2010; Shang, Y., et al., 2007). We isolated lateral excitation and recorded odor responses in VA6 after rearing in trans-2-hexenal. We did this by severing the antennal nerve and removing ORNs that synapse directly into the VA6 glomeruli. Any remaining odor-evoked excitation will occur through activation of palp ORNs. Interestingly, we found that trans-2-hexenal rearing increased odor-evoked lateral excitation in VA6 PNs. This finding suggests that trans-2-hexenal may be increasing global network activity or increasing the threshold for activation of eLNs. In the future, it will be interesting to understand how odor exposure effects eLN recruitment and activity across a larger sample of glomeruli.

References

Blakemore, C. and Cooper, G.F. (1970). Development of the brain depends on the visual environment. *Nature* 228, 477-8.

Couto, A., Alenius, M., and Dickson, B.J. (2005). Molecular, anatomical, and functional organization of the *Drosophila* olfactory system. *Curr. Biol.* 15, 1535-1547.

de Bruyne, M., Foster, K., and Carlson, J.R. (2001). Odor coding in the *Drosophila* antenna. *Neuron* 30, 537-52.

Devaud, J.M., Acebes, A., and Ferrus, A. (2001). Odor exposure causes central adaptation and morphological changes in selected olfactory glomeruli in *Drosophila*. *J. Neurosci.* 21, 6274-82.

Devaud, J.M., Acebes, A., Ramaswami, M., and Ferrús, A. (2003). Structural and functional changes in the olfactory pathway of adult *Drosophila* take place at a critical age. *J. of Neurobio.* 56, 13-23.

Dobritsa, A.A., van der Goes van Naters, W., Warr, C.G., Steinbrecht, R.A., and Carlson, J.R. (2003). Integrating the molecular and cellular basis of odor coding in the *Drosophila* antenna. *Neuron* 37, 827-41.

Gadenne, C., Barrozo, R.B., and Anton, S. (2016). Plasticity in Insect Olfaction: To Smell or Not to Smell? *Annual Review of Entomology* 61, 317-333.

Geramita, M. and Urban, N.N. (2016). Postnatal Odor Exposure Increases the Strength of Interglomerular Lateral Inhibition onto Olfactory Bulb Tufted Cells. *J. Neurosci.* **36**, 12321-12327.

Geramita, M. and Urban, N.N. (2017). Differences in Glomerular-Layer-Mediated Feedforward Inhibition onto Mitral and Tufted Cells Lead to Distinct Modes of Intensity Coding. *J. Neurosci.* **37**, 1428-1438.

Golovin, R.M., Vest, J., Vita, D.J., and Brodie, K. (2019). Activity-Dependent Remodeling of *Drosophila* Olfactory Sensory Neuron Brain Innervation during an Early-Life Critical Period. *J. Neurosci.* **39**, 2995-3012.

Hallem, E.A. and Carlson, J.R. (2006). Coding of odors by a receptor repertoire. *Cell* **125**, 143-60.

Hallem, E.A., Ho, M.G., and Carlson, J.R. (2004). The molecular basis of odor coding in the *Drosophila* antenna. *Cell* **117**, 965-79.

Hensch, T.K. and Fagiolini, M. (2005). Excitatory-inhibitory balance and critical period plasticity in developing visual cortex. *Prog Brain Res* **147**, 115-24.

Hong, E.J. and Wilson, R.I. (2015). Simultaneous encoding of odors by channels with diverse sensitivity to inhibition. *Neuron* **85**, 573-89.

Iyengar, A., Chakraborty, T.S., Goswami, S. P., Wu, C., and Siddiqi, O. (2010). Post-eclosion odor experience modifies olfactory receptor neuron coding in *Drosophila*. *Proc Natl Acad Sci* **107**, 9855-60.

Keene, A.C. and Waddell, S. (2007). *Drosophila* olfactory memory: single genes to complex neural circuits. *Nat Rev Neurosci.* 8, 341-54.

Keesey, I.W., Knaden, M., and Hansson, B.S. (2015). Olfactory specialization in *Drosophila suzukii* supports an ecological shift in host preference from rotten to fresh fruit. *J. Chem Ecol.* 41, 121-8.

Kidd, S., Struhl, G., and Lieber, T. (2015). Notch is required in adult *Drosophila* sensory neurons for morphological and functional plasticity of the olfactory circuit. *PLoS Genet.* 11.

Linz, J., Baschwitz, A., Strutz, A., Dweck, H. K. M., Sachse, S., Hansson, B.S., and Stensmyr, M. C. (2013). Host plant-driven sensory specialization in *Drosophila erecta*. *Proc Biol Sci.* 280.

Liu, A. and Urban, N.N. (2017). Prenatal and Early Postnatal Odorant Exposure Heightens Odor-Evoked Mitral Cell Responses in the Mouse Olfactory Bulb. *eNeuro.* 4.

Martin, J.P., Beyerlein, A., Dacks, A.M., Reisenman, C.E., Riffell, J.A., Lei, H., Hildebrand, J.G. (2011). The neurobiology of insect olfaction: sensory processing in a comparative context. *Prog Neurobiol* 95, 427-47.

Nagel, K.I., Hong, E.J., and Wilson, R.I. (2015). Synaptic and circuit mechanisms promoting broadband transmission of olfactory stimulus dynamics. *Nat Neurosci.* 18, 56-65.

Olsen, S.R. and Wilson, R.I. (2008). Lateral presynaptic inhibition mediates gain control in an olfactory circuit. *Nature* *452*, 956-60.

Olsen, S.R., Bhandawat, V., and Wilson, R.I. (2010). Divisive normalization in olfactory population codes. *Neuron* *66*, 287-99.

Sachse, S., Rueckert, E., Keller, A., Okada, R., Tanaka, N.K., Ito, K., and Vosshall, L.B. (2007). Activity-dependent plasticity in an olfactory circuit. *Neuron* *56*, 838-50.

Shang, Y., Claridge-Chang, A., Sjulson, L., Pypaert, M., Miesenbock, G. (2007). Excitatory local circuits and their implications for olfactory processing in the fly antennal lobe. *Cell* *128*, 601-12.

Shimizu, K. and Stopfer, M. (2017). A Population of Projection Neurons that Inhibits the Lateral Horn but Excites the Antennal Lobe through Chemical Synapses in *Drosophila*. *Front. Neural Circuits* *11*.

Si, G.W., Kanwal, J.K., Hu, Y., Tabone, C.J., Baron, J., Berck, M., Vignoud, G., Samuel, A.D.T. (2019). Structured Odorant Response Patterns across a Complete Olfactory Receptor Neuron Population. *Neuron* *101*, 950-962.

Staples, J.K., Krall, B.S., Bartelt, R.J., and Whitman D.W. (2001). Chemical defense in the plant bug *Lopidea robiniae* (Uhler). *J Chem Ecol.* *28*, 601-15.

Tian, N. and Copenhagen, D.R. (2003). Visual stimulation is required for refinement of ON and OFF pathways in postnatal retina. *Neuron* *39*, 85-96.

Turrigiano, G., (2011). Too many cooks? Intrinsic and synaptic homeostatic mechanisms in cortical circuit refinement. *Annu. Rev. Neurosci.* 34, 89-103.

Wilson, R.I., (2013). Early Olfactory Processing in *Drosophila*: Mechanisms and Principles. *Annu. Rev. of Neurosci.* 36, 217-241.

Yaksi, E. and Wilson, R.I. (2010). Electrical coupling between olfactory glomeruli. *Neuron* 67, 1034-47.

Chapter 2: Effect of odor rearing on antennal lobe PNs

Abstract

We reared flies in odor for two days post-eclosion. Unlike prior rearing paradigms that used continuous stimulation and high concentrations of odor, we pulse dilute concentrations of a specific odor to selectively stimulate a targeted olfactory receptor neuron and glomerulus. Flies were exposed to trans-2-hexenal, 2-butanone, and geranyl acetate to stimulate the DL5, VM7 and VA6 glomeruli, respectively. These experiments are referred to as directly reared. Rearing in trans-2-hexenal selectively increases DL5 PN responses to low odor concentrations as measured by whole-cell patch-clamp physiology. We did not see any changes in odor-evoked responses in VM7 or VA6 PNs after rearing in odors selective for the presynaptic ORNs. We find that the effects of odor exposure do not generalize across glomeruli, and we hypothesize that the strength of the stimulus may influence the effects of rearing. Given the effect of trans-2-hexenal exposure on DL5 PNs, we wondered if other PNs can also be affected by this odor. We exposed flies in trans-2-hexenal as before and recorded odor-evoked responses in PNs that are not activated by this odor during rearing, termed indirectly reared. We find that the effects of trans-2-hexenal exposure on other PNs is complex. In VM7, indirect rearing resulted in a dramatic increase in the afterhyperpolarization amplitude compared to mock-reared PNs. In VA6, indirect rearing significantly increased odor-evoked membrane potential in response to dilute odors. The increase in membrane potential, however, was small and did not result in a change in odor-evoked spike rate. Overall, we find that trans-2-hexenal is capable of changing PN response dynamics globally. This suggests that even selective odor stimulation can recruit lateral inputs and result in global plasticity in the antennal lobe. We note that the effects of naturalistic odor rearing

on antennal lobe PNs are small and changes in behavior likely arise due to higher brain circuits.

Introduction

A novel aspect of our rearing paradigm is our ability to precisely control the odor stimulus throughout the odor exposure experiment. Prior work in olfactory plasticity used simple chambers that exposed flies to odor through passive diffusion. Most studies included a perforated vessel containing a high concentration of odor near the vicinity of fly vials or simply placed fly bottles into an odorized chamber. It is unclear how many ORNs were targeted in these exposure paradigms, how stable the stimulus was over the course of days and how many more spikes were recruited in the olfactory circuit throughout exposure. We extended prior work by designing a constant odor rearing paradigm. Next, we exposed flies in odor for two days post-eclosion and performed whole-cell patch-clamp recordings from olfactory projection neurons. We compared PN spike responses in odor reared flies to those of flies reared in just the paraffin oil solvent. Selective odor ligands were used to stimulate DL5, VM7 and VA6 PNs using trans-2-hexenal, 2-butanone and geranyl acetate, respectively. We used odor concentrations that were known to activate PNs selectively and were near PN saturation (Olsen, S.R., et al., 2010). Our direct rearing results show that selective odor rearing with dilute odors has modest effects on the DL5 glomerulus. The main result is that direct odor rearing increases DL5 spike rates to low trans-2-hexenal odor concentrations. This effect was not seen in the VM7 or VA6 glomerulus, suggesting that the effects of targeted, dilute odor rearing does not generalize across different olfactory glomeruli.

Design of a constant odor exposure paradigm

We were first interested in designing an odor rearing chamber that would maintain odor pulse stability. We used a standard olfactometer to control pulsing of odor through

solenoid valves. Flow meters were used to set the wind speed entering into the fly chambers and control odor mixing into a carrier air stream. We selected flow rates that did not interfere with standard fly behavior (data not shown) and that allowed for a consistent stimulus amplitude to be delivered for several hours. To achieve this, we modified previously published olfactometer designs to fit onto a standard fly food bottle. We punched two holes through fly bottle cotton plugs and placed thin-wall stainless steel pipes into each hole. Carrier air and odorized air were mixed in the olfactometer, and this air was connected to one of the steel pipes leading directly into the fly bottle. Output air was allowed to ventilate through the remaining pipe, and this was connected to a loose vacuum (Figure 2.1A). We validated the stability of the odor pulse with a photoionization detector, and found that we could optimize odor stability by continuously stirring the liquid contents of an odor vial (Figure 2.1B). All stimulation vials were placed on a magnetic stir plate to equalize the headspace of stimulus vials and prevent rapid depletion during odor exposure. We emphasize that stirring was vital to achieve a reliable stimulus pulse long-term.

We recorded odor responses from a sample PN in response to the rearing parameters used for odor exposure (Figure 2.1C, D). To do this, we presented trans-2-hexenal diluted to 10^{-7} and mixed it into a carrier air stream that was odorized with fly food. DL5 responses recorded across 90 consecutive trials demonstrate that we can recruit 200Hz of stimulus-evoked activity across individual trials in a single DL5 PN (Figure 2.1D) with our rearing parameters. As a control, we delivered solvent (paraffin oil) into the food-infused carrier air and measured weak responses in the PN (Figure 2.1C, D). This suggests that our odor exposure parameters can reliably and robustly activate odor responses in PNs. To confirm that the PN of interest remained stable throughout our recording, we plot the input resistance in red and display baseline spike rates as black open circles (Figure 2.1C). Odor-evoked spike rates, shown as black filled circles, were quantified during 500ms of odor exposure (Figure 2.1C). DL5 spike rates to

the paraffin-oil solvent are plotted as gray filled circles (Figure 2.1C) and quantified in 50ms bins as a peristimulus-time histogram (Figure 2.1D, gray lines). The total odor pulse delivered was 1s and the inter-pulse interval was 20s to mimic the exact exposure protocol for all experiments.

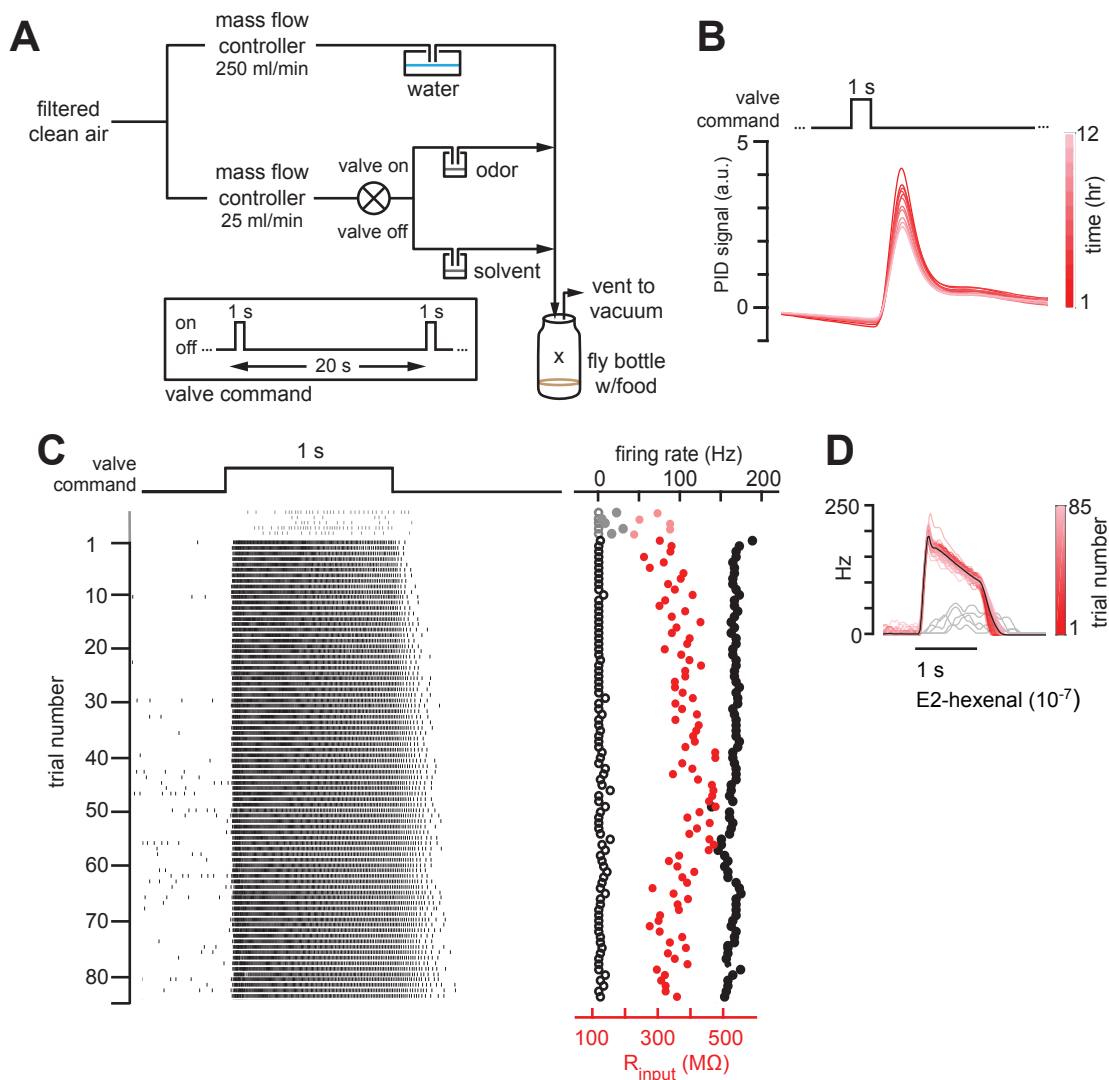


Figure 2.1: Chronic stimulation of olfactory neurons in a controlled odor environment

A) Diagram of chronic odor-rearing paradigm showing olfactometer and fly rearing bottle. Charcoal filtered air is split and sent to a high mass flow controlled, set to 250mL/min, or a low flow controller, set to 25mL/min. Low flow air is passed into a normally-closed

solenoid valve that controls whether air flows through an odor vial or a control (mock vial) containing just the solvent, paraffin oil. The valve receives input from an olfactometer that consists of a 1s 5V command with a 20s inter-pulse interval during which air is passing from the mock vial only. Odors are pulsed into fly bottles and exit through a port connected to a loose vacuum. **B)** The odor pulse was measured by placing a photoionization detector probe into the center of a fly bottle (designated by 'x' in panel. **C)** Raw spike rasters showing the response of a DL5 PN to mock (gray) and trans-2-hexenal 10^{-7} (black) presented across consecutive trials to mimic mock and odor rearing conditions. Baseline spike rate (open circles), odor-evoked spike rate (filled circles) and input resistance (red circles) are plotted for each trial. **D)** Peri-stimulus time histogram (PSTH) of trials 1-85 in response to trans-2-hexenal 10^{-7} stimulation with average evoked PSTH across all trials is plotted (black trace). Paraffin oil PSTH responses are overlaid in gray.

Chronic activation of direct ORN input can modestly increase PN responses to weak odors

To investigate how odors that are overrepresented in the flies' environment are encoded by the olfactory system, we exposed flies to one second pulses of odor in the bottle in which they normally grow (Figure 2.1A). We chose specific odors at concentrations previously shown to selectively activate a single ORN type (Olsen 2010), in order to facilitate the subsequent analysis of the impact of the manipulation on olfactory neurons receiving direct versus indirect persistent input. An additional criterion was that the odor stimuli drive strong and consistent levels of neural firing in the PNs receiving direct input from the activated ORN type. Indeed, photoionization measurements of the odor stimulus in the rearing bottle demonstrated that the stimulus was stable across more than 24 hours (Figure 2.1B). Odors were pulsed to avoid long-term neural adaptation to the odor, and the interval between odor pulses delivered to the bottle was 20 seconds.

Pilot recordings showed that, at this interstimulus interval, the odor stimulus reliably activated its cognate PN to saturating or near saturating firing rates over many trials, with little adaptation of the PN response to the odor (Figure 2.1C and data not shown; see also Figure 2.4 and Olsen 2010). Thus, the odor concentrations to which we exposed the flies were significantly lower than what has been used in prior studies investigating olfactory plasticity (Sachse, S., et al., 2007; Kidd, S., et al., 2015; Devaud, J.M., et al., 2001; Devaud, J.M., et al., 2003), but they drove strong, persistent, and saturating levels of neuronal activity in PNs.

We reared flies in odors that have previously been used to strongly activate a single olfactory receptor neuron type (Olsen, S., et al., 2010). Flies were exposed to odor in a highly controlled odor environment that is designed to maintain a constant odor amplitude throughout rearing (Figure 2.1A, B, and see Methods). Unlike prior odor exposure paradigms (Sachse, S., et al., 2007; Kidd, S., et al., 2015; Devaud, J.M., et al., 2001; Devaud, J.M., et al., 2003), we used an olfactometer to pulse odor for 1 second every 20 seconds into a carrier air stream that connects to a rearing bottle. We recorded responses from DL5 to verify that our stimulation parameters did not lead to habituation across trials (Figure 2.1C-E). We presented trans-2-hexenal diluted to 10^{-7} and mixed it into a carrier air stream that was odorized with fly food. As a control, we delivered solvent (paraffin oil) into the food-infused carrier air and measured weak responses in the PN (Figure 2.1C-D).

Using these conditions, newly eclosed flies were chronically exposed to trans-2-hexenal (10^{-7}), which selectively activates ORNs projecting to glomerulus DL5, or solvent (as a control), for two days (see Methods). On day three, we established whole-cell current clamp recordings from uniglomerular PNs receiving direct input from the DL5 glomerulus (hereafter referred to as DL5 PNs, Figure 2.2A) and measured their responses to a concentration series of trans-2-hexenal. In response to low concentrations of trans-2-hexenal (10^{-10} to 10^{-9}), we observed a modest increase in the

average amount of odor-evoked membrane depolarization in DL5 PNs. This heightened depolarization of DL5 PNs by weak odors corresponded to higher average rates of odor-evoked spiking. However, in response to moderate to high concentrations of trans-2-hexenal ($>10^{-8}$), DL5 PNs in trans-2-hexenal exposed and control solvent-exposed flies responded similarly.

We next examined the extent to which these results generalize to other glomeruli. Using the same approach, we exposed flies to either 2-butanone (10^{-4}), which selectively activates ORNs projecting to glomerulus VM7 (Figure 2.2G), or geranyl acetate (10^{-4}), which selectively activates ORNs projecting to glomerulus VA6 (Figure 2.2K). The concentrations of each of these odors was chosen because they selectively elicit similarly high average firing rates (>100 - 150 Hz) in their corresponding PNs, as trans-2-hexenal (10^{-7}) does in DL5 PNs. Again, we chronically exposed flies for two days to each of these stimuli, and measured the responses in each cognate PN (corresponding to the glomerulus receiving direct input from the activated ORNs) to a concentration series of each odor. We observed that the effect of chronic activation of direct ORN input on PN odor responses varied across different glomeruli. Similar to the DL5 glomerulus, VM7 PNs in 2-butanone exposed flies exhibited increased odor-evoked depolarization in responses to 2-butanone as compared to control flies, and these effects were more pronounced at weak concentrations (10^{-7}). Due to the small size of VM7 PN somata, VM7 PN spikes are small and filtered in comparison to those of other PNs, and odor-evoked spikes riding on large depolarizations could not be reliably counted across all firing rates in our data set. Therefore, for VM7 PNs only, we report odor responses only in terms of membrane depolarization.

In contrast, chronic activation of direct ORN input to VA6 PNs by exposure to geranyl acetate did not alter PN odor responses to the odor across the entire range of concentrations tested at the level of membrane depolarization or firing rate. These concentrations elicited levels of membrane depolarization (~ 10 - 30 mV) which were

similar to those at which other PN types exhibited differences in odor-evoked responses after chronic exposure. Additionally, odor exposure did not alter the input resistance of any cell that we recorded from (Figure 2.2D, J, N). Together, these results demonstrate that, in some glomeruli, chronic activation of direct ORN input can modestly enhance the strength of PN odor responses to weak direct odor inputs. However, this effect does not appear to be universal across all glomeruli.

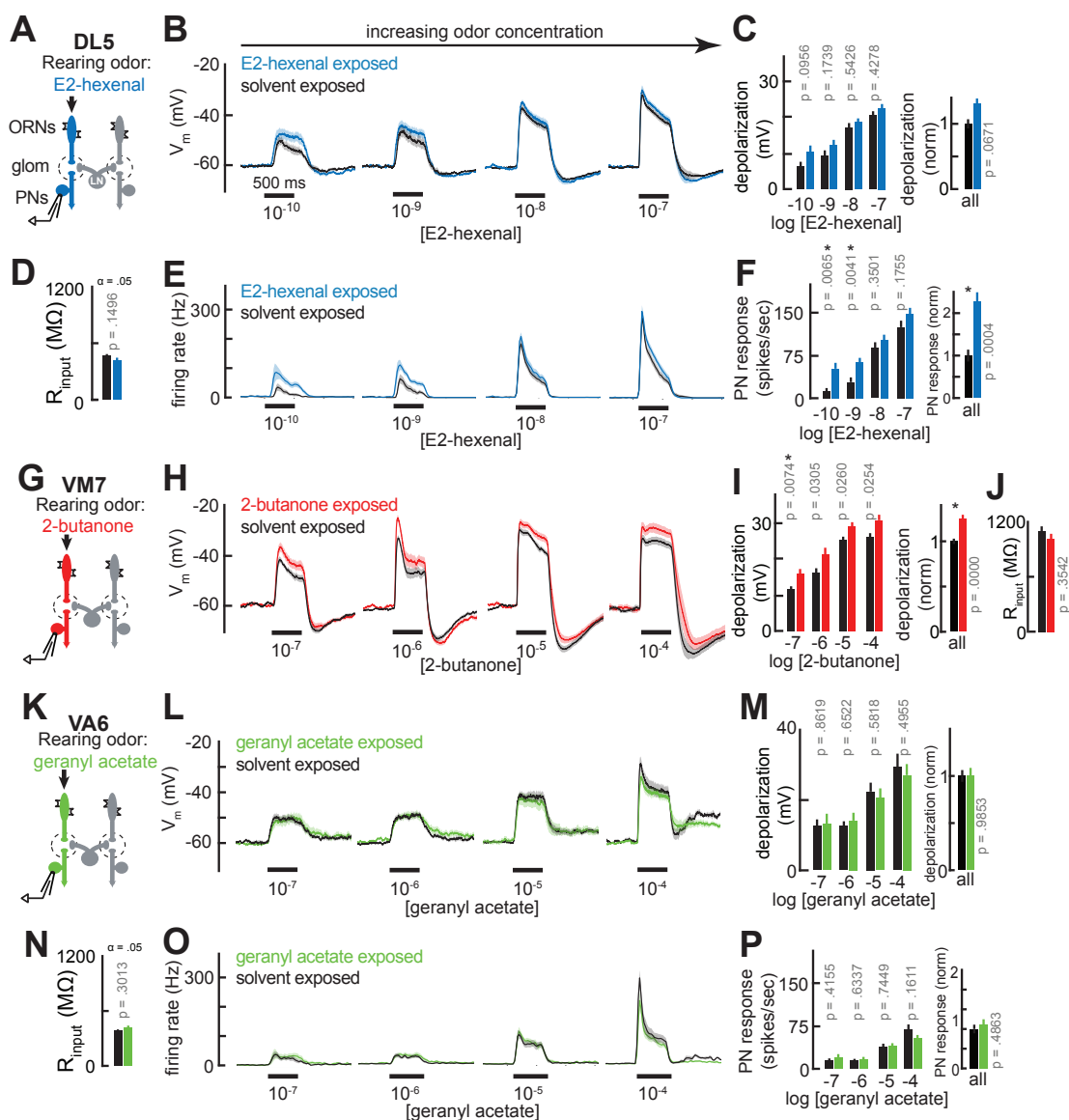


Figure 2.2: Effects of direct odor rearing on PN responses

A, G, K) Schematic of direct odor rearing and patch-clamp recordings targeting PNs. (a) DL5 reared in trans-2-hexenal (E2-hexenal; blue), (g) VM7 reared in 2-butanone (2but; red), and (k) VA6 reared in geranyl acetate (ga; green). Concentrations used for rearing: trans-2-hexenal 10^{-7} , 2-butanone 10^{-4} , geranyl acetate 10^{-4} . **B, H, L)** Average PN membrane potential following direct odor rearing and mock rearing in paraffin oil (black). (b) DL5 responses to trans-2-hexenal 10^{-10} , 10^{-9} , 10^{-8} , 10^{-7} , (h) VM7 responses to 2-butanone 10^{-7} , 10^{-6} , 10^{-5} , 10^{-4} , and (l) VA6 responses to geranyl acetate 10^{-7} , 10^{-6} , 10^{-5} , 10^{-4} . **C, I, M)** Left: Average odor-evoked depolarization of (c) DL5, (i) VM7 and (m) VA6

in direct rearing and mock rearing conditions. Right: Total normalized PN membrane depolarization computed across all odor stimuli. **D, J, N**) Average input resistance for (d) DL5, (j) VM7 and (n) VA6 PNs. **E, O**) Average PN spike rates following direct odor rearing and mock rearing in paraffin oil (black). (e) DL5 responses to trans-2-hexenal 10^{-10} , 10^{-9} , 10^{-8} , 10^{-7} , (o) VA6 responses to geranyl acetate 10^{-7} , 10^{-6} , 10^{-5} , 10^{-4} . **F, P**) Left: Average baseline-subtracted odor-evoked spike rate for (f) DL5 and (p) VA6 PNs. Right: Total normalized PN evoked spike rate. Raw Bootstrap p-values after 10,000 random draws are shown for each statistical comparison. Threshold for statistical significance is $p < 0.0125$ for concentration series and $p < 0.05$ for total normalized responses and R_{input} . Values are Bonferroni corrected.

We quantified these effects by calculating the total depolarization and average evoked firing rate during the first 500 ms after nominal stimulus onset (Figure 2.2C, F, I, M, P). To determine if any differences were arising by chance, we used permutation testing to iteratively shuffle the experimental labels of the data (odor trans-2-hexenal versus solvent exposure) within each stimulus. P-values were calculated directly from the fraction of 10,000 shuffled trials in which the absolute difference between the simulated group means was larger than the actual observed mean difference (see Methods), and the significance level was corrected for multiple comparisons within the concentration series. This statistical analysis confirmed that trans-2-hexenal exposure increased odor-evoked firing rates in DL5 PNs to weak, but not moderate or strong, stimuli. When firing rates in odor-exposed brains were normalized to controls within each stimulus, we observed an overall increase in odor-evoked DL5 PN firing rate due to trans-2-hexenal exposure (see Methods). Differences in the level of membrane depolarization between odor- and solvent-exposed groups did not reach statistical significance at any stimulus concentration, suggesting that a small, but systematic increase in membrane

depolarization was nonlinearly amplified by its interaction with spike threshold in DL5 PNs.

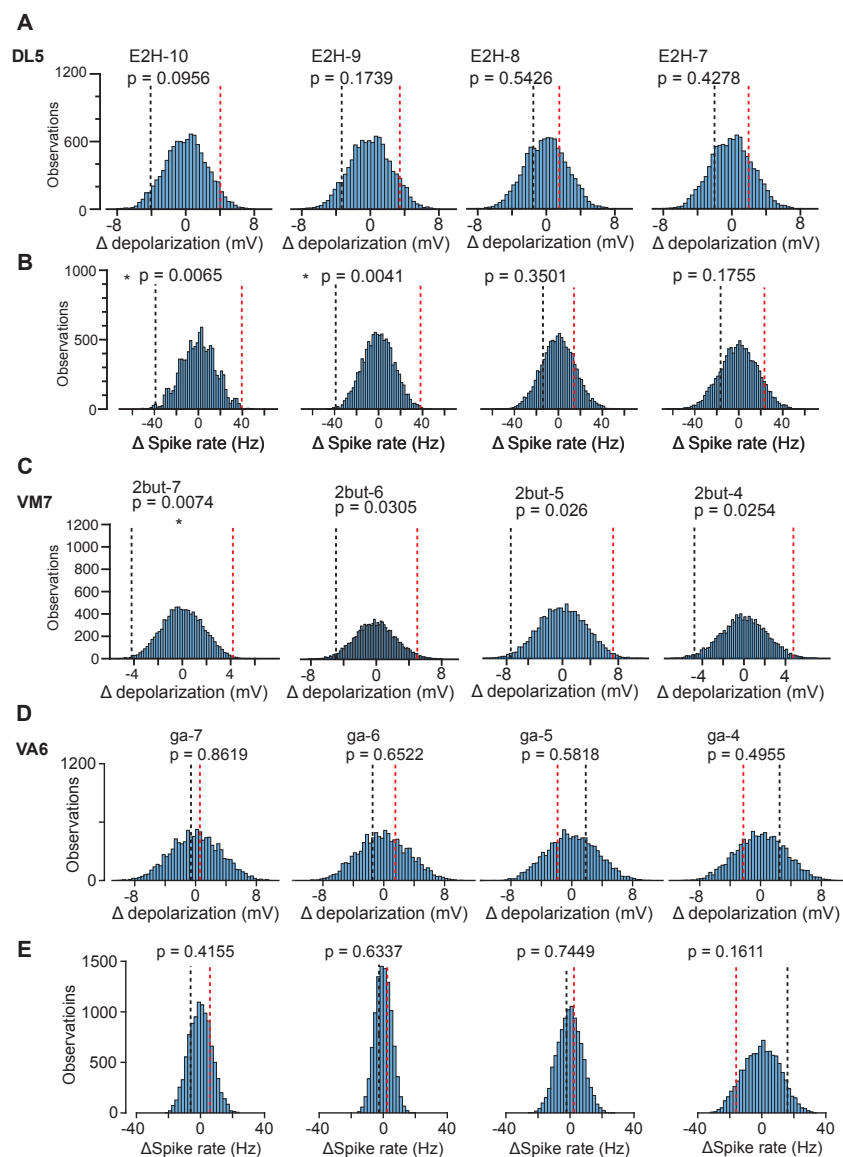


Figure 2.3: Statistical analysis of direct rearing results in PNs

A, C, D) Histograms of 10,000 permuted samples of average odor-evoked membrane potential in response to increasing concentrations of trans-2-hexenal (E2H) in DL5 (a), 2-butanone (2but) in VM7 (c), and geranyl acetate (ga) in VA6 (d). **B, E)** Same as above, but for average odor-evoked spike rates computed during the 500ms odor-stimulation

window for DL5 (b) and VA6 (e) PNs. Dotted lines indicate two-sided statistical threshold. Red lines are the actual differences between odor-reared and mock-reared responses. Bootstrap p-values are displayed in each histogram. Threshold for significance is $p < 0.0125$. Values are Bonferroni corrected.

To summarize our direct channel results from above, we generate PN concentration curves by plotting PN spike rates or membrane depolarization versus odor concentration (Figure 2.4). We find that trans-2-hexenal heightens DL5 PN spiking responses to low odor concentrations of trans-2-hexenal in direct rearing. In VM7, we find that direct rearing in 2-butanone increases odor-evoked membrane potential to low odor concentrations of 2-butanone. Lastly, we did not see any effects of direct odor rearing in geranyl acetate on VA6 odor-evoked PN spike rates. The results so far suggest that the effects of rearing may be odor specific and glomerulus specific. Not all glomeruli show the same effects; thus, there does not appear to be a general rule of PN plasticity following direct odor exposure. An important feature of the observations in Figure 2.4 is that the reared concentrations we used were near PN saturation levels. This suggests that our stimuli were sufficiently strong across exposure experiments. We do see that VA6 can respond more strongly to geranyl acetate 10^{-3} than 10^{-4} . It is possible to recruit more spikes in VA6 PNs with a stronger odor than we used during our rearing experiments (Figure 2.4C).

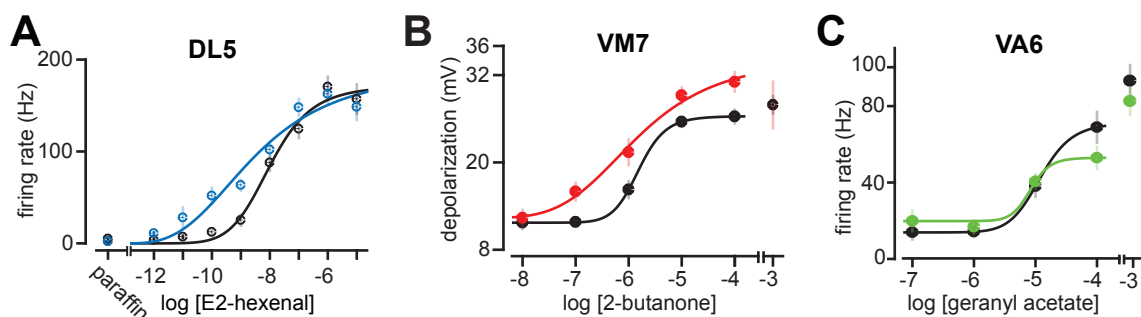


Figure 2.4: PN concentration curves following direct odor rearing

A-C) PN concentration curve in direct rearing for DL5 (a; blue), VM7 (b; red) and VA6 (c; green) and mock reared (black) conditions. For (b) and (c), responses to odor dilutions of 10^{-3} were not used to generate fits as these points likely recruit network mechanisms and are no longer selective odors. Odors used include (a) trans-2-hexenal (E2-hexenal) 10^{-12} , 10^{-11} , 10^{-10} , 10^{-9} , 10^{-8} , 10^{-7} , 10^{-6} , 10^{-5} ; (b) 2-butanone 10^{-8} , 10^{-7} , 10^{-6} , 10^{-5} , 10^{-4} , 10^{-3} ; and (c) geranyl acetate 10^{-7} , 10^{-6} , 10^{-5} , 10^{-4} , 10^{-3} .

Chronic elevation of indirect activity perturbs PN response properties

What determines whether PN odor-evoked responses will change after odor exposure? Directly rearing DL5 in trans-2-hexenal resulted in an increase in PN spike rates that we did not see in other directly reared glomeruli, VM7 and VA6. We reasoned two possible scenarios to explain our direct rearing results: a glomerulus may be responsible for the effects seen following rearing or the rearing odor used may influence the effects seen at a glomerulus. If the former is true, we would expect to see the same effect on individual PNs independent of the rearing odor. In contrast, the latter case suggests that each rearing odor is unique and therefore can influence the effects seen at PNs.

Although olfactory input is compartmentalized into parallel processing channels organized around each glomerulus, odor processing depends on an extensive network of local neurons that mediate lateral excitatory and inhibitory interactions across glomeruli. Thus, the odor response of a given PN depends on both the direct and

indirect synaptic input it receives. Having observed that chronic activity in a single ORN type can elicit plasticity in PNs directly postsynaptic to it, we next asked whether this plasticity is selective to PNs receiving direct input from the chronically activated glomerulus, or whether odor responses of PNs belonging to other glomeruli are also impacted. To address this question, we focused on evaluating odor responses in VM7 and VA6 PNs from flies chronically exposed to trans-2-hexenal (10^{-7}), which should evoke indirect neural activity in these neurons (Figure 2.5 A, I).

Intracellular recordings from non-DL5 PNs revealed that chronic exposure to trans-2-hexenal elicited subtle changes in the odor-evoked response properties of these PNs. For instance, spontaneous activity in VM7 PNs from trans-2-hexenal was mildly elevated (Figure 2.5 G, H). Similar to what was observed in the case of chronic direct activation, chronic activation of indirect activity resulted in a trend towards mild enhancement of PN odor responses to weak odors (Figure 2.5 J, K, M, N). This trend was small, but was observed in VA6 at the level of odor-evoked depolarization and spike rates in response to a subset of stimuli.

Additionally, chronic engagement of indirect input impacted the post-stimulus odor response in PNs. For example, odor-evoked depolarization measured in VM7 PNs in trans-2-hexenal exposed flies had a much more pronounced and prolonged afterhyperpolarization as compared to controls, or even as compared to flies that experienced chronic activation of direct input via 2-butanone exposure (Figure 2.5 B, D-F). This effect does not appear to generalize to all glomeruli. VA6 PNs exhibited a very different type of post-stimulus response, dominated by an extended period of excitation. In recordings from VA6 PNs in trans-2-hexenal exposed flies, odor responses in this post-stimulus epoch were enhanced across multiple odor concentrations, as compared to solvent-exposed controls. Together, these experiments demonstrated that chronic, focal activation of a single ORN class can lead to changes in odor response properties in multiple glomeruli, including in glomeruli not receiving direct synaptic input from the

chronically activated ORN class. This observation suggests that local lateral circuitry in the antennal lobe may participate in plasticity evoked by perturbations in the odor environment.

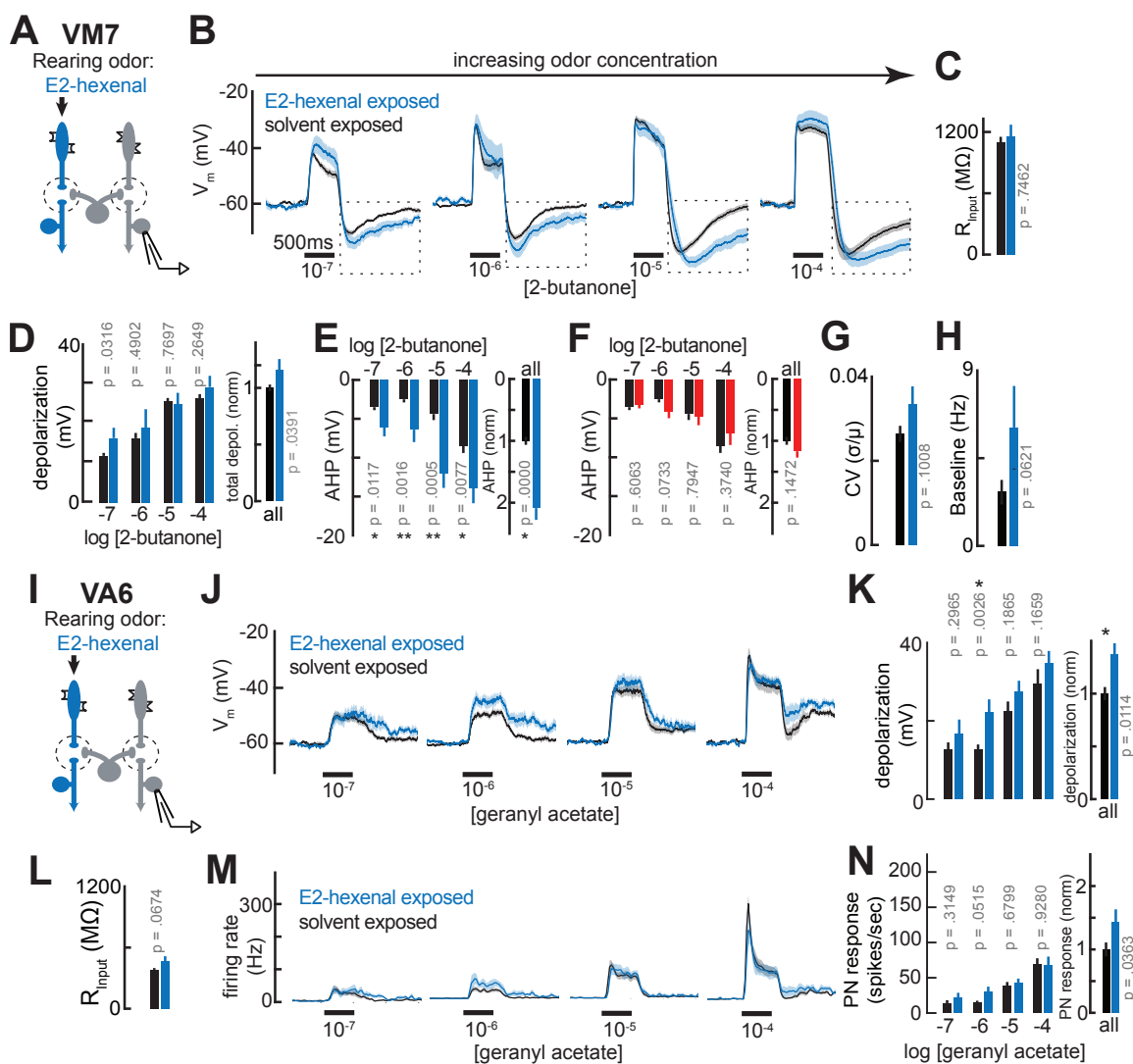


Figure 2.5: Effect of indirect rearing on PN responses

A, I) Schematic of indirect odor rearing and patch-clamp recordings targeting PNs. (a) VM7 and (i) VA6 reared in trans-2-hexenal (E2-hexenal 10^{-7} ; blue). **B, J)** Average PN membrane potential following indirect odor rearing and mock rearing in paraffin oil (black). (b) VM7 responses to 2-butanone 10^{-7} , 10^{-6} , 10^{-5} , 10^{-4} , and (j) VA6 responses to geranyl acetate 10^{-7} , 10^{-6} , 10^{-5} , 10^{-4} . **C, L)** Average input resistance for (c) VM7 and (l)

VA6 PNs. **D, K)** Left: Average PN membrane depolarization for (d) VM7 and (k) VA6 PNs. Right: Total normalized PN evoked spike rate. **E, F)** Left: Average VM7 afterhyperpolarization (AHP) potential following indirect odor rearing (e; blue) and direct odor rearing in 2-butanone 10^{-4} (f; red) computed for 2.5 seconds post-stimulation. Right: Total AHP averaged across stimuli. **G)** Average coefficient of variation (CV) computed for 5 seconds before odor stimulation. **H)** Average spontaneous firing rate computed for 5 seconds before odor stimulation. **M)** Average VA6 odor-evoked spike rate following indirect odor rearing. **N)** Left: Average VA6 odor-evoked spike rate computed during 500ms stimulus presentation. Right: Total normalized VA6 evoked spike rate. All traces show mean \pm SEM. Raw Bootstrap p-values after 10,000 random draws are shown for each statistical comparison. Threshold for statistical significance is $p < 0.0125$ for concentration series and $p < 0.05$ for total normalized responses and R_{input} . Values are Bonferroni corrected.

Discussion

We find that the effects of odor exposure do not greatly influence PN coding and vary between glomeruli. By using selective odor ligands to activate individual olfactory receptor neurons, we show that naturalistic odor conditions have small effects on both directly targeted and indirectly targeted PNs, though the effects are odor-dependent. Our exposure paradigm is fairly naturalistic in the sense that the odor concentrations we use for rearing closely resemble the concentrations at which the specific monomolecular compounds are typically found in nature. For example, trans-2-hexenal is a leaf aldehyde that occurs in leaves at concentrations of 10^{-11} (Kunishima, M., et al., 2016). Prior work showing effects on PNs and ORNs following exposure to high concentrations of odor may be problematic because of the borderline toxic odor concentrations used for exposure throughout the animal's development. While our odor concentrations used for exposure are dilute, we show that the targeted PNs fire near saturation to our stimuli.

This suggests that higher concentrations of odor will not further activate individual PNs, but instead will act as broad odors and activate more cells overall. With our work, we show that the early olfactory circuit of *Drosophila* is fairly hard-wired, and the effects of odor exposure on PN odor-responses are small.

The strongest effect of odor exposure was seen in response to the leaf aldehyde, trans-2-hexenal. We find that DL5 PNs increase sensitivity to low odor concentrations following direct odor exposure (Figure 2.2 B, C, E, F; Figure 2.4 A). It is possible that trans-2-hexenal exposed flies may be able to behaviorally discern dilute concentrations of trans-2-hexenal better than controls. Why would PNs increase sensitivity to dilute concentrations of the exposed odors rather than show habituation? We hypothesize that the design of our odor-exposure paradigm may be an important factor in mediating this distinction. For one, we present an odor pulse and allow the odor to dissipate completely during the inter-pulse interval period. This pulsing paradigm appears to be sufficient to 'refresh' PN sensitivity to odors, and this stimulus design is widely used across insect olfactory neurophysiology (Olsen, S.R., 2010 and many others). The presentation of odor with food may also be an important factor behind our observations, though we do not test the effects of odor-exposure in an odor-less food substrate or on sucrose-based food. Another possibility is the potential ethological importance of DL5 and trans-2-hexenal to the fly. Previous work shows that Or7a can mediate *Drosophila* oviposition through pheromone detection, and activation of Or7a via trans-2-hexenal in our experiments may be mediating similar effects in the fly (Lin, C.C., et al., 2015).

The effects of indirect rearing are small and most of the results are not significantly different than control responses. We noticed that trans-2-hexenal rearing significantly increased VA6 odor-evoked membrane potential in a 1s time window to a 500ms stimulus. The effect was only seen to low odor concentrations. Similarly, we noted a trending increase in VM7 odor-evoked spike rate to low odor concentrations, but the effect was not significantly different than control VM7 spike rates. Interestingly, the

effects we observed occurred within a similar stimulus range as we had seen in DL5 after direct rearing in trans-2-hexenal. The observation that VA6 odor-evoked membrane depolarization is significantly different during a 1s time window is unclear. PNs typically have unique response properties characterized by several features such as spike rate, membrane potential, and input resistance. In our data set, we note that PNs can differ in the overall shape of their responses, particularly during the post-stimulus period.

The afterhyperpolarization phase of VM7 PNs are strikingly pronounced compared to VA6, which typically does not hyperpolarize following stimulus presentation. Surprisingly, whereas 2-butanone rearing did not have any effect of VM7 odor-evoked spike rates, we see that indirect rearing in trans-2-hexenal induces a robust change in post-stimulus afterhyperpolarization of VM7 membrane potential that scales with odor strength. The afterhyperpolarization is not increased in amplitude, but instead shows that the cell requires more time to reach its resting membrane potential. Changes in membrane afterhyperpolarization have not previously been reported in *Drosophila* antennal lobe PNs following odor exposure. The membrane afterhyperpolarization phase is a complex interplay of voltage-gated ion channels and pumps that work together to bring the cell membrane potential back to baseline. It is possible that the different membrane dynamics of individual PNs may result from the unique genetic expression of voltage-sensitive machinery. Prior work suggests that PNs can be grouped into discernible clusters using gene expression analysis (Li, H., et al., 2017). While we did not investigate the cause of the increased afterhyperpolarization in VM7 following trans-2-hexenal exposure, we propose that the source may be a potassium-sensitive current. Prior work shows that there is an electrogenic sodium pump which regulates membrane afterhyperpolarization (Smith, P.A. and F.F., 1977; Schlue, W.R., 1991). Interestingly, the afterhyperpolarization disappears in K⁺-free saline and in ouabain, an electrogenic sodium pump blocker (Schlue, W.R., 1991). It is possible that the effect of odor exposure may involve the electrogenic sodium pump. If so, the pump may be more

sensitive to changes in membrane potential or may be over-expressed as a result of exposure.

VA6 has different membrane response dynamics than VM7; for example, we find subthreshold increases in odor-evoked membrane potential which have no effect on spike rate to low odors such as geranyl acetate 10^{-6} . Thus, rearing in trans-2-hexenal tends to increase responses in antennal lobe PNs but the magnitude of plasticity and response characteristics are unique to each glomerulus. VA6 odor-evoked membrane potential after trans-2-hexenal rearing was significantly greater than VA6 control responses. This suggests that indirect rearing in trans-2-hexenal may increase excitatory input into other glomeruli. The observation that trans-2-hexenal rearing does not result in a significant change in odor-evoked spike rate may suggest that the effects of rearing may not be computationally important in VA6. Overall, we see that trans-2-hexenal appears to be capable of mediating small changes in PN responses following chronic exposure. It will be interesting to perform a large-scale screen of different monomolecular odors to determine which other ligands are capable of altering PN responses as well. Is this effect aldehyde-specific or dependent on the targeted glomerulus, DL5? To address this question, one can expose flies to another odor which selectively activates DL5 or use light to selectively activate Or7a ORNs (Lin, C.C., et al., 2015).

Methods

Flies

The line *NP3481-Gal4, UAS-CD8-GFP* was used for all single-sensillar recordings and all patch-clamp experiments targeting DL5 and VM7. All patch-clamp recordings of VA6 PNs were performed in *UAS-CD8-GFP; Mz612-Gal4, UAS-CD8-GFP*.

Rearing

We designed a rearing set-up that allows us to group-rear flies in a controlled odor environment. Flies were reared on standard fly bottles with modified cotton plugs containing stainless steel rods for air input and output (McMaster Carr #89535K162). The bottom of the cotton plug was lined with mesh (McMaster-Carr #9318T45) to prevent flies from entering the rods. The inlet port was fit with a luer connector so each bottle could be easily positioned into the rearing set-up. Air delivery into the rearing system is controlled using an olfactometer as previously published with some modifications. For rearing, charcoal filtered air is split and passed through a low-range flowmeter (Cole-Parmer) set to 25mL/min and a high-range flowmeter (Cole-Parmer) set to 250mL/min. The high flow carrier air is passed into a humidifier bottle containing water, while the low flow is directed into a normally closed solenoid valve. Upon receiving a 5V signal, the valve switches the direction of flow into the rearing odor vial. This switching is cycled throughout the duration of rearing with 1 second of odor delivery followed by 20 seconds of solvent. Odors are mixed directly into the carrier air flow, and the total volumetric flow rate (odor/mock + carrier air) of 275mL/min is passed into the rearing bottle. Tygon tubing is used throughout the set-up except at site of odor mixing, where we use PTFE tubing. A loose vacuum is attached onto the outlet of the bottle.

We achieve stable pulse-to-pulse odor amplitude by continuously stirring the odor on a magnetic stir plate (Adventures in Homebrewing). We verified the long-term stability of the odor using a photoionization detector (Aurora Instruments) by inserting

the PID probe into the center of an empty fly bottle and measuring odor amplitude over the course of 24 hours. We used 2-butanone diluted at 10^{-4} as our test odor for rearing validation and set the PID at 10x gain.

For rearing experiments, we used bottles ~12 days post-seeding. Prior to rearing, flies were briefly anesthetized with CO_2 and all adult flies were emptied from the bottle. Any remaining adult flies that were stuck in the bottle were stirred into the fly food to ensure that there were no adults present at the start of rearing. The flies were set-up in the evening (day 0). The next morning, all eclosed flies were flipped into a new bottle and reconnected into the same rearing set-up where they remained for 2 days. Stimulus vials were changed every ~12 hours to maintain a consistent stimulus amplitude.

Electrophysiology

All electrophysiological experiments were performed in current-clamp mode on 2-day-old female flies except for EPSCs measurements, in which we used voltage-clamp mode. Patch-clamp recordings were conducted as previously described. Briefly, we filled our pipettes with K^+ aspartate internal solution for all recordings except for EPSC recordings where we used K^+ aspartate and Cs^+ -based internal solution. Internal solution contained 140mM of KOH, 140mM aspartic acid, 10mM HEPES, 1mM EGTA, 1mM KCl, 4mM MgATP, 0.5mM Na_3GTP and 13mM biocytin. The final pH values were adjusted to 7.1-7.3 and final osmolarity to 262-268 mOsm. For Cs -based internal, we replaced 140mM KOH with 140mM of CsOH. Patch electrodes were freshly pulled everyday (Sutter) and had a resistance of ~6-10 MOhm. The silver recording wire (A-M Systems #782500) was chlorided with bleach every ~1-2 weeks and thoroughly washed with water. Recordings were performed on electrophysiological rigs (Scientifica), signals were amplified (AxonClamp) and all data input/output was controlled using custom scripts in Matlab (Mathworks) communicating through an acquisition board (National Instruments BNC2120).

Flies were dissected in *Drosophila* saline containing 103mM NaCl, 3mM KCl, 5mM TES, 8mM trehalose 2H₂O, 10mM glucose, 26 mM NaHCO₃, 1mM NaH₂PO₄ H₂O, 4mM MgCl 6 H₂O, and 1.5 mM CaCl₂ 2H₂O with pH ~ 7.25 and osmolarity adjusted to 270-275 mOsm. Saline was oxygenated with a 5% CO₂/95% O₂ air mixture (Airgas #Z02OX951200C4H9) during dissections and perfused during all electrophysiological experiments. Flies were anesthetized on ice and stabilized into stainless steel foils with a small application of wax (Almore Electra waxer #66000) around the eyes and abdomen. The antennal lobe PNs were exposed by carefully removing the cuticle and desheathed with forceps as previously described (Olsen, S.R., 2008; Olsen, S.R., 2010 and others). For EPSC and current injection experiments, the antennal nerve was carefully severed using fine forceps. For all recordings, we targeted GFP+ PNs. We used a 5X objective (Olympus) for coarse alignment and switched to a 40X water-immersion objective (Olympus) while patching. After locating flies with a white LED, we switched to an IR LED shining below the head to locate cell somata. We briefly pulsed wide-field blue light (Sutter TLED+) to locate GFP-expressing PNs and visualized IR-GFP signals through long-pass filters (Olympus). During experiments, cell identity was verified using diagnostic odor panels and verified post-hoc by imaging biocytin fills in most of the cells recorded. When measuring odor-evoked responses, we excluded cells that had low spontaneous activity, suggesting nerve damage. Recordings were stopped if there was a ~20% drift in input resistance.

Histology and confocal imaging

Tissue histology was performed as previously described. Briefly, after rearing for two days as, flies were transferred to a scintillation vial and anesthetized on ice. Female flies were selected for dissection and fixation, and dissections were performed in *Drosophila* saline. The head capsule was removed from the body and the cuticle was carefully removed from the brain. Fine forceps were used to remove trachea and fat droplets

surrounding the brain. Samples were fixed in 4% paraformaldehyde for 14-16 minutes and then washed three times in phosphate buffered saline (PBS) for seven minutes each. After washing, samples were placed in blocking buffer solution consisting of 5% normal goat serum in PBS with triton (PBST) (0.2% Triton-X in PBS) for 20 minutes. After blocking, samples were transferred to a primary antibody solution consisting of a fresh mixture of blocking buffer plus primary antibodies. We used the following antibodies: rat anti-CD8 (1:50; Thermo Fisher #MA5-17594) and mouse anti-nc82 (1:40; DSHB #AB_2314866). Samples were placed in 4°C rocking for 24 hours. After incubation, a quick 1X wash was performed in PBST followed by three washes of 15 minutes each on the rocker. Samples were again incubated 4°C rocking for 24 hours in secondary antibody solution consisting of a fresh blocking buffer and secondary antibodies: goat anti rat Alexa 488 (1:250; Abcam #ab150157), goat anti mouse Alexa 633 (1:250; Thermo Fisher #A21050), and Streptavidin Alexa 568 conjugate to visualize biocytin (1:1000; Thermo Fisher #S11226). After incubation, samples were washed as previously described for the primary antibody step and washed at 4°C overnight. Confocal imaging was performed using a Leica SP8 confocal with a 40X oil immersion objective. Images were acquired as z-stacks with one micron step sizes between each plane.

Odor presentation for electrophysiology

Odors were presented using custom olfactometers controlling normally-closed solenoid valves. For all physiological measurements, air flow was controlled using mass flow controllers (Alicat), with the carrier air set to 2L/min and stimulus to 220mL/min. We presented a 500ms odor pulse for all experiments unless otherwise noted. We computed input resistance by measuring the voltage response to a 300ms hyperpolarizing current injection at the start of every recording. Resting membrane potential was estimated by computing the average membrane potential between 3-4 seconds of the recording,

odors were presented after a 6 second delay from the start of the trial, and the total trial length was 10 seconds. The inter-trial-interval was set to 30 seconds, and each odor was presented for 6 trials for PNs and 5 trials for ORNs. In concentration series presentations, we presented paraffin oil first followed by odors from low to high concentrations to minimize contamination. Between flies, clean air was passed through the olfactometer for ~15 minutes. Odorants were presented in a two-channel olfactometer and mixed in the carrier air stream. In experiments where we only used one odor for stimulation, the remaining port was connected to vials containing just the solvent. In odor blends, we presented two odorants simultaneously through different valves.

Analysis of odor-evoked responses

Spikes were counted using a custom GUI in Matlab (Mathworks) that identifies spikes by thresholding the first and second voltage derivatives as described previously. Thresholds were manually adjusted and all spikes were manually inspected. Peristimulus-time histograms of PN and ORN spiking responses were quantified as previously described using 50ms bins and a 25ms overlap. The PN response to the first trial of each stimulus was not included in analysis. All data plotted is the population mean and SEM. The odor-evoked response for DL5 and VM7 PNs were analyzed from 6.1 to 6.6 seconds during odor delivery and accounts for any mechanical delay in stimulus presentation (data not shown). VA6 odor-evoked responses were quantified from 6.1 to 7.1 seconds to account for the prolonged depolarization following stimulus presentation in this cell type.

Statistics

Statistical analysis was conducted using nonparametric permutation methods. Cell averages across rearing conditions were permuted such that each sample was randomly selected without replacement. Labels from the data were removed to create permuted

samples consisting of mock and odor data selected at random. The total number of samples per each rearing condition matched that of the experimental groups. Permutations were drawn 10,000 times and shuffled distributions for pseudo-mock and odor conditions were generated. We computed a t-statistic to compare whether the difference between the shuffled responses were significantly different than the difference between the actual measured mean odor and control responses for each odor. To do this, we computed a p-value using a two-sided t-test. We counted the total number of observations that the shuffled mean was greater than or equal to the observed mean. The cut-off for significance was adjusted using a Bonferroni correction to account for multiple comparisons across odor stimuli. This statistical analysis was applied to average spike rate, depolarization area, and peak calcium fluorescence as indicated in the main text and figure legends.

References

Devaud, J.M., Acebes, A., and Ferrus, A. (2001). Odor exposure causes central adaptation and morphological changes in selected olfactory glomeruli in *Drosophila*.

J. Neurosci. *21*, 6274-82.

Devaud, J.M., Acebes, A., Ramaswami, M., and Ferrús, A. (2003). Structural and functional changes in the olfactory pathway of adult *Drosophila* take place at a critical age. *J. of Neurobio.* *56*, 13-23.

Kidd, S., Struhl, G., Lieber, T. (2015). Notch is required in adult *Drosophila* sensory neurons for morphological and functional plasticity of the olfactory circuit. *PLoS Genet* *11*.

Kunishima, M., Yamauchi, Y., Mizutani, M., Kuse, M., Takikawa, H., Sugimoto, Y. (2016). Identification of (Z)-3:(E)-2-Hexenal Isomerases Essential to the Production of the Leaf Aldehyde in Plants. *J Biol. Chem.* *291*, 14023-33.

Li, H., Horns, F., Wu, B., Xie, Q., Li, J., Li, T., Luginbuhl, D.J., Quake, S.R., Luo, L. (2017). Classifying *Drosophila* Olfactory Projection Neuron Subtypes by Single-Cell RNA Sequencing. *Cell* *171*, 1206-1220.

Lin, C.C. and Potter, C.J. (2015). Food odors trigger *Drosophila* males to deposit a pheromone that guides aggregation and female oviposition decisions. *Elife* *4*.

Olsen, S.R., Bhandawat, V., and Wilson, R.I. (2010). Divisive normalization in olfactory population codes. *Neuron* *66*, 287-99.

Sachse, S., Rueckert, E., Keller, A., Okada, R., Tanaka, N.K., Ito, K., and Vosshall, L.B. (2007). Activity-dependent plasticity in an olfactory circuit. *Neuron* 56, 838-50.

Schlue, W.R. (1991). Effects of Ouabain on Intracellular Ion Activities of Sensory Neurons of the Leech Central-Nervous-System. *J. Neurophysiol.* 65, 736-746.

Smith, P.A. and Weight, F.F. (1977). Role of electrogenic sodium pump in slow synaptic inhibition is re-evaluated. *Nature* 267, 68-70.

Chapter 3: Effect of odor rearing on ORNs and ORN-PN synapses

Abstract

What causes PNs to alter odor-evoked responses following direct and indirect odor exposure? One possibility is that PNs inherit changes from feed-forward olfactory receptor neurons (ORNs). To determine if rearing alters ORN responses, we performed single-sensillar recordings and GCaMP calcium imaging of ORN terminals following odor exposure. We found that ORN responses to odor do not change; thus, the effect at PNs must occur within the antennal lobe. Next, we measured ORN-PN synaptic strength by recruiting unitary excitatory post-synaptic currents (uEPSCs) in PNs using optogenetics. Overall, we found no difference in current peak amplitude or decay rate of the uEPSCs between rearing conditions. Finally, we recorded PN responses to current injections and found no changes across rearing conditions. These results suggest that effects of rearing do not occur at the ORNs, ORN-PN synapses, or intrinsically at the PN. We hypothesize that odor exposure may change PN responses through lateral circuit mechanisms.

Introduction

To identify the source of the increase in excitation in DL5 PNs, we recorded spiking responses from cognate ORNs, Or7a. After following the same odor exposure protocol, we recorded single-sensillar responses from directly reared ORNs and found that there is no effect on any ORN responses tested. This suggests that PN responses cannot be explained by responses at the ORN level. In the following chapters, we look into what synaptic and circuit mechanisms may be important in mediating the selective increase in excitation in the DL5 glomerulus.

Increases in DL5 responses to low odor concentrations following direct odor rearing in trans-2-hexenal may be a result of a change in ORN-PN synapse strength. We

developed a method to artificially recruit uEPSCs into PNs using light stimulation. We show that light results in reliable uEPSCs and allows for targeted stimulation of genetically labeled ORN dendrites. To determine if increases in DL5 are due to changes in ORN-PN synaptic strength, we measured uEPSCs in DL5 PNs while stimulating ORN axons. We did not find that trans-2-hexenal rearing influenced the total uEPSC size compared to that of solvent-reared flies. We acknowledge that the spread of EPSC data is high and small changes may be difficult to measure.

ORN response properties are unaffected by their chronic, persistent activation

We wondered if, in flies chronically exposed to some odors, enhanced PN responses to weak odors might arise directly from changes in the sensitivity of ORNs. Prior studies have suggested that chronic odor exposure increases the sensitivity of ORNs (Iyengar, A., et al., 2010). Direct feedforward excitation might be impacted by chronic odor exposure, but not be apparent in measurements of PN responses to stronger odors, perhaps due to compensation from circuit mechanisms such as lateral inhibition.

Therefore, we exposed flies to trans-2-hexenal (10^{-7}) or 2-butanone (10^{-4}) as before, and recorded extracellular spiking activity from the ORN classes selectively activated by each odor (see Methods). We observed that chronic activation of either ORN type – ab4a ORNs in trans-2-hexenal exposed flies or pb1a ORNs in 2-butanone and trans-2-hexenal exposed flies (Figure 3.1A, D, G) – did not significantly impact their odor responses at concentrations at which we observed increased responses in their cognate PNs (Figure 3.1B, C, E, F, H, I). We quantified ORN responses by calculating the average firing rate during a 500-ms window after the stimulus, and observed that ORN responses to their cognate odor across a broad range of concentrations were unaffected by chronic odor exposure (Figure 3.1C, F). In addition, we evaluated pb1a odor sensitivity in trans-2-hexenal exposed flies, since VM7 PN responses were altered

by chronic activation of trans-2-hexenal driven indirect input. These experiments showed that pb1a odor responses were largely unaffected by trans-2-hexenal exposure. Although we observed a small decrease in response to 2-butanone at a concentration of 10^{-4} , this difference did not consistently trend at nearby concentrations (10^{-5} or 10^{-3}) and did not reach statistical significance (Figure 3.1H, I).

We next considered the possibility that very small changes in ORN firing rate might not be resolvable in extracellular recordings from individual neurons, but that the high convergence of ~ 10 to ~ 100 ORNs onto PNs could amplify a small difference in ORN firing into a measurable increase in PN response. Therefore, we used functional imaging to measure the population response of all ab4a ORNs summed in the DL5 glomerulus, where the many ab4a ORN axon terminals converge in a small physical volume of about $\sim 200 \mu\text{m}^3$ (Figure 3.1J, K). As before, we chronically exposed flies expressing the genetically encoded calcium indicator GCaMP6f in ab4a ORNs (under the control of the Or7a promoter) to trans-2-hexenal or solvent, and measured odor-evoked ORN calcium signals in the DL5 glomerulus using two-photon imaging (Figure 3.1J, K). The increased sensitivity of ORN population imaging, as compared to single ORN recordings, for detecting odor responses was evident from the ability of functional imaging to resolve ab4a responses to trans-2-hexenal at 10^{-10} concentration, an odor stimulus that was not distinguishable from solvent controls in single ORN recordings from either condition. However, odor-evoked population responses from ab4a ORNs in DL5 were indistinguishable between trans-2-hexenal exposed and control flies across the entire concentration curve (Figure 3.1L, M). Taken together, these results indicate that ORN odor responses are unaffected by perturbations in the odor environment that drive over a million additional spikes in the ORN over the course of two days of exposure. They also imply that the limited PN plasticity we observe likely stems from central circuit mechanisms, rather than changes in input from the periphery.

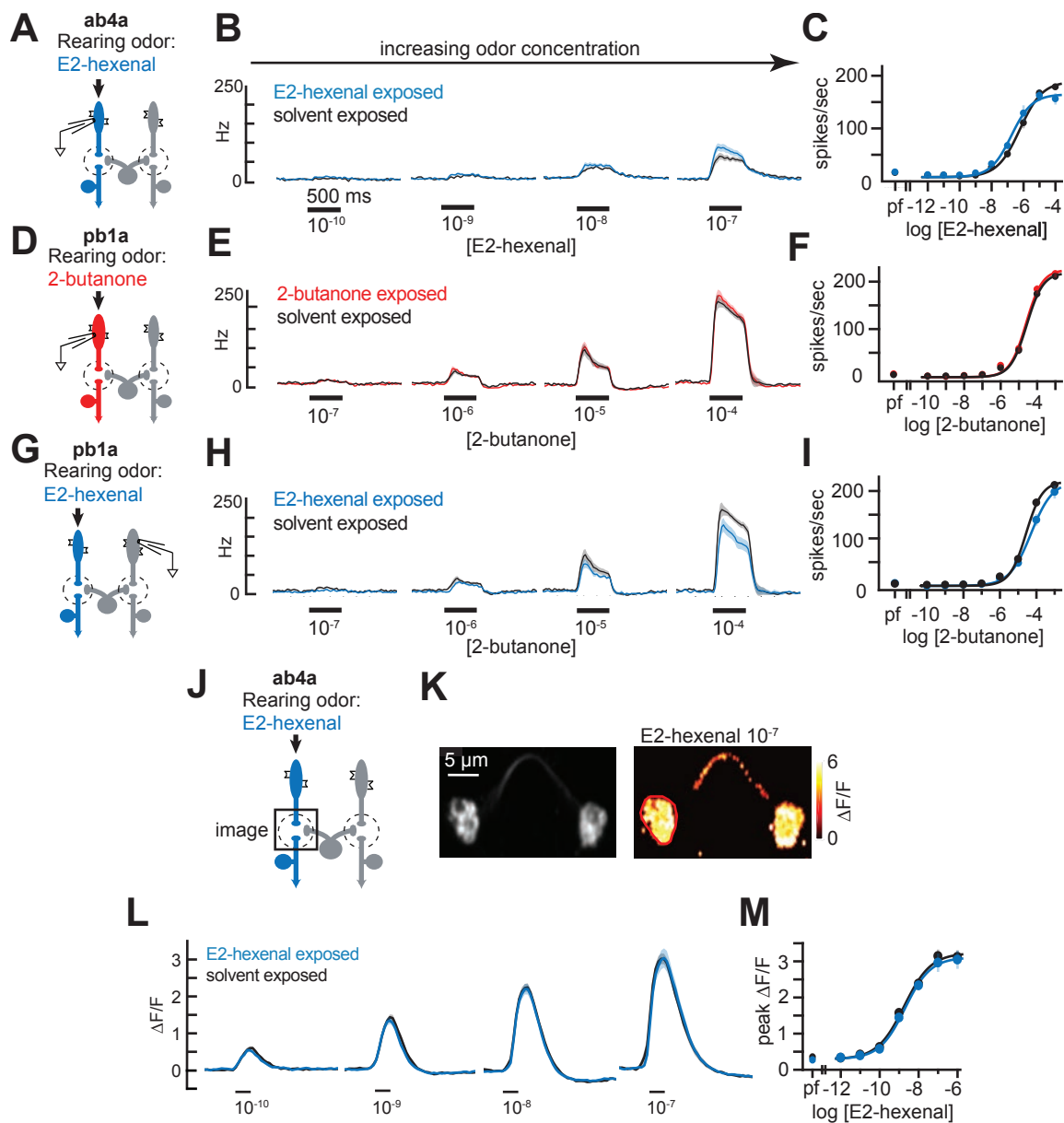


Figure 3.1: ORN responses do not explain the effects of rearing on PNs

A, D, G) Schematic of odor rearing conditions and targeted single-sensillar recordings (SSR) in trans-2-hexenal reared ab4a ORNs (a; blue), 2-butanone reared pb1a ORNs (d; red) and trans-2-hexenal reared pb1a ORNs (g; 2but). **B, E, H**) PSTH of odor-evoked spike rates in trans-2-hexenal reared ab4a (b), 2-butanone reared pb1a (e) and trans-2-hexenal reared pb1a (h) ORNs. **C, F, I**) Concentration series showing baseline-subtracted ORN responses computed during the 500ms of stimulus presentation for

trans-2-hexenal reared ab4a responses (c), 2-butanone reared pb1a (f) and trans-2-hexenal reared pb1a (i). The average paraffin oil (pf) response is plotted to the left. **J)** Schematic of direct odor rearing and imaging window. Or7a terminals, projecting into the DL5 glomerulus, were imaged. **K)** Left: Maximum intensity projection of imaging plane. Right: Delta F/F response to trans-2-hexenal 10^{-7} in a mock-reared fly. Scale bar 5 μ m. **L)** Average delta F/F responses of Or7a terminals after direct (blue) and mock (black) rearing conditions to trans-2-hexenal 10^{-10} , 10^{-9} , 10^{-8} and 10^{-7} . Scale bar 0.5 seconds. **M)** Average and SEM of peak delta F/F responses were computed during stimulus presentation. Paraffin is shown to the left, followed by responses to a concentration series of trans-2-hexenal.

We permuted ORN spike rates and calcium fluorescence 10,000 and quantified p-values by counting the ratio that the difference between permuted conditions are different than the actual means across all 10,000 shuffled samples. Significance thresholds were determined using a Bonferroni correction. The distributions we obtained are shown in Figure 3.2 for ab4a direct rearing (a), pb1a direct (a) and indirect rearing (c), and Or7a direct rearing (d). A quantification of baseline spike rates and distribution of permuted samples is provided in Figure 3.2A-C in the right panel. We note that we did not find any effect on spontaneous spike rate at the ORN. This is in contrast to the weak effect of trans-2-hexenal rearing on VM7 spontaneous activity (Figure 2.5G, H).

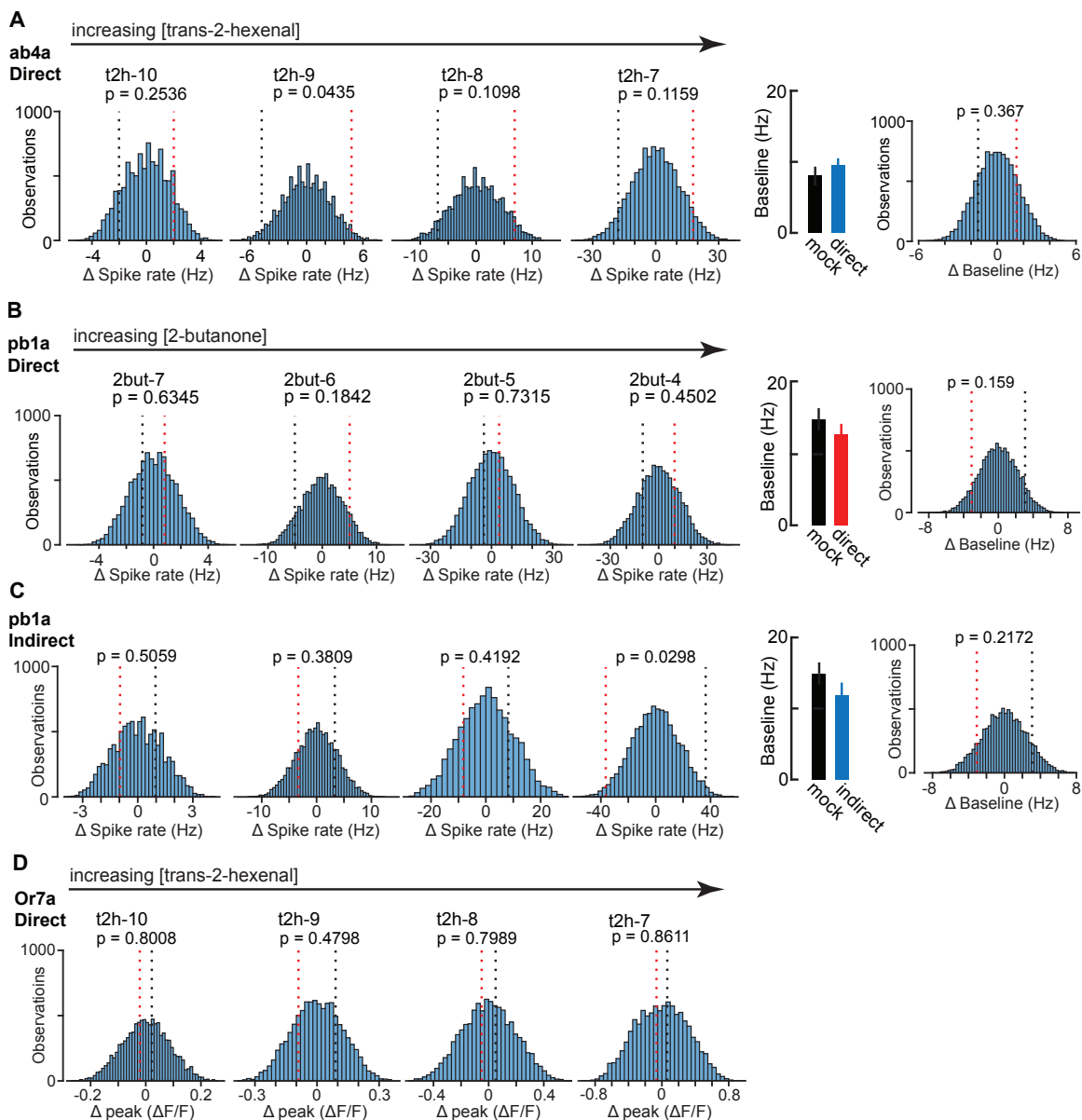


Figure 3.2: Statistical analysis of ORN spiking responses in direct and indirect rearing conditions

A-C) Left: Histogram of 10,000 permuted samples taken from average odor-evoked ORN spike rates. **Right:** Average baseline spiking activity was computed prior to odor stimulation across rearing conditions. Direct E2H-reared ab4a to trans-2-hexenal (a), direct 2-butanone reared pb1a to 2but (b) and trans-2-hexenal indirect pb1a to 2-butanone (c) are shown. **D)** Statistical analysis of delta F/F responses in Or7a ORN

axon terminals following direct trans-2-hexenal 10^{-7} rearing. All responses are shown to increasing concentrations of odor stimuli from left to right. Dotted lines indicate two-sided statistical threshold. Red lines are the actual differences between odor-reared and mock-reared responses. Threshold for statistical significance was $p < 0.0125$ for concentration series and $p < 0.05$ for baseline spike rates. Values are Bonferroni corrected. Bootstrap p-values are displayed in each histogram.

Next, we wondered if there was a change in the total amount of ORN neurites innervating the DL5 glomerulus following trans-2-hexenal exposure. A change in total ORN innervation may reflect changes in the total population of Or7a ORNs or an increase in innervation density from a conserved population of ORNs. One way to measure total ORN innervation is by quantifying the total baseline calcium fluorescence in Or7a>opGCaMP6f terminals. We used our existing 2-photon imaging data to extract the pre-stimulus baseline fluorescence responses of our data in trans-2-hexenal and solvent exposed Or7a terminals (Figure 3.3). We did not find any effects of odor exposure on Or7a baseline fluorescence.

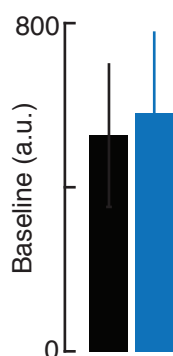


Figure 3.3: Baseline calcium fluorescence of Or7a>opGCaMP6f terminals in DL5

Baseline fluorescence (a.u.) is plotted for mock exposed (black) and trans-2-hexenal 10^{-7} exposed conditions. With our statistical analysis, we did not find that odor exposure had significant effects on baseline calcium fluorescence.

The role of central mechanisms in olfactory plasticity

We next investigated possible central mechanisms that might contribute to olfactory plasticity in the weak odor regime. First, we asked whether receiving increased sensory input might change the intrinsic excitability of PNs. Overall, the input resistance of PNs was unaltered in flies chronically exposed to any of the odors in our study, regardless of whether they were receiving direct or indirect chronic stimulation (Figure 2.2D, J, N). To measure f-I responses in PNs, it was necessary to remove the spontaneous activity in PNs to ensure our measurements were not impacted by presynaptic inputs arising from the ORNs (Figure 3.4A). Consistent with these observations, f-I curves directly evaluating the spiking response of deafferented DL5 PNs in response to current injection at the soma were similar between control and trans-2-hexenal exposed flies (Figure 3.4B, Figure 3.5A, B). These results indicate that the intrinsic excitability of PNs is unaltered by chronic odor exposure and does not account for the increase in PN responses to weak odors.

Next, we asked whether ORN-PN synaptic strength might be impacted by chronic odor exposure. In each glomerulus, many ORN axons of the same type synapse onto each PN, and each ORN communicates with each PN via multiple active zones (Kazama, H. and Wilson, R.I., 2008; Tobin, W.F., et al., 2017; Horne, J.A., et al., 2018). We refer to the combined action of all the neurotransmitter release sites between an ORN and a PN as the “ORN-PN synapse.” To measure the strength of a unitary synaptic connection between ab4a ORNs and DL5 PNs in trans-2-hexenal exposed flies, we adapted a previously established minimal stimulation protocol (Kazama, H. and Wilson, R.I., 2008) for use with an optogenetic-based method to recruit ORN activity. Presently, we are aware of one other study that uses a light-based optical method to recruit EPSCs in post-synaptic cells on a rodent model (Burke, K.J., et al., 2018). To our knowledge, we employ the first use of Chrimson to recruit light-evoked EPSCs in *Drosophila*. We placed the channelrhodopsin variant Chrimson under the control of the Or7a promoter, driving

its expression in all ab4a ORNs. Or7a>Chrimson flies were housed in light-proof bottles on ATR-supplemented food (Figure 3.3C). We acutely removed the antennae to eliminate spontaneous feedforward activity. Next, we stimulated ORNs using wide-field delivery of light through the imaging objective while monitoring synaptic responses in DL5 PNs using genetically targeted whole-cell voltage-clamp recordings (Figure 3.4D).

We employed a minimal stimulation protocol to isolate unitary excitatory postsynaptic currents (uEPSCs) evoked by a single presynaptic ORN spike. Stimulation with initially low levels of light elicited no synaptic response in the PN. As the power density was gradually increased, trials of mostly failures were interspersed with the abrupt appearance of an EPSC in an all-or-none manner. Further ramping the light in small increments had no effect on the amplitude of the EPSC in the PN, until a power density was reached where the EPSC amplitude abruptly doubled, as compared to the amplitude of the initially recruited EPSC (Figure 3.4E). Light-evoked EPSCs were entirely dependent on supplying flies with the rhodopsin chromophore all trans-retinal in their food. The step-like profile of EPSC amplitudes as a function of power density reflects the discrete recruitment of individual ORN axon fibers with increasing stimulation. In particular, the sharp transition from mostly failures to a reliably evoked current is consistent with the response stemming from the activation of a single ORN input. The time from the onset of light stimulation to the onset of the evoked EPSC was variable and averaged around ~22 ms (Figure 3.5C), which was similar to the properties of the latency to the recruitment of the first ORN spike at comparable light intensities (Jeanne, J.M. and Wilson, R.I., 2015). In order to compare response amplitudes and kinetics across different trials, individual uEPSCs from each condition were aligned by their peaks and averaged. In control flies, DL5 uEPSC amplitude (~40 pA) and kinetics were similar to previous measurements made using conventional electrical stimulation of the antennal nerve (Kazama, H. and Wilson, R.I. 2008). We used these methods to record uEPSCs from DL5 PNs in flies chronically exposed to either solvent or trans-2-

hexenal, which drives direct activity in DL5. Average DL5 uEPSC amplitudes and response kinetics were indistinguishable in flies solvent and trans-2-hexenal exposed flies (Figure 3.4F). Thus, ORN-PN strength appeared unchanged by chronic odor exposure, and is unlikely to account for the observed increases in DL5 PN responses to weak odors.

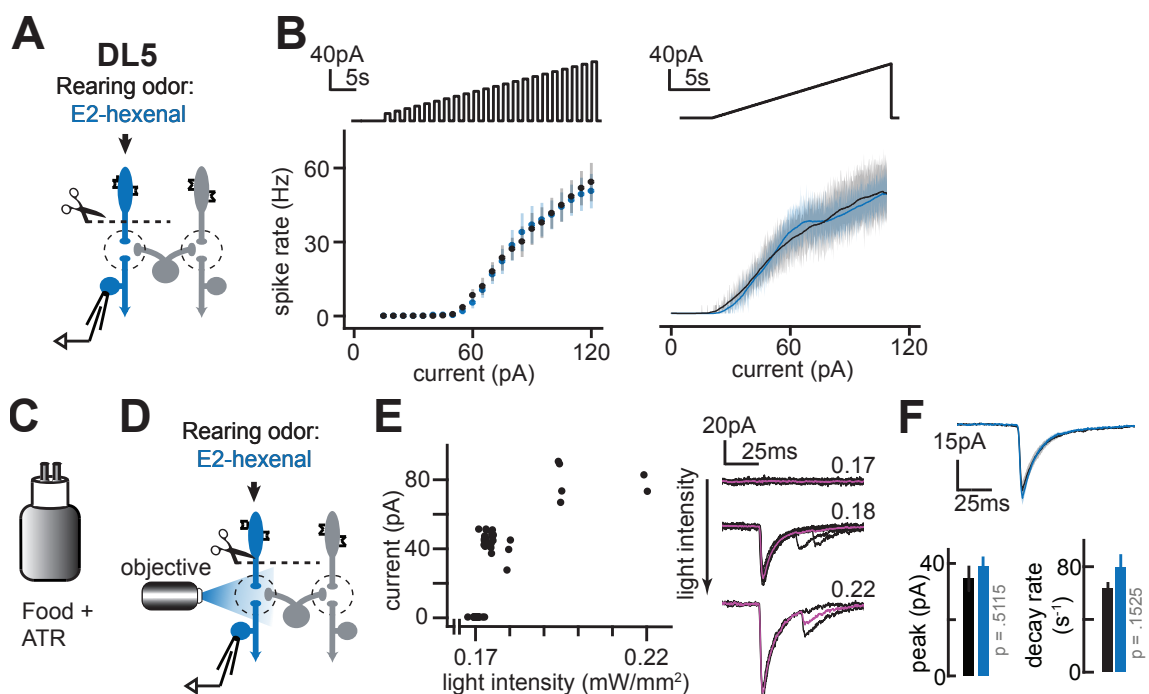


Figure 3.4: Cellular and synaptic effects following direct rearing

A) Flies were reared directly in trans-2-hexenal to target DL5 glomeruli or mock as before. Prior to recording, the antennal nerve was severed to silence spontaneous activity in the antennal PNs. **B)** Spike rates were measured in response to current injection step (left) and ramp (right) protocols. For current step response, spike rates were quantified as the total spike count per 100ms current step. For ramp response, spike rates were quantified in 50ms bins with 25ms overlap. **C)** Flies expressing Chrimson in Or7a ORNs were raised in foil-wrapped, light-proof bottles on standard medium. ATR was mixed into food for control and odor-reared experiments prior to rearing. **D)** Schematic of direct odor rearing in trans-2-hexenal 10^{-7} (blue). The antennal

nerve was severed, and DL5 PNs were targeted for patch-clamp recordings. Blue light was passed through a 40X objective to stimulate Or7a terminals and recruit uEPSCs on post-synaptic DL5 PNs. **E)** Left: EPSC current amplitude is plotted versus light intensity. Right: As light intensity is increased, light-evoked EPSCs show a doubling in current amplitude. **F)** Top: Average EPSC after direct rearing in E2H (blue) and mock (black). Bottom right: Average EPSC peak (pA). Bottom left: Average decay rate (s^{-1}). Bootstrap p-values are shown in gray.

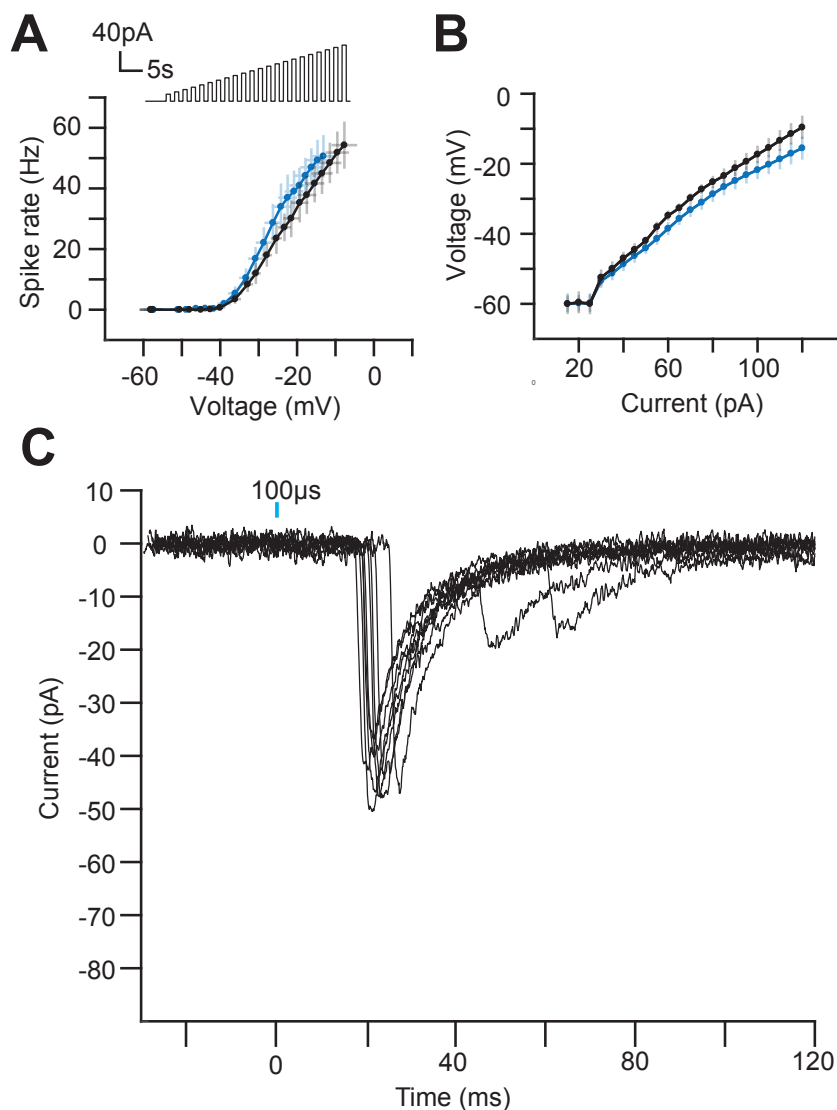


Figure 3.5: Supplement to Cellular and synaptic mechanisms following rearing

A-B) Spike rate versus voltage (a) and voltage versus current (b) responses plotted in direct E2H-reared DL5 PNs to a step current injection protocol. **C)** Raw, unaligned EPSC responses in mock-reared DL5 PNs in response to light-evoked Chrimson activation. A 100 μ s light pulse (to scale) was used to stimulate Or7a terminals and recruit unitary EPSCs in cognate DL5 PNs.

In order to compare uEPSC kinetics, we fit each uEPSC with an exponential model. We computed the average time constant by extracting the minimum peak to the steady state response of the data and fitting the traces using the following equation: $A \times e^{(-Bx)}$, where A has units of pA and B seconds. Overlaid raw data and model fits are shown below in Figure 3.5. We show mock exposed uEPSC (Figure 32.6A) and trans-2-hexenal exposed uEPSC (Figure 3.6B) with fits.

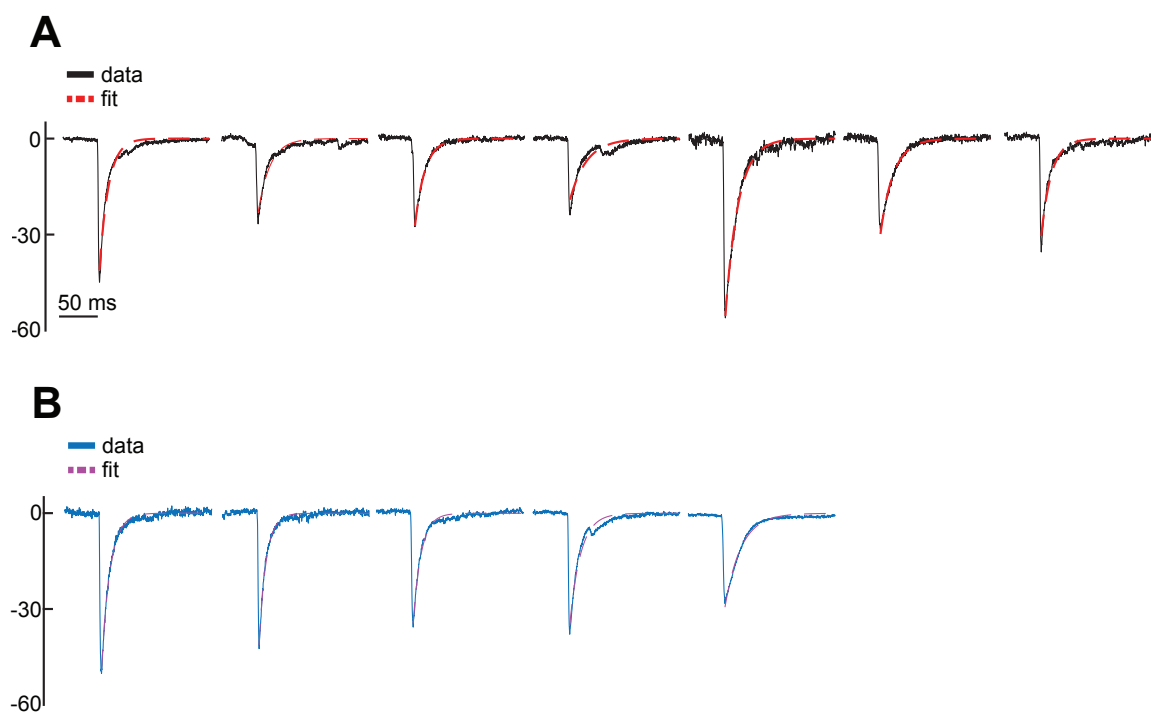


Figure 3.6: Raw uEPSCs and exponential model fit overlay

A-B) Average EPSCs for data recorded from individual flies are plotted for mock (a; black) and trans-2-hexenal (b; blue) exposure conditions. Data are fit with an exponential model to compare decay rates between rearing conditions. Exponential fits are plotted for mock (a; red dash) and trans-2-hexenal (b; purple dash) conditions.

ORN-PN transforms after direct odor rearing using known models

Given that DL5 PN responses were heightened at low odor concentrations while Or7a responses were unchanged, we hypothesized that the PNs were boosting weak ORN inputs. We reasoned that there may be a change in the ORN-PN transform function that may reflect an increase in input gain control at the PN. Thus, we wanted to determine whether the ORN-PN transform is altered in response to rearing and compare the effects across glomeruli. To investigate this, we utilized a known framework to observe the input-output function arising between ORN and PN synapses. Following the formulation described in Olsen et al., we applied the input gain control model (Eq. 2), a variation of the hyperbolic ratio function, to the ORN-PN transform data of Or7a and DL5 responses after rearing in paraffin and trans-2-hexenal. While we find that there is a slight boost in PN responses at the low end, this effect is not captured by the Olsen model (Figure 3.4A). We repeated the same process, but this time for pb1a and VM7 responses following direct and indirect odor exposure conditions. We see that the ORN-PN transform does not capture differences in the PN responses for VM7 either (Figure 3.7A, B) as we see when analyzing the PN concentration curves alone (Figure 2.4A-C). DL5 PN responses are changed at low concentrations, and the transform model does not capture the small amplification in the data arising at the PN. In VM7, we see small change in the saturation region of the PN (Figure 3.7B). This observation suggests that direct rearing in 2-butanone may change the ORN-PN transform and the effect may be described by a change in the saturation region via a response gain model. Overall, the effects of rearing are best captured by looking at the PN concentration curves and PSTHs (Figures 2.1 & 2.4).

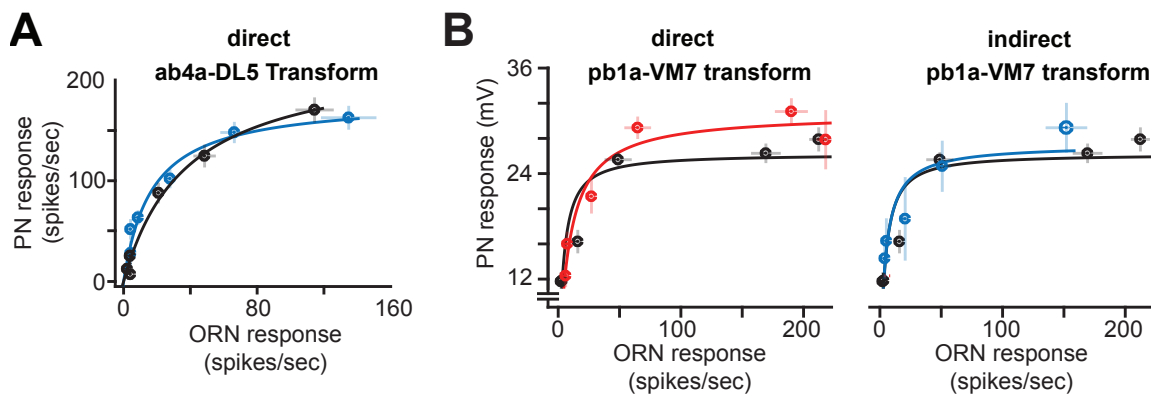


Figure 3.7: ORN-PN transforms in direct and indirect rearing conditions

A) ORN-PN transforms for (a) ab4a-DL5 responses after direct rearing in trans-2-hexenal (blue) and mock rearing in solvent (black). **B)** ORN-PN transforms for pb1a-VM7 responses. Left: Direct odor rearing in 2-butanone 10^{-4} (red) and mock rearing (black). Right: Indirect odor rearing in trans-2-hexenal 10^{-7} (blue) and mock rearing (black). ORN and PN responses are quantified as the average odor-evoked spike rates during the 500ms odor stimulation. ab4a-DL5 responses are plotted to trans-2-hexenal 10^{-11} , 10^{-10} , 10^{-9} , 10^{-8} , 10^{-7} and 10^{-6} . pb1a-VM7 responses are plotted to 2-butanone 10^{-8} , 10^{-7} , 10^{-6} , 10^{-5} , 10^{-4} and 10^{-3} .

Discussion

In this chapter, we investigated potential presynaptic and cell intrinsic mechanisms that may explain the effects of odor exposure on PNs. This chapter represents several experiments we performed to characterize the inputs arising into PNs with high resolution. Our analysis confirms that the effect of odor exposure on PNs is not explained by changes in peripheral odor responses or in ORN-PN synaptic strength. It is possible that network level activity may be responsible for the effects we see on PNs, and we investigate different circuit mechanisms in Chapter 4.

Overall, our results suggests that ORN responses may be robust and resistant to plasticity following our odor-exposure paradigm. Our observation complements prior work in olfactory plasticity that report a consistent total ORN number or ORN glomerular innervation between odor rearing and control flies (Sachse, S., et al., 2007). Other studies reported effects of rearing on ORNs both at a physiological (Iyengar, A., et al., 2010) and anatomical (Golovin, R.M., et al., 2019) level. The discrepancies among the different bodies of work may be due to the difference in exposure paradigms, monomolecular odors and odor concentrations used. It is possible that chronically exposing flies to high concentrations of specific chemical compounds can be toxic. Odorants may enter through the lymph and disrupt internal homeostasis or the olfactory receptor itself may be damaged. For example, CO₂ influences spiracle dilation on the *Drosophila* thorax, and increasing CO₂ concentrations can result in *Drosophila* desiccation due to the heightened need for oxygen (Badre, N.H., et al., 2005; Wigglesworth, V.B. 1942). We propose that chronically exposing flies to monomolecular odorants at naturalistic concentrations does not change ORN spiking responses. Future work may seek to understand whether our observations generalize across a diversity of chemical classes.

In our experiments, we developed a novel method to recruit uEPSCs in post-synaptic neurons while performing GFP-guided whole-cell patch-clamp physiology.

Unlike traditional nerve stimulation experiments where all ORN fibers are activated near the vicinity of the stimulation electrode, our light stimulation method allows for a single population of ORN fibers to be activated. This technique can be combined with any gene expression methods including Gal4/UAS, *lexA/lexAop*, and QF/QUAS systems. Our method has a few benefits over conventional nerve shock experiments. Experimenters needing to record EPSCs from PNs receiving inputs from the palp cannot use nerve shock because the maxillary nerve is located deep within the head capsule. It is possible to overcome this challenge by expressing light-sensitive opsins in palp ORNs and using wide-field light to activate release from terminals. Additionally, it is possible to identify unlabeled PNs in patch-clamp recordings by determining whether light stimulation from a defined population of ORNs recruits activity.

We confirm that the shape of recruited uEPSCs is consistent with those of prior published works using conventional nerve shock in *Drosophila* (Kazama, H., and Wilson, R.I., 2008). Our results suggest that rearing does not alter the amplitude or the kinetics of uEPSCs in DL5 PNs. It is important to note that the variance in EPSC amplitude across populations is high (Kazama, H., and Wilson, R.I., 2008), and it is possible that we are unable to resolve effects of rearing from the noise. We conclude that the EPSC is unchanged in response to odor exposure. We acknowledge that current methods cannot resolve effects, and it is possible synaptic strength may be affected after rearing.

Methods

Flies

Single-sensillar recordings were performed in NP3481-Gal4, UAS-CD8-GFP female flies. Unitary EPSC experiments were conducted in NP3481-Gal4, UAS-CD8-GFP; 13X-IVS-lexAop2-Cs-Chrimson.mVenus/+; Or7a-lexA/+ (see also Chapter 5 Methods). For calcium imaging of ORN terminals, we used *Or7a-KI-Gal4/+*; *20XUAS-IVS-Syn21-OpGCaMP6f-p10/+*.

Histology and confocal imaging

Histology and confocal imaging was performed as previously described in Chapter 2.

Odor stimulation

Odors were diluted w/w in paraffin oil to a final concentration of 10^{-2} . A broad panel of odorants were used to activate the palp including isobutyl acetate, pentyl acetate, p-cresol, trans-2-hexenal, 2-butanone and 2-heptanone. We presented a paraffin solvent to flies in mock and odor rearing conditions. Odors were presented via a custom olfactometer and presented for 500 ms as described in Chapter 2. Odorants were purchased from Sigma or Fischer Scientific in the highest purity available.

Light-activated EPSC recruitment

EPSCs were isolated using light stimulation for the first time to our knowledge in flies. All fly crosses containing the Chrimson reporter were wrapped in foil to prevent any chance of light-activation. For light-activation experiments, flies were fed food supplemented with a mixture of all trans-retinal (ATR; Sigma #R2500) at least 24 hours prior to recordings. A 35mM ATR stock was prepared in 95% ethanol, wrapped in foil and stored in the dark at -20°C . We supplemented 50mL of food with 500uL of ATR once at the start of rearing

and kept fly bottles wrapped in foil for the duration of rearing. ATR was added to both odor and mock reared bottles.

Flies were dissected to expose the antennal lobe and both antennal nerves were severed. Electrophysiology rigs were light-proofed, and patch-clamp recordings were performed in voltage-clamp mode. We used wide-field blue light stimulation using a 460nm light source (Sutter TLED+) to selectively stimulate ORN terminals to recruit unitary EPSCs (uEPSCs) directly into DL5. This method has several advantages over conventional nerve shock techniques. Because we sever the antennal nerve to isolate uEPSCs, we lose our ability to identify cell identity using an odor panel. Genetically expressing Chrimson in Or7a ORNs allows us to minimize uncertainty in experimental recordings by recording from PNs that only show light-evoked responses. In addition, this method will allow future recordings of uEPSCs in the maxillary palp. In an intact fly prep, it is challenging to find the maxillary nerve for nerve stimulation. Using light would bypass this issue and allow for easy accessibility to the terminals of maxillary palp ORNs. We tested several methods of optical stimulation and found that wide field blue light worked best. When we used optrodes for pilot experiments, we found that light was highly sensitive to the optrode position relative to the antennal nerve. In effect, there was large variability in the required stimulus pulse length needed to successfully stimulate ORN terminals. In all experiments with wide-field stimulation, we maintained a 100us pulse length and adjusted the total light intensity across flies to recruit single or double uEPSCs when necessary.

Single-sensillar recordings

Single-sensillar recordings were performed as previously described. Flies were positioned at the end of a cut pipette tip and stabilized with wax. The antennae or palp were stabilized on a glass coverslip with a glass pipette controlled by a micro-manipulator (Scientifica). Flies were coarsely adjusted under a 5X objective, then finely

adjusted under a 50X air objective (Olympus). Ground and recording electrodes were filled with saline and flicked to remove any air bubbles. We carefully inserted ground electrodes into the eye. A sharp recording pipette was inserted into sensilla, and sensillar identity was confirmed using diagnostic odor panels. We used fluorescence-guided SSR in pilot experiments to learn the morphology and anatomical location of our target sensilla (Lin, C.C. and Potter, C.J., 2015).

Calcium imaging

We performed calcium imaging using a 2-photon microscope (Thor Labs) with a Ti-Sapphire laser through a 20X water objective (Olympus). Images were acquired at 11 frames per second with frame size of 256x96 pixels and a dwell time of 2 μ s/pixel. Frames were aligned to stimulus commands in Thor Sync software. We collected 8 seconds of baseline activity prior to presenting a 0.5 second odor pulse for a total trial length of 15 seconds. Odors were presented for 3 trials, with 45 second inter-trial-interval during which the shutter was closed to prevent bleaching of the sample.

Analysis of calcium imaging data

Each frame was first background subtracted to the mean fluorescence of an ROI drawn outside of the neuropil. Odor was presented at frame 93 for a total of 6 frames. We extracted 70 frames before the start of each trial and 60 frames post-odor presentation for analysis. Baseline fluorescence responses were computed as the average pixel intensity across the first 70 frames prior to odor presentation for each trial, and then subtracted frame-by-frame. We computed delta F/F values by normalizing the background-subtracted signal by the average pre-stimulus background and averaged across trials for each stimulus. Peak fluorescence was computed by finding the maximum of the delta F/F during stimulus presentation. Heat-maps were generated

using the same methods as described above. We chose representative heat-maps by identifying the maximum intensity projection taken across the entire recording (ImageJ).

References

- Badre, N.H., Martin, M.E., and Cooper, R.L. (2005). The physiological and behavioral effects of carbon dioxide on *Drosophila melanogaster* larvae. *Comp. Biochem. Physiol. A Mol. Integr. Physiol.* *140*, 363-76.
- Burke, K.J. Jr., Keeshen, C.M., and Bender, K.J. (2018). Two Forms of Synaptic Depression Produced by Differential Neuromodulation of Presynaptic Calcium Channels. *Neuron* *99*, 969-984.
- Horne, J.A., Langille, C., McLin, S., Wiederman, M., Lu, Z., Xu, C.S., Plaza, S.M., Scheffer, L.K., Hess, H.F., and Meinertzhagen, I.A. (2018). A resource for the *Drosophila* antennal lobe provided by the connectome of glomerulus VA1v. *Elife* *7*.
- Iyengar, A., Chakraborty, T.S., Goswami, S. P., Wu, C., and Siddiqi, O. (2010). Post-eclosion odor experience modifies olfactory receptor neuron coding in *Drosophila*. *Proc Natl Acad Sci* *107*, 9855-60.
- Jeanne, J.M. and Wilson, R.I. (2015). Convergence, Divergence, and Reconvergence in a Feedforward Network Improves Neural Speed and Accuracy. *Neuron* *88*, 1014-1026.
- Kazama, H. and Wilson, R.I. (2008). Homeostatic matching and nonlinear amplification at identified central synapses. *Neuron* *58*, 401-13.
- Lin, C.C. and Potter, C.J. (2015). Re-Classification of *Drosophila melanogaster* Trichoid and Intermediate Sensilla Using Fluorescence-Guided Single Sensillum Recording. *PLoS One* *10*.

Olsen, S.R., Bhandawat, V., and Wilson, R.I. (2010). Divisive normalization in olfactory population codes. *Neuron* 66, 287-99

Sachse, S., Rueckert, E., Keller, A., Okada, R., Tanaka, N.K., Ito, K., and Vosshall, L.B. (2007). Activity-dependent plasticity in an olfactory circuit. *Neuron* 56, 838-50.

Tobin, W.F., Wilson, R.I., and Lee, W.C.A. (2017). Wiring variations that enable and constrain neural computation in a sensory microcircuit. *Elife* 6.

Wigglesworth, V.B. (1942). *The Principles of insect physiology*. 2nd ed. London, Methuen & Co. LTD.

Chapter 4: Network-level effects after rearing

Abstract

In Chapters 2-3, we investigated the effects of rearing on PNs in the antennal lobe. PNs receive direct feedforward inputs from cognate ORNs that project into the same glomerulus. While ORNs are a main source of excitation onto PNs, additional circuit-level inputs are important components to PN odor responses. Lateral inhibition and lateral excitation is broadly signaled across the antennal lobe. Promiscuous odors are particularly strong activators of lateral inputs, and these inputs are understood to innervate the antennal lobe glomeruli globally. To determine whether rearing affects lateral inputs, we measure lateral inhibition and lateral excitation within the antennal lobe. We use a genetic strategy to label most of the GABAergic antennal lobe inhibitory local neurons (iLNs) and perform confocal fluorescence microscopy to quantify innervation density across a subset of antennal lobe glomeruli. We find that trans-2-hexenal rearing induced an increase in iLN innervation density while 2-butanone rearing had no effect. The effect of increased iLN innervation density was driven by a change in the volume of antennal lobe glomeruli while the raw iLN fluorescence was unchanged.

Next, we wondered if the effects of trans-2-hexenal can be explained by changes in lateral excitatory inputs in the antennal lobe. We reared flies in trans-2-hexenal and recorded from VA6 PNs in a severed-nerve preparation. By removing direct excitation from the feedforward ORNs, any remaining excitation in the VA6 glomerulus is a result of lateral inputs. We find that odor-evoked membrane depolarization is increased in trans-2-hexenal exposed VA6 PNs. This finding suggests that trans-2-hexenal exposure may increase lateral excitatory inputs into some olfactory glomeruli. All in all, these findings suggest that trans-2-hexenal may influence physiology and anatomy of global antennal lobe networks.

Introduction

Each individual glomerulus in the *Drosophila* antennal lobe receives direct excitation from feedforward ORNs that synapse onto PNs. ORNs typically increase in firing rates as odor concentrations increase, whereas PN responses appear to saturate (Wilson, R.I., 2013). Global circuit mechanisms help shape the PN output arising in response to ORN input. A major computational component within antennal lobe glomeruli involves inhibition via pre- and post-synaptic local neurons (LNs) (Olsen, S.R. and Wilson, R.I., 2008). LNs act as a turn-dial volume control within the antennal lobe by maintaining a homeostatic balance of odor outputs from the antennal lobe. Typically, the more ORNs that an odor activates, the more LNs also become activated (Hong, E.J. and Wilson, R.I., 2015). In effect, the inhibitory inputs prevent synapse depletion between ORNs and PNs and normalize PN responses to odor. Inhibition innervates glomeruli globally and appears to have uniform physiological inputs across the antennal lobe. While the population of inhibitory LNs (iLNs) is heterogenous, the majority of the population signals via GABAergic neurotransmission. Thus, each glomerulus is a complex bundle of fibers containing ORN terminals, LN terminals and PN dendrites.

Lateral inhibition is recruited by broad odors which typically activate several populations of ORNs simultaneously. In nature, flies rarely encounter monomolecular odors as we present in the lab. Instead, natural odors are present as complex mixtures containing dozens of monomolecular odors. An odor that we associate as a single entity, i.e. a ripe banana, contains several odorants that smell like the characteristic fruit when combined together. One way to mimic natural odorants in the lab is to present a mixture of monomolecular odorants to flies while recording odor responses. Mixing fixed compounds allows for experiments to be comparable across days and gives the experimenter control of the concentrations of each odorant. In this chapter, we present odor mixtures and record from VM7 PNs following rearing. While we found that rearing can alter responses to monomolecular compounds in Chapter 2, our goal in this chapter

is to determine if rearing alters PN responses to more naturalistic stimuli.

Aside from iLN input, the antennal lobe also contains a population of lateral excitatory neurons (eLNs) which broadly innervate glomeruli. Like iLNs, eLNs appear to broadly respond to odors. Direct excitation from feedforward ORNs is the dominant source of excitation that forms PN odor responses. Lateral excitation becomes noticeable when these inputs are disrupted (Yaksi, E. and Wilson, R.I., 2010); yet, it has never been reported to depolarize the cell membrane towards spike threshold. While the purpose of lateral excitation is unclear, it may serve as a back-up system to ensure all channels receive some form of excitation. Interestingly, lateral excitation is mediated via electrical rather than chemical synapses. More work needs to be done to understand the computational roles of lateral excitation and how these populations of neurons are affected across perturbations to the circuitry. We were drawn to investigate features of lateral excitation following our rearing paradigms because of the magnitude of our effects. Specifically, we wondered if lateral excitatory inputs are capable of undergoing plasticity in response to chronic odor exposure.

Chronic odor exposure can elicit global perturbation in glomerular volume

Our observations suggested that lateral connectivity may be important for the effects of chronic odor exposure on PN responses, and prior work had implicated local GABAergic inhibition in olfactory plasticity (Sachse, S., et al., 2007). Therefore, we next examined whether LN innervation density is impacted by chronic odor exposure. We expressed membrane-targeted GFP (CD8:GFP) under the control of the NP3056-Gal4 driver, which targets a large subset of GABAergic LNs, and exposed these flies for two days to trans-2-hexenal, 2-butanone, or solvent as described. The labeled LNs were reconstructed by volumetric confocal imaging, and the 3D boundaries of each of a subset of easily identifiable glomeruli were manually segmented in each brain using a

neuropil co-stain (nc82) (Figure 4.1A). In order to determine if rearing results in any anatomical changes across the antennal lobe, we focused on quantifying glomerular volume after trans-2-hexenal and 2-butanone odor exposure (Figure 4.1B). In addition, we characterized LN innervation density by measuring raw fluorescence and normalizing by each glomerular volume (Figure 4.1C). We found that trans-2-hexenal rearing resulted in a global decrease in LN fluorescence intensity.

As expected, identified glomeruli of the same type had a characteristic size that was consistent across brains within a condition (Figure 4.1B). Across the glomeruli in our subset, glomerular volumes varied as much as ~5 to 6-fold. We found that glomeruli in flies chronically exposed to trans-2-hexenal were smaller than their counterparts in control solvent-exposed flies. This downward trend was relatively consistent across all glomeruli measured; DL5, the glomerulus that receives direct input from trans-2-hexenal (10^{-7}), was not notably different. We pooled our measurements across glomeruli by computing the normalized volume of each glomerulus in the odor-reared condition, relative to its average in the control group. We found that the average glomerular volume in trans-2-hexenal exposed flies was smaller than that of control flies (Figure 4.1B). We then quantified the amount of LN neurites (CD8:GFP) in each glomerulus using the 3D ROI generated from the neuropil co-stain. Whereas the absolute level of LN signal was similar between trans-2-hexenal and control exposed flies, the overall density of LN innervation in each glomerulus was higher in trans-2-hexenal exposed flies, driven by the reduction in glomerular volume (Figure 4.1C). These effects were specific to trans-2-hexenal exposure. Flies chronically exposed in parallel to 2-butanone showed no significant changes in either glomerular volume or in LN density, including in glomerulus VM7, which receives direct input from 2-butanone (10^{-4}) (Figure 4.1B, C). These results show that chronic exposure to some, but not all, odors can elicit widespread anatomical perturbations in the olfactory circuit. In contrast with previous reports, however, these

effects are not glomeruli-specific and extend globally beyond the chronically activated glomerulus (Sachse, S., et al., 2007; Kidd, S., et al., 2015; Golovin, R.M., et al., 2019).

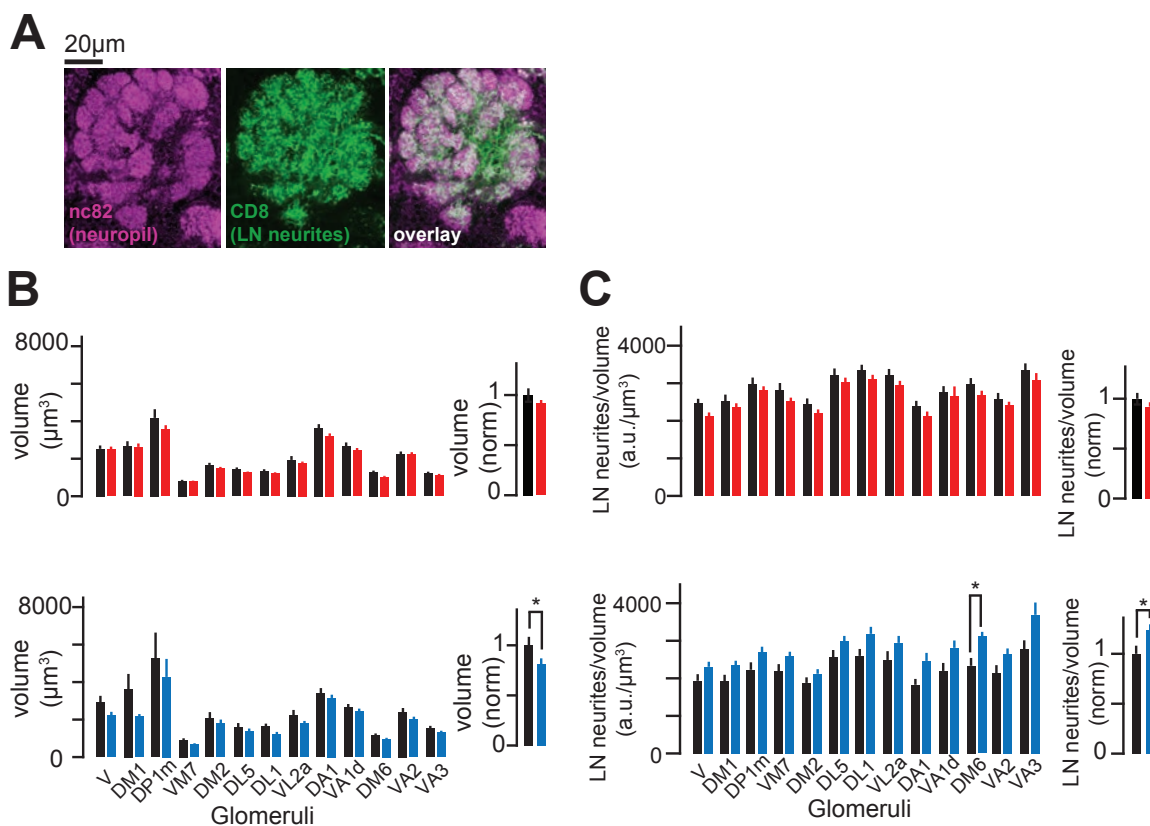


Figure 4.1: Anatomical characterization of rearing effects in the antennal lobe

A) Sample section of neuropil (magenta), LN neurites (green) and expression overlay (white) in the antennal lobe. Scale bar 20µm. **B)** Left: Volume measured for 13 antennal lobe glomeruli in 2but (red; top), E2H (blue; bottom) and mock (black) reared flies. Right: Total normalized volume. **C)** Left: LN neurite density in 2but (red; top) and E2H (blue; bottom) reared flies. Right: Total normalized LN density across rearing conditions.

In addition to glomerular volume and LN density, we quantified raw LN fluorescence intensity (Figure 4.2A, B), neuropil intensity (Figure 4.2C, D), LN intensity per neuropil (Figure 4.2E, F) and neuropil density (Figure 4.2G, H) as supplemental analyses. Following trans-2-hexenal rearing, we did not see any effect on any additional metrics (Figure 4.2A, C, E, G). We note that 2-butanone rearing resulted in a significant decrease in the total LN neurite intensity (Figure 4.2B) which is also significantly decreased for the glomerulus DM6. This result suggests that the total LN innervation may be scaling proportionally to volume (Figure 4.1B) and fixed LN innervation density may be maintained between 2-butanone rearing and mock rearing conditions (Figure 4.1C, Figure 4.2F). It is possible that the effects on anatomy may have a significant signaling contribution on the cellular and circuit level. We next wanted to determine whether there are physiological consequences of an increase in LN density following trans-2-hexenal rearing or LN intensity following 2-butanone rearing by activating the iLN population with our stimulus set.

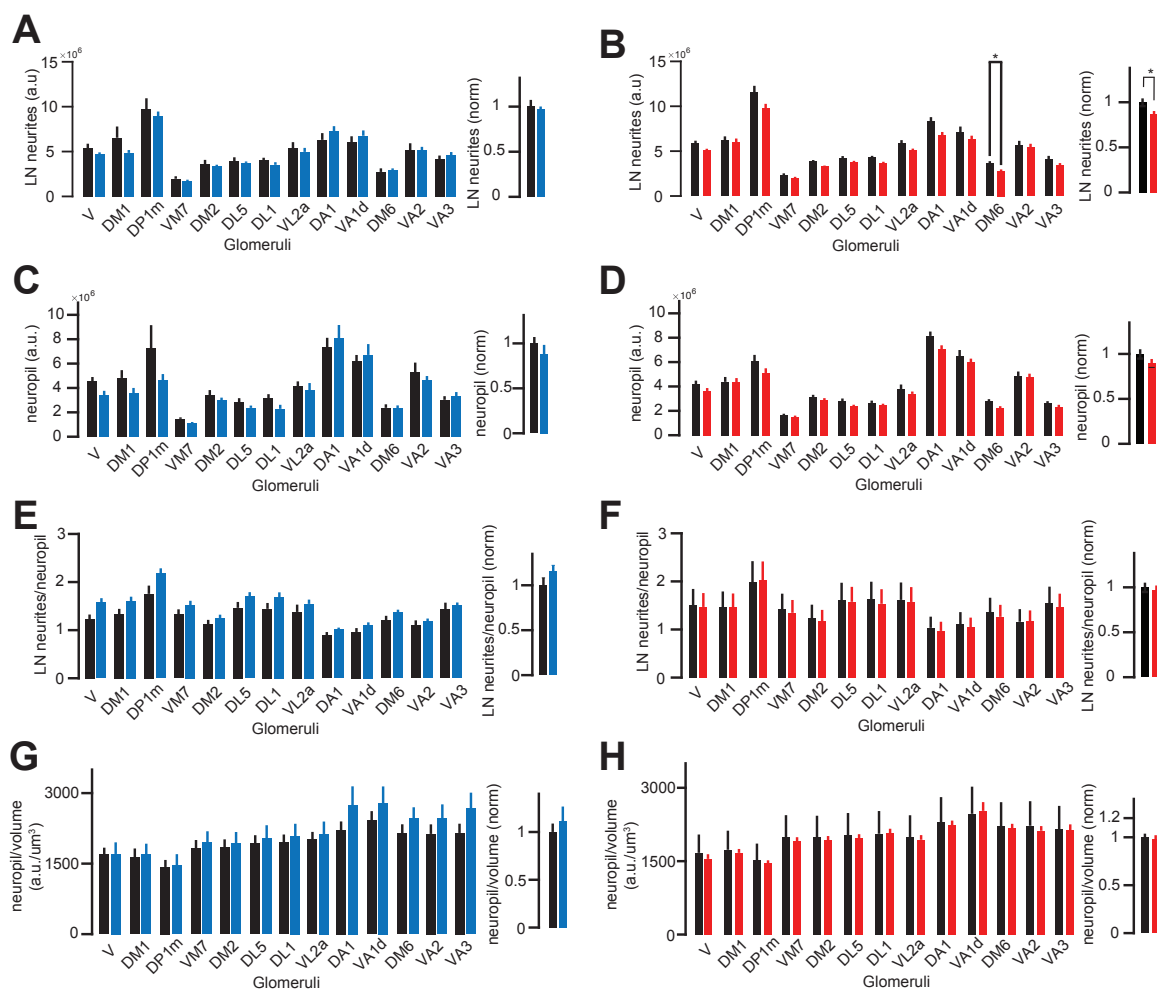


Figure 4.2: Additional data on antennal lobe anatomy

A, B) Left: Raw LN neurite intensity across 13 glomeruli following rearing in trans-2-hexenal 10⁻⁷ (a; blue) and 2-butanone 10⁻⁴ (b; red) with mock reared control glomeruli (black). Right: Normalized total LN neurites summed across glomeruli. **C, D)** Left: Raw nc82 intensity following trans-2-hexenal 10⁻⁷ (c) and 2-butanone 10⁻⁴ (d) rearing. Right: Normalized total nc82 intensity summed across AL glomeruli. **E, F)** Left: LN neurite intensity normalized to nc82 following trans-2-hexenal 10⁻⁷ (e) and 2-butanone 10⁻⁴ (f) rearing. Right: Normalized total LN neurite intensity per neuropil intensity summed across AL glomeruli. **G, H)** Left: nc82 normalized to antennal lobe volume following trans-2-hexenal 10⁻⁷ (g) and 2-butanone 10⁻⁴ (h) rearing. Right: Normalized total neuropil density summed across AL glomeruli.

PN coding of odor mixtures is unaffected by chronic odor exposure

So far we have evaluated PN responses using only atypical odor stimuli, specifically chosen to provide selective input to a single ORN class. We started with this approach so that the source of ORN input with respect to each PN type is unambiguous. However, typical odors activate multiple odorant receptor neuron classes, and the odor response in each PN usually reflects both direct input, from its presynaptic ORN partners, and indirect input, arising from activity in other glomeruli and received via local lateral circuitry. Thus, we next investigated how chronic odor exposure impacts PN responses to more typical odor stimuli that elicit direct and indirect synaptic input to PNs. Additionally, we wondered what the physiological consequences of a decrease in LN innervation are. In all of the physiological experiments we have thus far shown, we measured responses of individual cells to highly selective monomolecular odorants. In this set of experiments, we chose to focus on VM7 because this PN has previously been shown to be suppressed by the broad odorant, pentyl acetate (Olsen, S.R. et al., 2010). We then tested whether direct and indirect odor rearing has an effect on VM7 responses to blends of pentyl acetate and the selective odor, 2-butanone.

As before, we recorded from VM7 PNs in flies chronically exposed to trans-2-hexenal, 2-butanone, or solvent (Figure 4.3A-C, F, I). We mixed a fixed concentration of pentyl acetate (10^{-3}), a broadly activating odor that drives activity in many ORN types (but does not activate pb1a, the VM7 ORN), with increasing concentrations of 2-butanone, the odor that drives direct input to VM7 (Olsen, S.R., et al., 2010). As previously described, mixing in pentyl acetate generally reduced VM7 responses to its direct odor 2-butanone (Figure 4.3A-C), a consequence of the recruitment of lateral GABAergic inhibition onto VM7, driven by activity in non-VM7 ORNs (Olsen, S.R. and Wilson, R.I., 2008; Olsen, S.R., et al., 2010). Each rearing paradigm is plotted with responses to pure monomolecular odor, 2-butanone (solid line), and odor mixtures

(dashed line) overlaid. Mixtures of pentyl acetate and 2-butanone result in a reduction in odor-evoked membrane potential to dilute concentrations of 2-butanone, particularly at a concentration of 10^{-8} (Figure 4.3A-C). This suggests that the feedforward direct excitatory input onto VM7 is fairly strong and counteracts the effects of inhibition from concentrations of 10^{-7} to 10^{-4} (Figure 4.3A-C). We quantify the change in depolarization between pure odor responses and mixture responses for mock, 2-butanone and trans-2-hexenal rearing conditions (Figure 4.3D, E). Overall, there is no difference between the total suppression in response magnitude across rearing conditions. We find that the difference between response magnitudes shows an effect at 2-butanone 10^{-4} , and this is driven by the observation that 2-butanone rearing enhances the odor-evoked amplitude to the pure odor (Figure 4.3D, Figure 2.2H, I).

When we plot the same data but compare mixture responses across rearing conditions (Figure 4.3F, I), we see that there are no differences to any stimulus (Figure 3.3G, H, J, K). This result suggests that odor mixtures normalize responses and abolish any changes that result from direct feedforward excitation. Whereas we observed that the afterhyperpolarization responses of VM7 PNs to pure direct input (driven by 2-butanone) were modestly enhanced in odor-exposed flies (Figure 2.2H, I), VM7 responses to mixed direct and indirect input (driven by mixtures of 2-butanone and pentyl acetate) were similar in control and odor-exposed flies (Figure 4.3G, H, J, K). This effect was observed across the entire range of concentrations we evaluated. This observation suggests that the local GABAergic inhibitory network may act to counter modest changes in excitability elicited by perturbations in the odor environment, thereby maintaining stable PN responses to most typical odors.

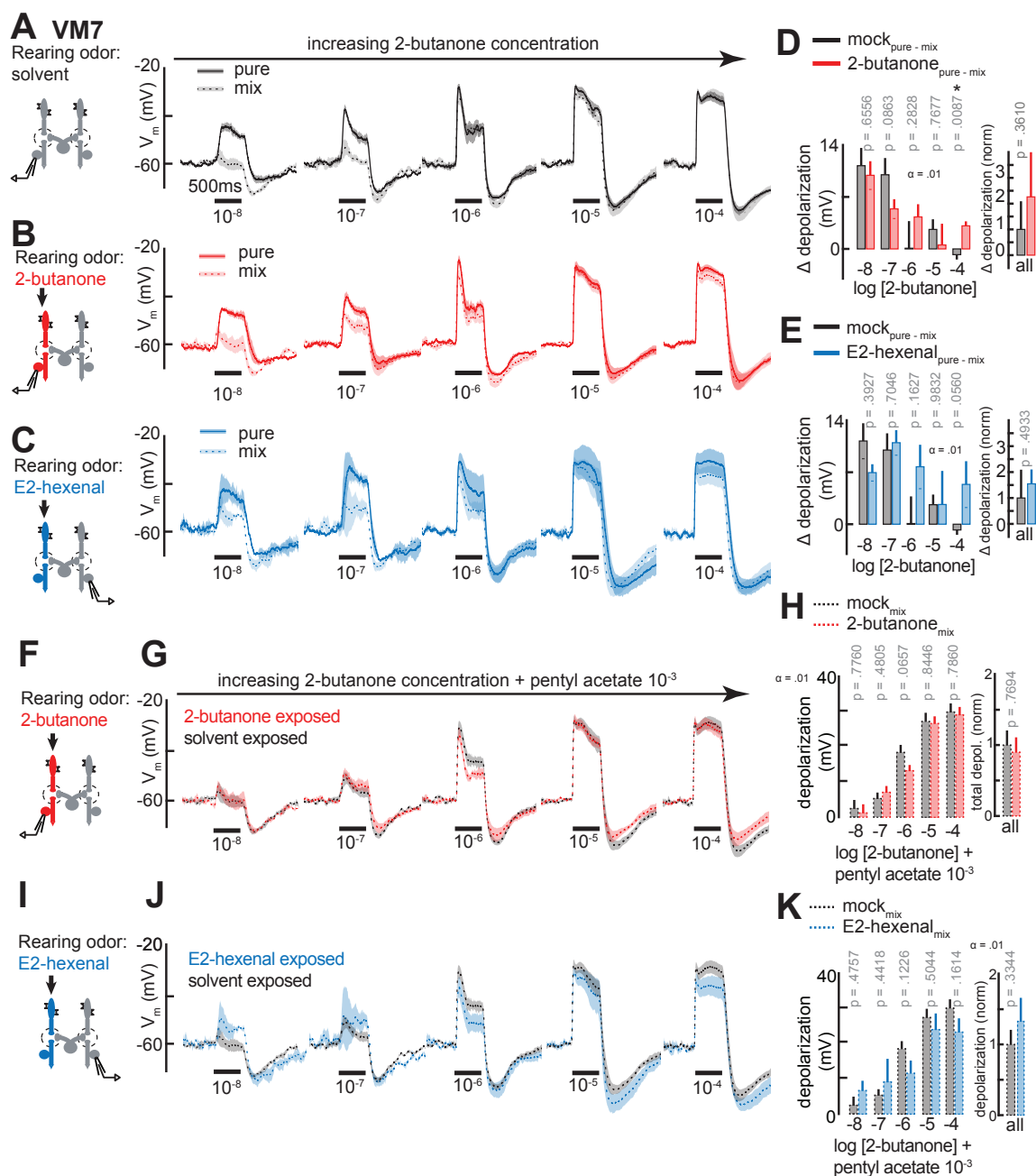


Figure 4.3: Odor exposure does not affect PN responses to mixtures

A-C) Left: Schematic of rearing condition and VM7 patch-clamp recordings for (a) mock rearing (black), (b) 2-butanone 10^{-4} direct rearing (red), and (c) trans-2-hexenal (E2-hexenal) 10^{-7} indirect rearing (blue). Right: Average odor-evoked membrane potential in VM7 PNs in response to pure odor stimulation (2-butanone; dark solid line) and mix (2-butanone with pentyl acetate; light dotted line). 2-butanone was presented at 10^{-8} , 10^{-7} ,

10^{-6} , 10^{-5} and 10^{-4} concentrations. Pentyl acetate was fixed at 10^{-3} in mixtures. **D-E)** Left: Average change in odor-evoked membrane depolarization between pure and mix responses following mock rearing, (d) 2-butanone 10^{-4} rearing and (e) trans-2-hexenal (E2-hexenal) 10^{-7} rearing. Right: Total change in odor-evoked membrane depolarization between pure and mix VM7 responses across rearing conditions. **F, I)** Schematic of rearing condition and VM7 patch-clamp recordings. (f) direct 2-butanone 10^{-4} rearing (red), and indirect trans-2-hexenal (E2-hexenal) 10^{-7} rearing (blue). **G, J)** Average odor-evoked membrane depolarization of VM7 PNs in responses to odor mixtures of increasing concentrations of 2-butanone with pentyl acetate. **H, K)** Left: Average membrane depolarization across odor mixtures in mock vs. 2-butanone (h) and trans-2-hexenal (E2-hexenal) (k) reared conditions. Right: Average total membrane depolarization computed across odor mixtures.

Indirect odor rearing may increase lateral excitation globally

The majority of network-level activity is mediated through presynaptic inputs from inhibitory local neurons. Antennal lobe PNs are also known to receive small amounts of lateral excitation from gap junctions. Different PNs receive different amounts of lateral excitation, and the excitation is odor-dependent. Lateral excitation is typically very small, providing around 10mV subthreshold depolarization into the PNs. We wondered if odor exposure can alter the amount of lateral excitation that a PN receives. Our data shows that PN responses have small changes in odor-evoked depolarization after rearing. In VA6 in particular, indirect rearing in trans-2-hexenal lead to small, subthreshold changes in odor-evoked membrane potential. In this set of experiments, we aimed to isolate lateral excitation in VA6 after indirectly rearing in trans-2-hexenal. We chose this PN because the effects of trans-2-hexenal rearing resembled features of lateral excitation as previously described (Olsen, S.R., et al., 2007; Yaksi, E. and Wilson, R.I., 2010). For these recordings, we reared flies in trans-2-hexenal to indirectly target VA6 PNs. Prior to physiological recordings, we carefully severed the antennal nerve to remove all direct inputs into VA6 (Figure 4.4A). Any excitation that we see is thus mediated laterally through stimulation of maxillary palp ORNs.

We presented a panel of odorants that strongly activate broad ORN subtypes. Interestingly, we found that rearing in trans-2-hexenal increases odor-evoked membrane depolarization in VA6 PNs to a panel of broad odorants (Figure 4.4B, C). Notably, different odors recruit different amounts of lateral excitation and not all odors show the effect of enhanced depolarization. In particular, we found that pentyl acetate, 2-heptanone and trans-2-hexenal recruit increased odor-evoked in excitation after rearing whereas 2-butanone (Figure 4.4B, C) did not show any differences. We also tested responses to iso-butyl acetate and *p*-cresol, and did not see strong enhancements of lateral excitation. This result suggests that the effect of rearing on lateral excitation is

dependent on odor identity and a glomerulus can be uniquely tuned to different sources of lateral excitation.

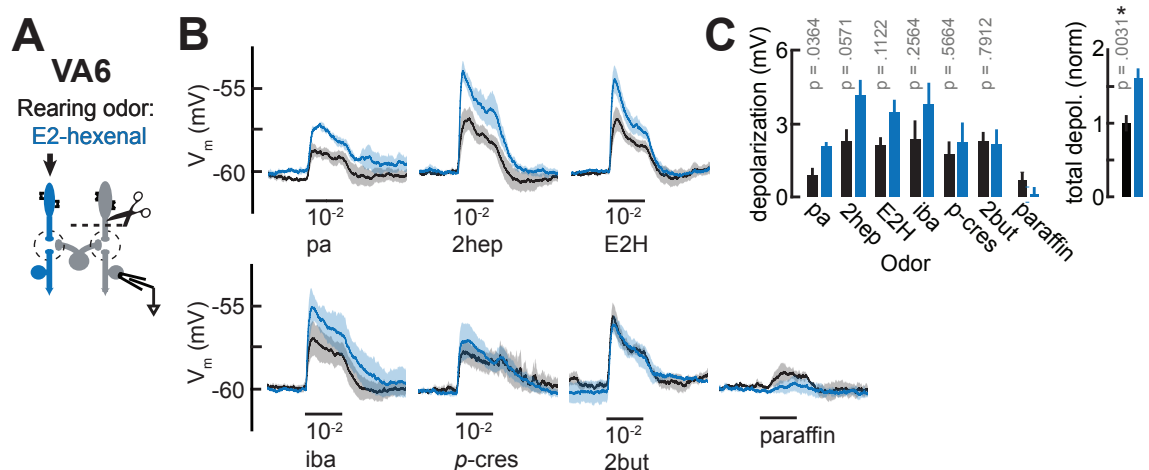


Figure 4.4: Lateral excitatory inputs may be increased after trans-2-hexenal exposure

A) Schematic of indirect odor rearing in trans-2-hexenal 10^{-7} and patch-clamp recording from VA6 PNs. The antennal nerve was severed prior to electrophysiological recording. **B)** Average VA6 odor-evoked membrane potential in response to lateral excitatory inputs. Odors used include pentyl acetate (pa), 2-heptanone (2hep), trans-2-hexenal (E2H), isobutyl acetate (iba), p-cresol (p-cres), 2-butanone (2but) and paraffin oil. All odors were diluted to 10^{-2} . **C)** Left: Average membrane depolarization of VA6 PNs in response to lateral excitatory inputs. Right: Total normalized membrane depolarization.

Methods

Flies

We used the following line for LN anatomy and glomerular volume measurement: UAS-brp-short strawberry/+; 20X-UAS-CD8-GFP/NP3056-Gal4. We did not quantify the short-stawrberry signal.

Odor stimulation

Odors were mixed in vapor phase in the carrier air stream. Odors were diluted as previously described. We presented a panel of increasing concentrations of the selective odor (2-butanone) while holding the concentration of the broad odor, pentyl acetate, at 10^{-3} . This concentration was previously shown to be effective at recruiting inhibition (Hong, E.J. and Wilson, R.I., 2015) and suppressing VM7 odor responses (Olsen, S.R., et al., 2010).

Electrophysiology

Electrophysiological measurements were performed as described in Chapter 2. To isolate lateral excitation in VA6, flies were dissected to expose the antennal lobe as described previously. Direct excitatory inputs into VA6 arise from ab5a ORNs, which are housed on the antennae. We removed directed excitatory inputs by carefully severing both antennal nerves with fine forceps. Any remaining excitation was mediated via ORN activation located on the palp and signaled into the antennal lobe via the maxillary nerve.

Histology and confocal imaging

Tissue histology was performed as previously described in Chapter 2. For LN anatomy experiments, Streptavidin was omitted from the secondary antibody solution.

Anatomical image analysis

Stacks were imported into ImageJ (NIH) and the 3D ROI toolkit was used to extract individual glomeruli. Several planes were manually traced across the upper and lower bounds of individual glomeruli and the remaining planes were automatically interpolated. Values for each region of interest were saved and exported into Matlab (Mathworks) and Excel (Microsoft Office) for further analysis.

Discussion

Overall, trans-2-hexenal odor exposure resulted in a global decrease in glomerular volume. In effect, we found that LN innervation density also decreased. This result is consistent with prior work that reported changes in glomerular volume. Our result, though, differs from published work because we see effects of rearing across multiple glomeruli rather than the target odor. This suggests that odor exposure paradigms are complex and may affect antennal lobe glomeruli through network circuits. We propose a global screen spanning chemical classes to determine whether the effects of rearing generalize across a certain dimension in odor space.

Odorants in nature are highly complex mixtures consisting of many monomolecular odorants in varying concentrations. In effect, naturalistic stimuli likely recruit many different ORN populations that can recruit both PNs and local neurons (LNs) to modulate total spiking responses in the antennal lobe. While we saw that VM7 PNs had increased afterhyperpolarization amplitude in response to pure monomolecular odor stimulation after indirect rearing (Figure 2.5B, E), we found that broad odor mixtures suppress these effects (Figure 4.3G, H, J, K). Future studies may look into how inhibitory neuron recruitment is effected after rearing and whether PN sensitivity to inhibition is altered.

Prior work has characterized the effects of lateral excitation across different antennal lobe glomeruli and identified that each glomerulus receives different amounts of lateral excitation in an odor-dependent manner (Yaksi, E. and Wilson, R.I., 2010; Olsen, S.R., et al., 2007; Shang, Y., et al., 2007). Yaksi et al. describe that different odorants can recruit different amounts of depolarization into glomeruli, yet the total depolarization is weak and is below spike threshold (Yaksi, E. and Wilson, R.I., 2010). Interestingly, lateral excitation mediated via eLNs is signaled via electrical, not chemical synapses and eLN inputs appear global. It is unclear why the antennal lobe needs lateral excitation and what computation advantages eLNs have within this stage of olfactory processing. One possibility is that electrical communication is much faster, which may allow for odor signals to be quickly propagated across the network. It is also possible that lateral excitation may serve as an auxiliary excitatory signaling input into glomeruli in case direct excitatory inputs are damaged. Since most odorants in nature are composed of complex mixtures that activate populations of ORNs, damages in individual ORN populations can result in an altered population code of odorants and therefore skew a fly's perception and behavioral response to odors. By activating glomeruli via another mechanism, the fly may be able to maintain a consistent odorant representation.

The observation that trans-2-hexenal rearing may increase the strength of lateral excitation into VA6 suggests that eLNs may be capable of undergoing odor-evoked plasticity. Typically, lateral excitation is seen in response to strong, broad odors. Given that flies are reared in low odor concentrations of trans-2-hexenal suggests that eLN sensitivity may be increased. It is important to note that trans-2-hexenal 10^{-7} did not recruit noticeable lateral excitation in VA6. With this observation, we can only suggest that this particular glomerulus does not receive strong lateral excitation in response to this odor. It is possible that trans-2-hexenal 10^{-7} may still recruit weak levels of eLN activity into other glomeruli which may strengthen global eLN connectivity. Future work would need to image eLN responses to trans-2-hexenal 10^{-7} to determine whether the

responses are present and whether rearing can increase eLN sensitivity to a panel of odorants. Whether the effects of lateral excitation after trans-2-hexenal rearing can occur across other glomeruli is unknown with our current dataset. It would be interesting to image PN calcium responses across the entire antennal lobe to identify other glomeruli which may be affected following trans-2-hexenal rearing. A caveat to imaging is the decreased measurement sensitivity in comparison to patch-clamp, though this may not be an issue with the new, high resolution calcium indicators available for use within *Drosophila*.

References

Golovin, R.M., Vest, J., Vita, D.J., and Broadie, K. (2019). Activity-Dependent Remodeling of *Drosophila* Olfactory Sensory Neuron Brain Innervation during an Early-Life Critical Period. *J. Neurosci.* **39**, 2995-3012.

Hong, E.J. and Wilson, R.I. (2015). Simultaneous encoding of odors by channels with diverse sensitivity to inhibition. *Neuron* **85**, 573-89.

Kidd, S., Struhl, G., Lieber, T. (2015). Notch is required in adult *Drosophila* sensory neurons for morphological and functional plasticity of the olfactory circuit. *PLoS Genet* **11**.

Olsen, S.R. and Wilson, R.I. (2008). Lateral presynaptic inhibition mediates gain control in an olfactory circuit. *Nature* **452**, 956-60.

Olsen, S.R., Bhandawat, V., and Wilson, R.I. (2007). Excitatory interactions between olfactory processing channels in the *Drosophila* antennal lobe. *Neuron* **54**, 667-667.

Olsen, S.R., Bhandawat, V., and Wilson, R.I. (2010). Divisive normalization in olfactory population codes. *Neuron* **66**, 287-99.

Sachse, S., Rueckert, E., Keller, A., Okada, R., Tanaka, N.K., Ito, K., and Vosshall, L.B. (2007). Activity-dependent plasticity in an olfactory circuit. *Neuron* **56**, 838-50

Shang, Y., Claridge-Chang, A., Sjulson, L., Pypaert, M., Miesenbock, G. (2007).

Excitatory local circuits and their implications for olfactory processing in the fly antennal lobe. *Cell* 128, 601-12.

Yaksi, E. and Wilson, R.I. (2010). Electrical coupling between olfactory glomeruli.

Neuron 67, 1034-47.

Chapter 5: Expressing Chrimson in ORNs

Introduction

In this short chapter, I provide sample recordings from antennal and palp ORNs in which I drove expression of the Chrimson light-activated ion channel. All of the driver lines used in this chapter were generated by our lab's first technician, Meike Lobb-Rabe. She generated both the Or42a-lexA and Or7a-lexA fly lines, both of which are expressed on the third chromosome. I recorded odor-evoked and light-evoked responses from Or42a ORNs located on the palp, which innervate the VM7 glomerulus. These ORNs are also known as pb1a neurons, and are housed in palp basiconic sensilla along with another neuron, pb1b. Light-evoked responses were achieved in Chrimson-expressing Or42a ORNs across a range of light intensities and wavelengths. To achieve high spatial precision during uEPSC recruitment, blue light was used to stimulate ORN terminals. However, for the recordings shown in this chapter, I use 660nm red LEDs attached to a rearing barrel. Surprisingly, driving Chrimson in OR42a ORNs abolished endogenous odor responses from these neurons, but light-evoked responses were functional. In effect, expressing Chrimson appeared to influence the endogenous expression or compromised the function of the Or42a receptor. This effect was seen in Or42a across all flies tested (n=2). Interestingly, while Or42a ORNs did not have odor responses, the ORNs housed in the same olfactory sensilla had strong odor-evoked responses that resembled responses in control flies without Chrimson expression. Chrimson expression did not always influence odor responses in ORNs. Driving Chrimson expression in Or7a ORNs, located on the antennae, induced reliable light-evoked responses. Importantly, odor-evoked responses via the endogenous Or7a receptor remained intact. These observations suggest that odor responses may be affected by Chrimson expression in ORNs. It is important to thoroughly test light-evoked and odor-evoked responses in ORNs if an experimenter needs to compare light-activated and receptor-mediated ORN

spiking activity. Lastly, I provide an example of an LED rearing barrel I built for the lab. I validated that the LEDs can successfully activate light-evoked responses in flies on the rig. While I did not use the barrels for experiments, I leave the assembly for future use in the lab.

Methods

Chrimson expression

Fruit flies were stored at 25°C throughout all phases of development. Chrimson was expressed in Or42a ORNs by crossing flies from the following genotypes:

NP3481-Gal4, UAS-CD8-GFP/(FM6) ; ; Or42a-lexA/TM6B

X

NP3481-Gal4, UAS-CD8-GFP/(FM7) ; 13X-IVS-lexAop2-Cs-Chrimson.mVenus/Cyo-actGFP ;

This yielded the genotype used in experiments:

NP3481-Gal4, UAS-CD8-GFP; 13X-IVS-lexAop2-Cs-Chrimson.mVenus/+; Or42a-lexA/+

Likewise, Chrimson expression in Or7a ORNs was accomplished using an identical schema:

NP3481-Gal4, UAS-CD8-GFP/(FM6) ; ; Or7a-lexA/MKRS

X

NP3481-Gal4, UAS-CD8-GFP/(FM7) ; 13X-IVS-lexAop2-Cs-Chrimson.mVenus/Cyo-actGFP ;

This yielded the genotype used in experiments:

NP3481-Gal4, UAS-CD8-GFP; 13X-IVS-lexAop2-Cs-Chrimson.mVenus/+; Or7a-lexA/+

Or42a-lexA and Or7a-lexA were generated in the Hong lab by our former lab technician, Meike Lobb-Rabe. These flies are currently maintained in the Hong lab fly stocks in case other experimenters wish to use these flies in future work.

For control recordings, we used the following line:

NP3481-Gal4, UAS-CD8-GFP;;

ATR and light-proofing

Once crosses were established, all fly bottles were carefully wrapped in aluminum foil to prevent the entrance of light. This is critical to ensure Chrimson does not cause unintended activation of the chosen olfactory receptor throughout development. Prior to recordings, all trans-retinal (ATR) was carefully added to the existing fly food. ATR was kept in a 35mM stock solution in 95% ethanol, and this was wrapped in foil and maintained at 4°C. On the day of experiments, flies were transferred into scintillation vials and wrapped in foil.

Electrophysiology

Extracellular single-sensillar recordings were performed as previously described. Briefly, flies were anesthetized on ice and a ~2-day-old female was chosen for recordings. The fly was positioned into the end of a modified 200uL pipette tip, and the head and abdomen were stabilized with a light application of wax. Recording and ground pipettes were freshly pulled each day before the start of experiments using a Sutter pipette puller. Both pipettes were filled with standard *Drosophila* saline. The flies were mounted on Scientific electrophysiology rigs, coarsely adjusted using a 5x Olympus objective and finely adjusted using a 50x Olympus air objective. A coarse manipulator was used to insert a ground electrode into one eye of the fruit fly. One antenna or palp was carefully positioned onto the top of a coverslip, also connected to a coarse manipulator. Once the sensilla of interest were identified, a fine manipulator was used to bring a recording electrode into view. The electrode tip was carefully inserted into the tip of an olfactory sensillum and sensillar identity was confirmed using a standard panel of diagnostic odors. This procedure was repeated until the sensilla of interest were found.

Light stimulation

A red LED barrel was positioned below the fly on the electrophysiology rig. The barrel

was aligned such that the antennae were positioned near the top and center of the LED barrel. Light stimulation was controlled using a Matlab program and DAQ (National instruments). A 500ms pulse of light was delivered to the fly and the intensity was manually adjusted on the LED barrel using a custom-built rotary switch (Figure A.1).

Results

In pb1, there are two neurons that have distinct odor tuning: pb1a (Or42a) responds strongly and selectively to 2-butanone, and pb1b (Or71a) to *p*-cresol (de Bryune, 1999; Couto, A., M., et al., 2005). In control flies that lack exogenous light-sensitive opsins in the olfactory system, all odor responses should be driven only by the specific olfactory receptor expressed on the ORN of interest. In ab4a, a typical odor response is shown in Figure 4.1. The traces represent representative raw extracellular recordings measured in a NP3481-Gal4, UAS-CD8-GFP female fly. Responses to trans-2-hexenal are strong: there is both a strong local field potential (LFP) response present as well as spontaneous and evoked spikes throughout the recording. Two olfactory receptor neurons (ORNs) are housed in the ab4a sensilla, and they are distinguished based on their spike amplitude. The Or7a-expressing ORN is termed ab4a due to its large spike amplitude, and this ORN is responsible for the robust response to trans-2-hexenal. In contrast, the smaller spikes belong to ab4b neuron which is not responsive to trans-2-hexenal.

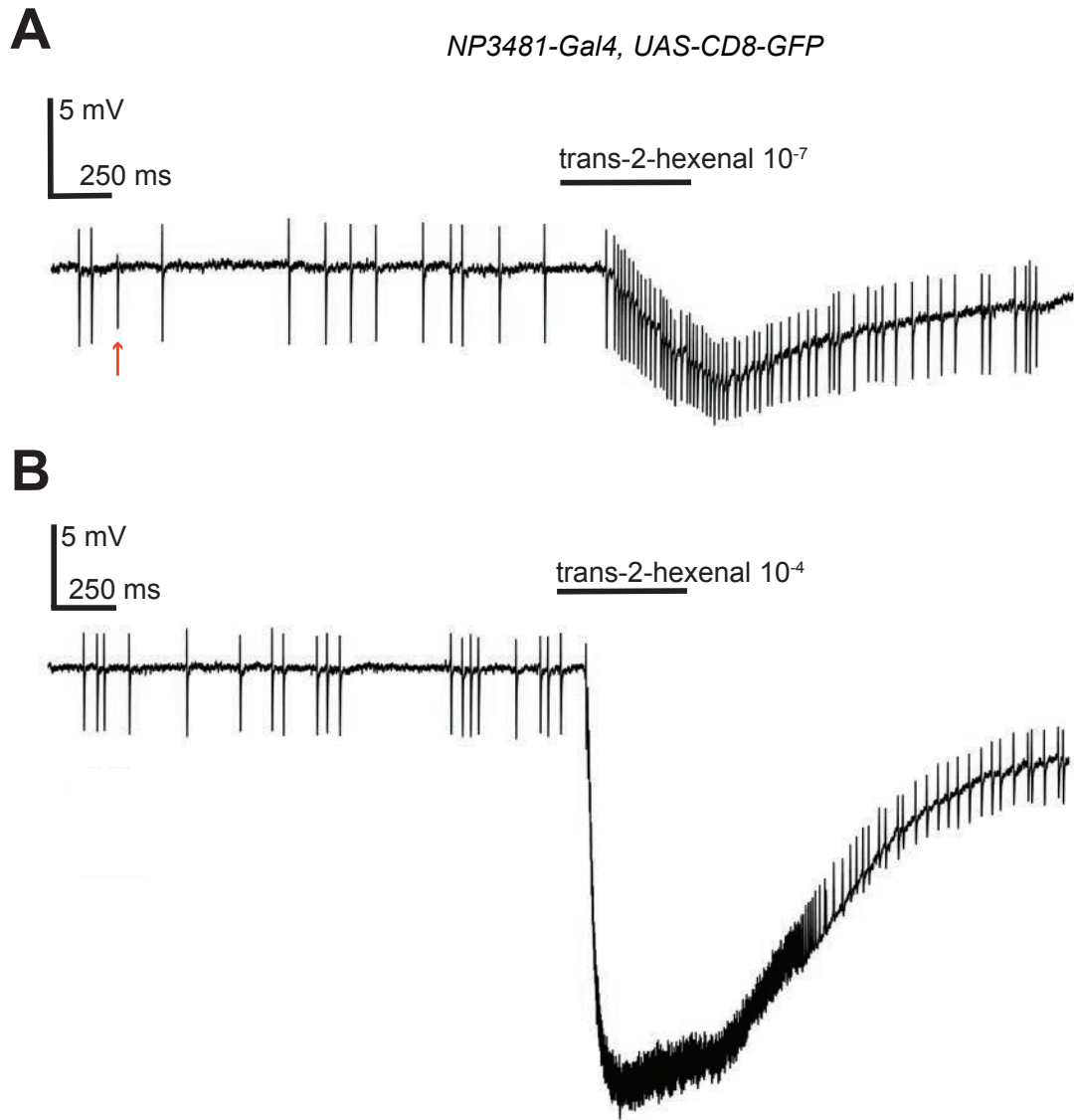


Figure 5.1: Odor-evoked response in ab4 sensilla of a control fly

Trans-2-hexenal was presented to the fly at (a) 10^{-7} and (b) 10^{-4} concentrations. Strong odor-evoked spiking responses are recruited during stimulation in ab4a ORNs. An LFP response is seen in both (a) and (b) odor-evoked responses. A red arrow in (a) designates a spike from ab4b, which fires sparsely and with a smaller amplitude. Genotype: *NP3481-Gal4, UAS-CD8-GFP*.

In order to perform light-activated uEPSC recordings in DL5 PNs, we expressed Chrimson in Or7a ORNs which project into the DL5 glomerulus. These ORNs are located within ab4 sensilla and are denoted as *ab4a* neurons due to the larger spike amplitude these cells have than the neighboring neuron, *ab4b*, within the same sensilla. In addition to EPSC experiments, we were also interested in the prospect of using light to chronically activate specific ORNs rather than using odorants as before. For light to work, we needed to ensure that we could recruit reliable and robust spiking responses in ORNs. First, we built a rearing chamber that is lined with red-emitting LEDs which we discuss in more detail in the Appendix. To test the efficacy of our design, we placed the rearing barrel within an electrophysiology rig just below the pipette tip holding a fly. About 1-2 days prior to recordings, female flies were sorted from male flies and placed in vials containing standard fly food with a droplet of ATR. For reference, we placed roughly 100uL of ATR-EtOH solution into the small fly vials and 500uL of ATR-EtOH into the large fly bottles. The fly vials were wrapped in aluminum foil, and flies were maintained in the incubator until ready for use. Flies were prepared according to the standard procedure for single-sensillar recordings as described in the Methods section in Chapter 3. We fixed the light intensity of the red LEDs to evoke maximum spiking, which was roughly midway on the rotary switch (see Appendix for more information). The electrophysiology rig was light-proofed to ensure the ORNs were not stimulated by ambient light. Without light-proofing, the spontaneous firing rate of Or7a ORNs was increased relative to control flies lacking Chrimson expression (data not shown). In light-proofed conditions, the spontaneous firing rate of the cell was similar to that of control flies, suggesting that Chrimson expression did not affect the spontaneous activity in Or7a ORNs (Figure 5.2). Care was taken to ensure the flies were exposed to ambient light for as little time as possible, though exposure to light could not be prevented during the placement of flies into the mounting pipette.

NP3481-Gal4, UAS-CD8-GFP ; 13X-IVS-lexAop2-CsChrimson.mVenus/+ ; Or7a-lexA/+

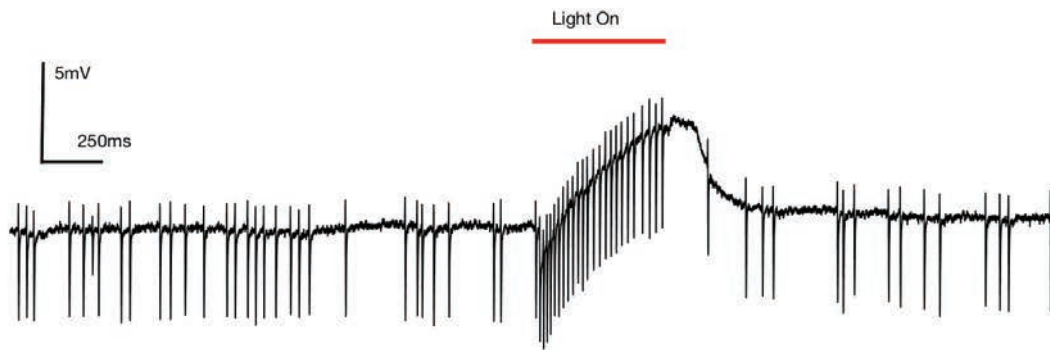


Figure 5.2: Light-evoked response in ab4 sensilla in Or7a>Chrimson fly

A light-evoked response in ab4 sensilla in Or7a>Chrimson fly is reliably recruited.

We presented a 500ms pulse of red light to the fly and measured light-evoked responses in Or7a. The results of a single recording are shown in Figure 5.2. Notably, light stimulation caused a robust increase in spiking that closely resembled responses to trans-2-hexenal 10^{-7} odor stimulation (Figure 5.1A, Figure 5.2). We see that ab4b neurons are still functioning as expected, with a visible spontaneous spike appearing early in the pre-stimulus phase of the sample trace (Figure 5.2). Interestingly, we do not see a transduction current during light stimulation (Figure 5.2) as we do with odor (Figure 5.1), suggesting that receptor-ligand interactions may be necessary for transduction currents to occur. Instead, we see that light causes a slight deflection with reversed polarity. The cause of this is likely due to an electrical artifact of stimulation that is detected by the recording headstage. All in all, we see that light stimulation causes robust firing in Or7a that is locked to the stimulus. We note that we could not achieve higher firing rates with more light, and this example roughly demonstrates the highest spiking response we could recruit in this ORN. The effect of increasing light was nonlinear, and high light intensities shunted ORN firing (Figure 5.5B). It may be possible

to increase the amount of light-evoked spikes using a genotype that includes two copies of the Chrimson reporter or Or7a driver, though we did not test this.

We were also interested in determining if odor-evoked responses were comparable between Or7a>Chrimson and control flies. To the same ORN that we show in Figure 5.2, we presented a series of trans-2-hexenal odor concentrations following the same methods used throughout our experiments in Chapter 3. In addition to observing reliable light-evoked responses, the neuron maintained robust odor-evoked responses (Figure 5.3). We conclude that expressing Chrimson in Or7a does not disrupt the function of the Or7a receptor. Thus, the Or7a>Chrimson fly line can be used to reliably recruit light- and odor-evoked spiking.

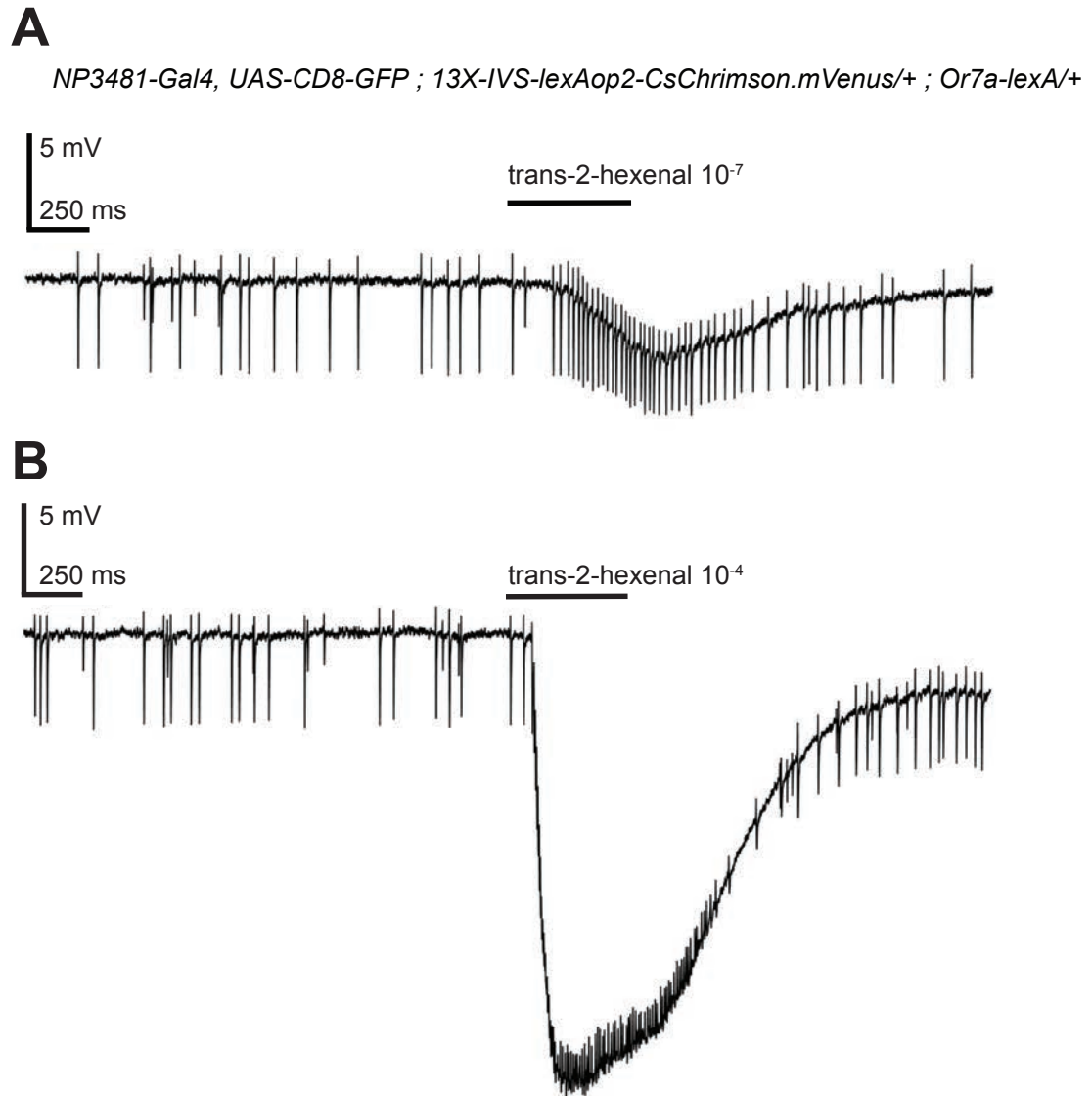


Figure 5.3: Odor-evoked responses in ab4 sensilla in Or7a>Chrimson fly

Odor-evoked responses are maintained in Or7a>Chrimson flies. Responses to trans-2-hexenal (a) 10^{-7} and (b) 10^{-4} are shown. Full genotype is written in figure above.

Another ORN we were interested in potentially rearing with light was the Or42a neuron that projects into the VM7 glomerulus. This ORN is located on the palp, and is known to be strongly selective to 2-butanone (Olsen, S.R., et al., 2010). The large amount of prior work focused on VM7 makes this ORN an attractive target for light-evoked rearing (Golovin, R.M., et al., 2019; Olsen, S.R., et al., 2010; Olsen S.R., and Wilson, R.I., 2008). First, we wanted to determine what typical odor-evoked responses look like in control flies. We presented a series of 2-butanone dilutions to our work-horse line, *NP3481-Gal4, UAS-CD8-GFP*. As expected, 2-butanone recruits robust firing and a pronounced transduction current in pb1a ORNs (Figure 5.4). Dilutions of 10^{-4} recruited strong spiking that was locked to the stimulus (Figure 5.4A), while 10^{-2} dilutions recruited a prolonged spiking response (Figure 5.4B).

The rearing concentration we used for VM7 throughout this thesis was 2-butanone at 10^{-4} , so we were interested to see if light could recruit comparable spiking. We expressed Chrimson in Or42a ORNs and performed the same experiments as described for Or7a>Chrimson. As before, we found that light stimulation evoked reliable and robust spiking in Or42a>Chrimson ORNs (Figure 5.5A). The traces we show represent the maximum spiking we could recruit, and higher light intensities shunted the ORN as we observed for Or7a (Figure 5.5B).

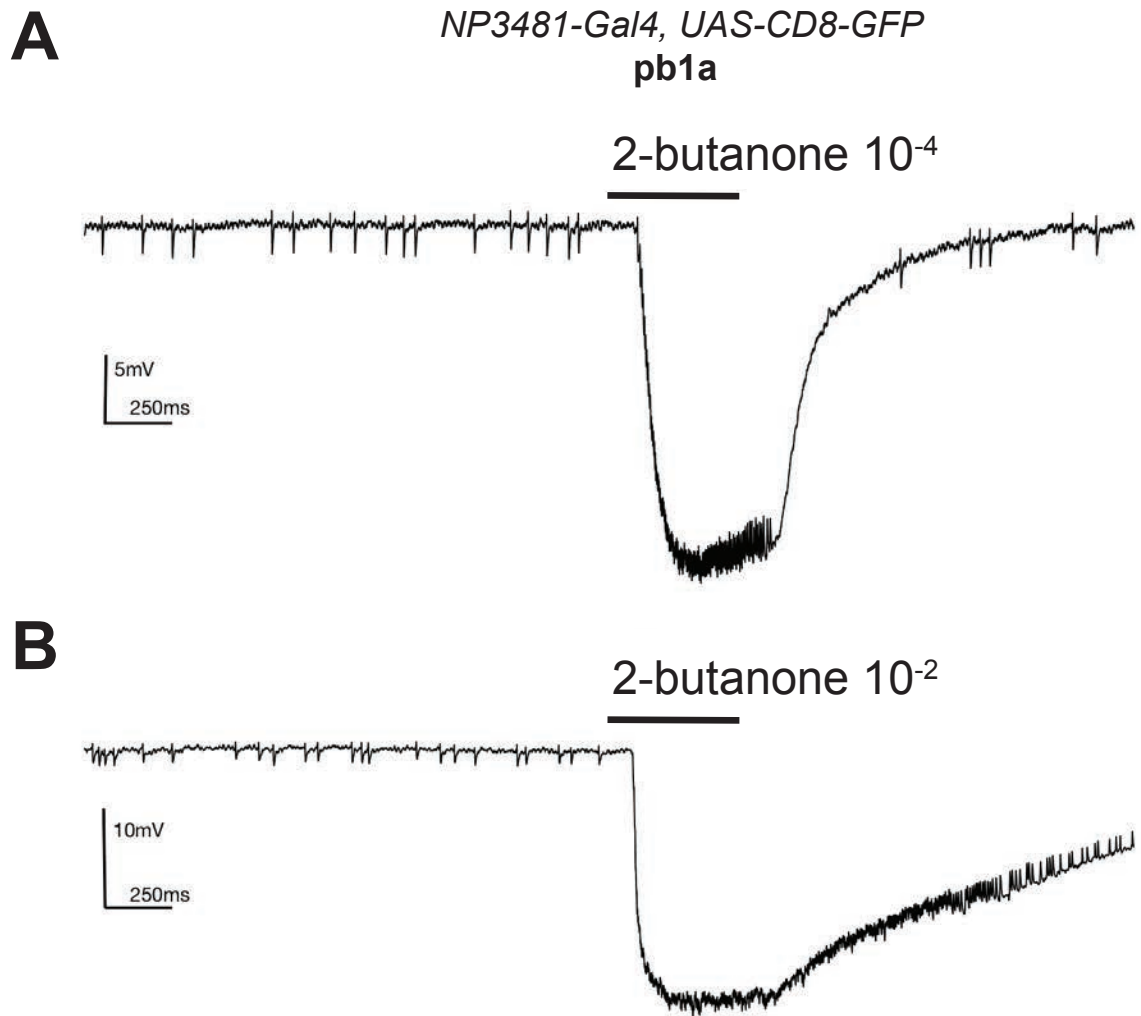


Figure 5.4: Odor-evoked responses in Or42a (pb1a) in a control fly

Representative odor-evoked responses in control pb1 sensilla to 2-butanone stimulation diluted to (a) 10^{-4} and (b) 10^{-2} . 2-butanone is a selective ligand for pb1a neurons, and responses are driven by pb1a neuronal activity. Genotype: *NP3481-Gal4, UAS-CD8-GFP*.

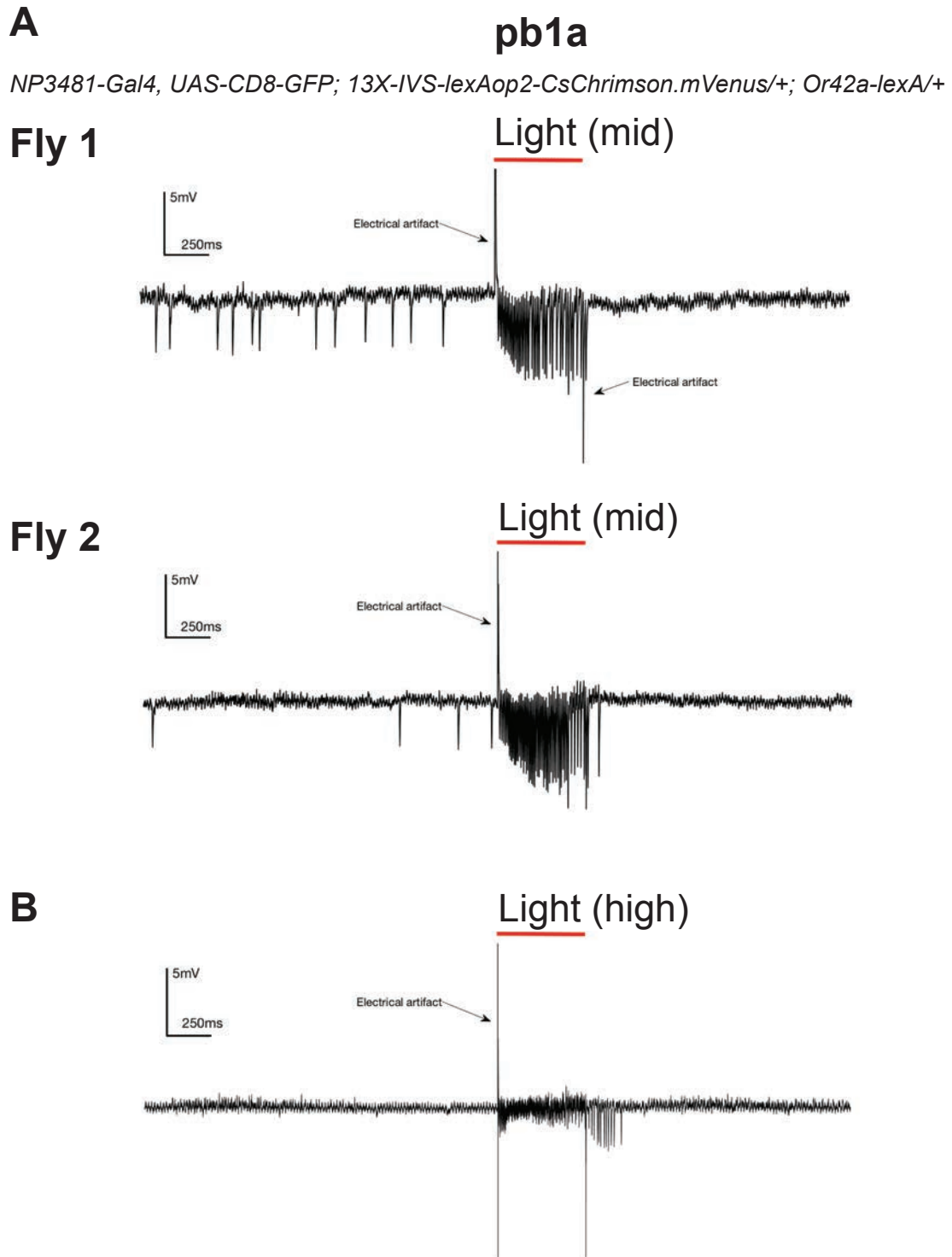


Figure 5.5: Light-evoked responses in *Or42a>Chrimson* (*pb1a*) ORNs.

A) A 500ms pulse of red light was used to stimulate *Or42a>Chrimson* ORNs. Representative raw traces are shown for recordings in two different flies. Light intensity

was set at a medium level. **B)** Representative trace showing light-evoked shunting of ORN responses with high light intensities. Genotype written in figure.

We wondered if Or42a>Chrimson flies exhibit reliable odor-evoked spiking in addition to light-evoked responses. We presented a 500ms pulse at different concentrations of 2-butanone to the same cells shown in Figure 5.5. To our surprise, we found that odor-evoked responses were completely abolished in Or42a>Chrimson ORNs (Figure 5.6). We did not see any transduction currents apparent in the ORN to 2-butanone 10^{-4} , suggesting that all odor-evoked dynamics are completely gone (Figure 5.6A). Since 2-butanone 10^{-2} is a broad odor, the transduction we see is likely due to the activity of other ORNs rather than pb1a given the lack of spiking in the cell (Figure 5.6B). Given how robustly Or42a ORNs respond to odor in control flies (Figure 5.4), we were not expecting to see this effect in Or42a>Chrimson ORNs. The lack of odor responses in Or42a>Chrimson suggests that Chrimson may somehow disrupt odor responses in some ORNs. We postulate a couple of possible mechanisms behind this observation. The exogenous expression of Chrimson may somehow interfere with the genetic expression of the Or42a receptor itself. Genetic profiling or histological analysis of receptor expression may reveal whether the receptor continues to be expressed in Or42a>Chrimson flies. It is also possible that the receptor is expressed, but is non-functional. Given that we see this observation in two different flies, we conclude that Or42a>Chrimson cannot be used in experiments requiring measurements of odor and light-evoked responses. We suggest that researchers always perform targeted single-sensillar recordings when they wish to drive Chrimson expression in different ORN populations.

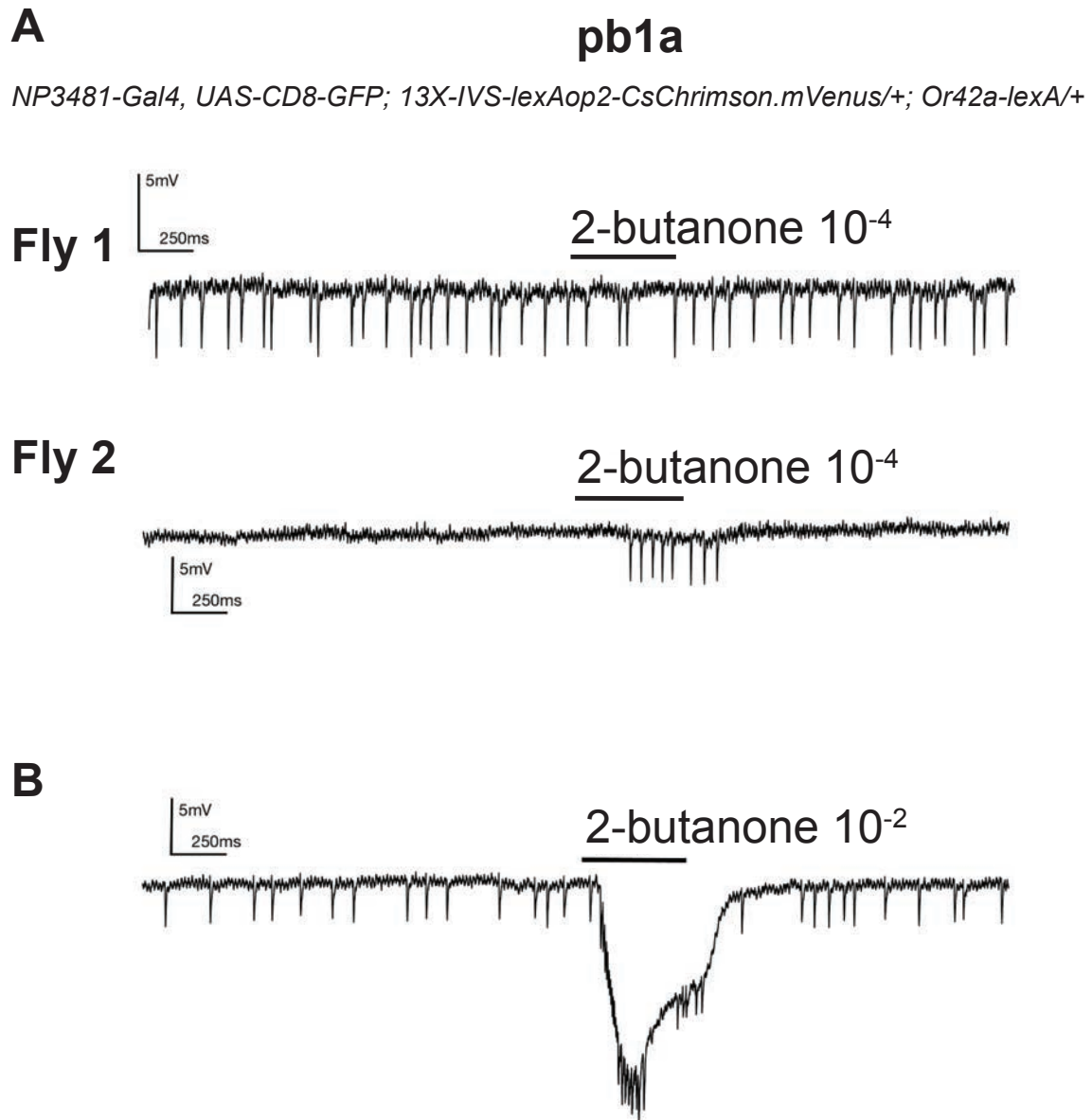


Figure 5.6: Odor-evoked responses are gone in Or42a>Chrimson (pb1a) ORNs

A,B) Or42a (pb1a) responses to a 500ms pulse of (a) 2-butanone at 10⁻⁴ is shown in two different flies and to (b) 2-butanone 10⁻² in Fly 1. Notably, expressing Chrimson in Or42a abolished odor responses. Full genotype listed in figure.

Next, we wondered if the effect of Chrimson expression in Or42a was selective. Conveniently, the pb1 sensilla contains another neuron which is highly selective for *p-cresol* (Figure 5.7). If the genotype disrupts odor responses non-selectively, we would expect to see a difference in pb1b neuronal responses.

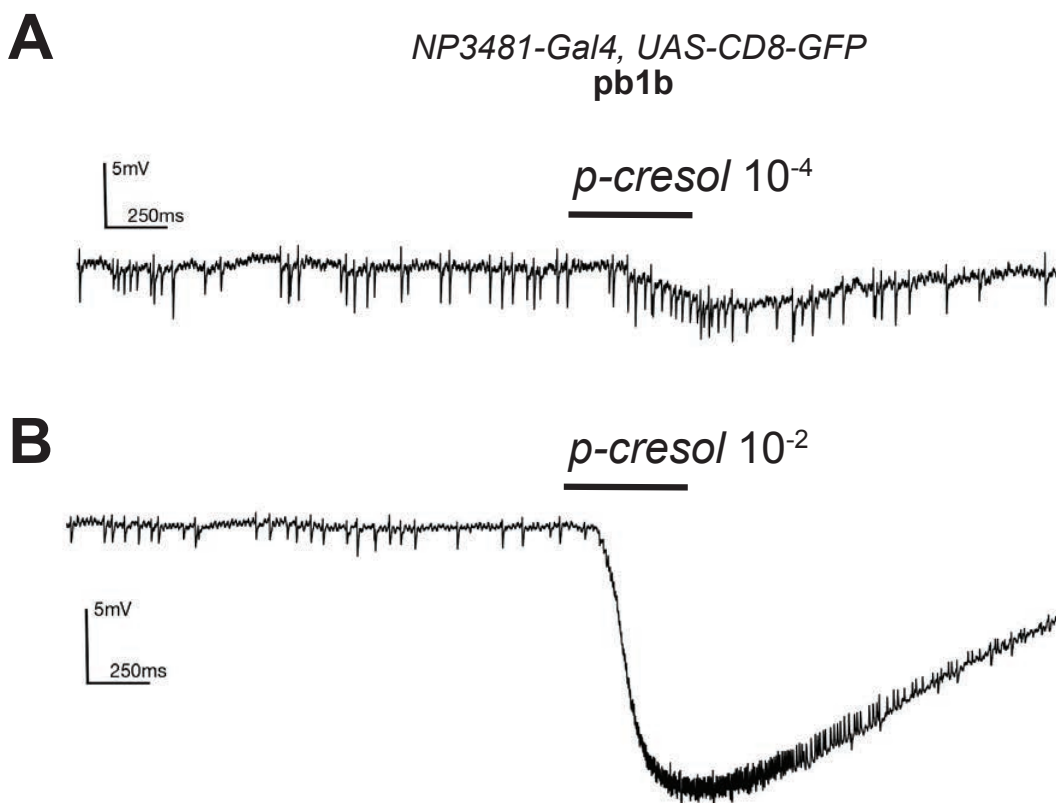


Figure 5.7: Odor-evoked responses in Or71a (pb1b) neuron in a control fly

Representative odor-evoked responses in control pb1 sensilla to *p-cresol* stimulation diluted to (a) 10^{-4} and (b) 10^{-2} . *p-cresol* is a selective ligand for pb1b neurons, and responses are driven by pb1b neuronal activity.

While recording from the same sensilla as shown in Figure 5.5 and 5.6, we presented *p*-cresol to activate Or71a (pb1b) neurons in Or42a>Chrimson flies. We see that odor responses in pb1b are intact (Figure 5.8) and comparable to control recordings (Figure 5.7). We note that the spontaneous activity of Or71a is low in both genotypes (Figure 5.7, 5.8) which is likely a standard characteristic of these ORNs. This finding suggests that the Or42a>Chrimson line specifically abolishes odor responses in the targeted ORNs rather than affecting odor responses globally. Thus, we rule out the possibility that this line is toxic and conclude that the targeted expression of Chrimson on Or42a neurons disrupts the endogenous Or42a receptor functionality and/or interferes with receptor expression.

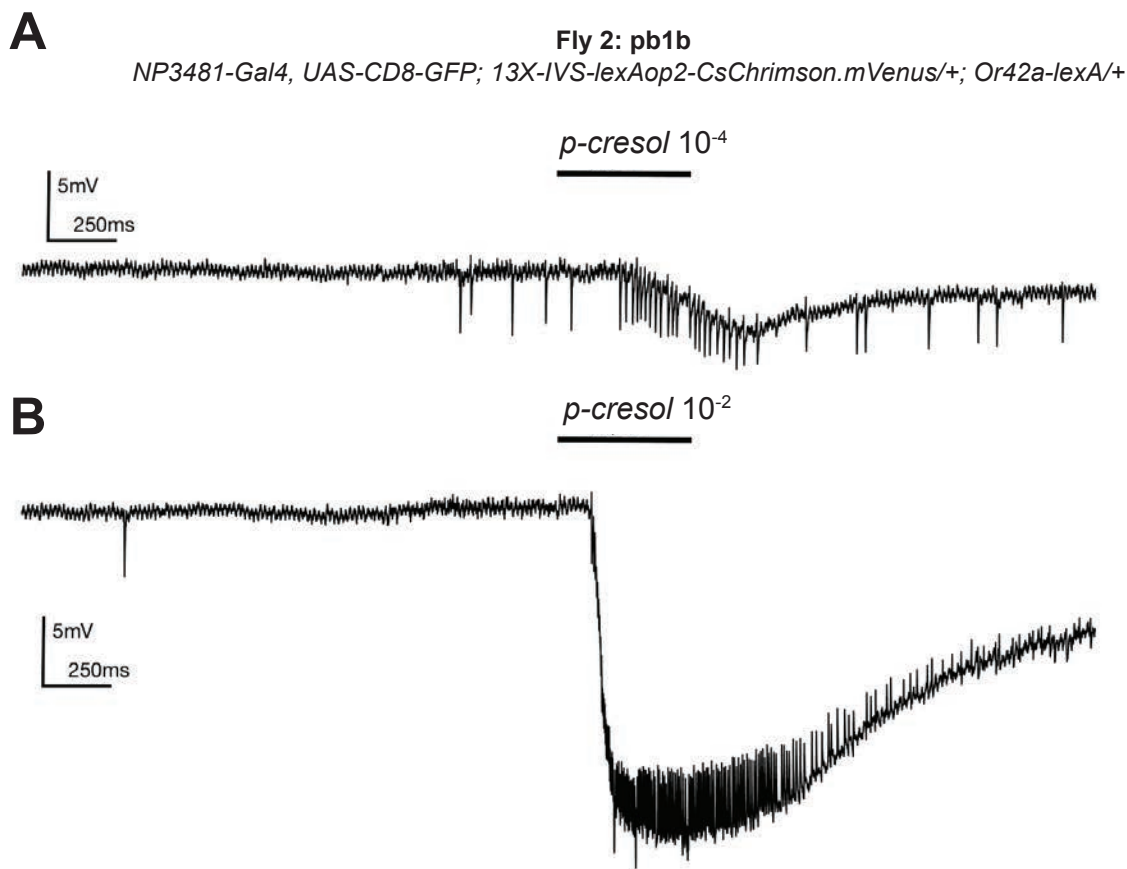


Figure 5.8: Odor-evoked responses are intact in Or71a (pb1b) ORNs in an Or42a>Chrimson fly

Responses to *p-cresol*, a known selective ligand for Or71a (pb1b) ORNs are shown. Odors were diluted to (a) 10^{-4} and (b) 10^{-2} . Note that pb1b odor responses are normal in Or42a>Chrimson flies. Genotype listed in figure.

We have shown that we can reliably recruit light-evoked spiking in two different ORNs including antennal Or7a and palp Or42a neurons. Both cells behave similarly during light stimulation: reliable time-locked spiking is apparent, responses lack transduction currents, spontaneous activity is maintained comparable to controls in light-proofed conditions, and high light intensities shunt ORN firing. We demonstrated that Or7a>Chrimson ORNs maintain odor-evoked responses comparable to control flies that lack Chrimson expression in Or7a ORNs. Surprisingly, we find that targeted Chrimson expression in Or42a ORNs abolishes odor-evoked responses completely and selectively in this cell type. We conclude that Chrimson may affect odor-evoked responses in a certain population of targeted ORNs. Measurements of odor- and light-evoked responses are encouraged should Chrimson be expressed in a different ORN type. We did not investigate the cause for the disrupted odor responses in Or42a>Chrimson ORNs, but this leaves an interesting open question in the genetic regulation of receptor expression and/or function in ORNs.

References

de Bruyne, M., Clyne, P.J., and Carlson, J.R. (1999). Odor coding in a model olfactory organ: the *Drosophila* maxillary palp. *J Neurosci.* *19*, 4520-32.

Couto, A., Alenius, M., and Dickson, B.J. (2005). Molecular, anatomical, and functional organization of the *Drosophila* olfactory system. *Curr. Biol.* *15*, 1535-1547.

Golovin, R.M., Vest, J., Vita, D.J., and Brodie, K. (2019). Activity-Dependent Remodeling of *Drosophila* Olfactory Sensory Neuron Brain Innervation during an Early-Life Critical Period. *J. Neurosci.* *39*, 2995-3012.

Olsen, S.R. and Wilson, R.I. (2008). Lateral presynaptic inhibition mediates gain control in an olfactory circuit. *Nature* *452*, 956-60.

Olsen, S.R., Bhandawat, V., and Wilson, R.I. (2010). Divisive normalization in olfactory population codes. *Neuron* *66*, 287-99.

Chapter 6 : Antennal LFP responses to odors

Introduction

All data presented in this chapter were collected by my sister, Caroline Gugel, during the summer of 2018 in the Hong lab. She worked as a research assistant on a project aimed to generate isointense odor curves for different commonly-used odors in the field of insect olfaction. I provided all training and assisted with data analysis throughout her project, though she became extremely independent and performed all experiments and analyses herself (including her own Matlab scripts). All data shown was collected, analyzed, and generated by Caroline while I formatted the final figures in Adobe Illustrator.

The purpose of this chapter is to provide experimenters with a reference dataset containing commonly used odorants in olfactory neuroscience. We presented four odorants from low to high concentrations while recording antennal local field potentials (LFP) from three different recording sites. Our purpose was to generate concentration curves for 2-heptanone (2hep), pentyl acetate (pa), trans-2-hexenal (t2h) and 2-butanone (2but) and identify concentrations at which these odors are isointense. We find that pentyl acetate recruits the largest local field potential (LFP) amplitude in the antennal lobe while 2-butanone recruits the least amount of activity. Most odors evoke LFP at concentrations that are 10^{-6} or above with the exception of trans-2-hexenal, which evokes measurable LFP activity when diluted to as low as 10^{-8} . The weakest odor appeared to be 2-butanone, which only evokes strong LFP in response to 10^{-5} dilutions. Overall, our data suggests that each odor evokes differing levels of population activity, and isointense stimuli can be created by slightly varying odor concentrations. We note that our dataset only includes antennal LFP, not maxillary palp LFP; thus, the responses measured to the odors are an underestimate of the total olfactory receptor neuron population LFP. About 90% of all ORNs are located on the antennae, with the remaining

10% on the maxillary palp (Couto, A.M., et al., 2005; de Bruyne, M., et al., 1999; de Bruyne, M., et al., 2001; Hallem, E.A., and Carlson, J.R., 2006);

Methods

We presented odors in increasing concentrations to the fly while recording total antennal activity. We used the following odors, all diluted by weight in paraffin oil: 2-butanone (2but), trans-2-hexenal (t2h), iso-butyl acetate (iba) and 2-heptanone (2hep). The concentrations ranged from 10^{-8} to 10^{-2} , and the flow rates were fixed to 2L/min for the carrier and 200mL/min for the odorant. Electroantennogram recordings were performed using the same set-up as single-sensillar recordings with a few modifications described below. Briefly, flies were anesthetized on ice and positioned into the end of a modified pipette tip. Antennae were positioned on coverslips and stabilized using a glass pipette. A ground electrode was inserted into one eye of the fruit fly, and a recording electrode was inserted into one of three locations on the antenna: proximal, medial, and distal. For each fly, the entire odor panel was presented at a single location. To ensure the reliability of odor-evoked responses and to prevent fruit fly desiccation, new flies were used for each location. Odors were averaged across locations and across flies. Isointense concentration curves were generated using peak voltage deflection and area during the 500ms odor stimulation period. We computed the peak and average deflection of the LFP responses across odor concentrations, recording locations, and averaged across all locations. Peak LFP was computed by finding absolute value of the minimum voltage deflection during the odor-evoked stimulation window. Average LFP was first computed as the integral of the voltage waveform during the odor-evoked stimulation window. The integral was then multiplied by the time window to obtain an estimate of the average evoked LFP.

Results

A concentration series was presented to each fly during a recording session. Odors were selected randomly and presented in order of increasing concentration. We found that most odors evoke strong local field potential (LFP) at high odor concentrations (Figure 6.1). The palp pb1a-selective odor, 2-butanone (2but), recruited the least amount of LFP at the antenna, with an average population response of 3mV. Responses to 2-butanone start at 2but 10^{-4} , suggesting that lower concentrations of 2-butanone are fairly weak activators (Figure 6.1A). Interestingly, while trans-2-hexenal recruits a maximum LFP amplitude of 4mV in the antenna, this odor recruited a stronger odor-evoked response at low concentrations (Figure 6.1B). Since trans-2-hexenal is a selective odor for ab4a ORNs that express the Or7a receptor, we expect that the LFP activity arises largely from this specific population of ORNs. The next strongest odor, 2-heptanone (2hep), recruited noticeable LFP through a range of odor concentrations and shows evidence of activation to concentrations as low as 10^{-6} (Figure 6.1C). As expected, pentyl acetate (pa) recruited the strongest LFP at high concentrations including 10^{-2} , 10^{-3} and 10^{-4} within the antennal lobe (Figure 6.1D). Previously, single-sensillar recordings of ORN odor responses have shown that pentyl acetate broadly activated many individual ORN classes. In effect, most antennal PNs are also responsive to pentyl acetate.

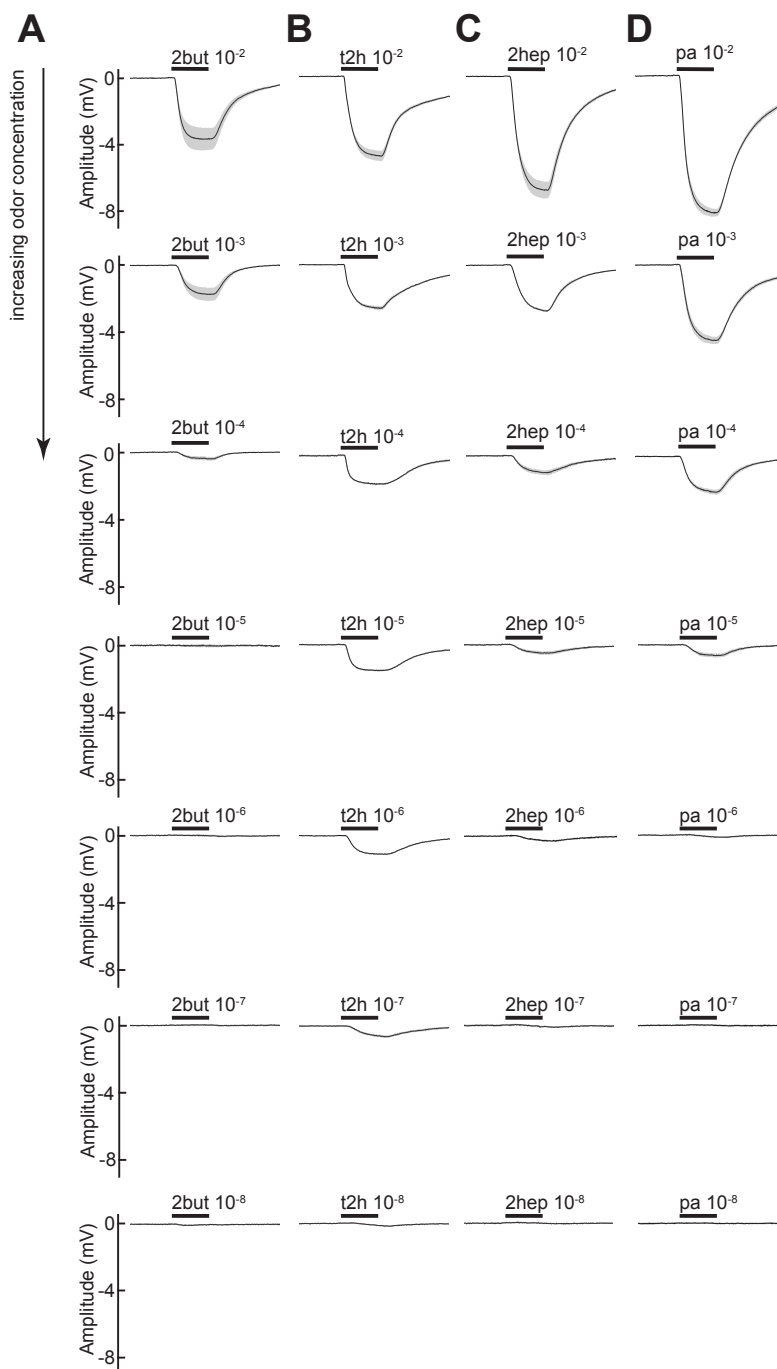


Figure 6.1: Antennal LFP recordings averaged across locations

Stimuli were presented from 10^{-8} to 10^{-2} dilutions for monomolecular odors including (a) 2-butanone, (b) trans-2-hexenal, (c) 2-heptanone and (d) pentyl acetate. Mean \pm SEM of the LFP response is computed across all recordings. Data are averaged across all recording locations, and SEM is computed across flies.

Next, we wanted to determine how LFP amplitude varies across different recording locations. To do this, we separated the data in Figure 6.1 based on the recording location along the third antennal segment including proximal, medial and distal to the second segment of the antennae (Figure 6.2A-C, respectively). All data represent the average peak LFP across flies. The peak was computed as the maximum deflection within the 500ms odor delivery window. Proximal recording locations resulted in the largest peak (Figure 6.2A) LFP deflection compared to medial (Figure 6.2B) and distal (Figure 6.2C) for 2-butanone, 2-heptanone and pentyl acetate. The peak magnitude decreased as the recording location was moved further along the third antennal segment for these three odors. In contrast, trans-2-hexenal recruited the largest peak deflection for medial recording locations (Figure 6.2B), followed by distal (Figure 6.2C), and finally the lowest detected LFP magnitude at proximal locations (Figure 6.2B). In general, each recording location produced greater peak deflections consistently across odor concentrations with a few exceptions (i.e. pentyl acetate 10^{-4} peak magnitudes were greater medially than proximally). Overall, the differences between recording sites are notably different between proximal and distal locations yet comparable between proximal and medial conditions. This data suggests that using proximal or medial locations may suffice for an estimate of total LFP, and these locations can be used to directly compare evoked LFP across a range of odors. We note that there is a population of ORNs strongly selective for 2-butanone that are located on the palp, and the antennal recordings are an underestimation of the total LFP recruited. It is likely the other odorants are also activating palp ORNs, but we suspect that 2-butanone-evoked LFPs may be underestimated to a larger extent than the rest of the stimulus panel.

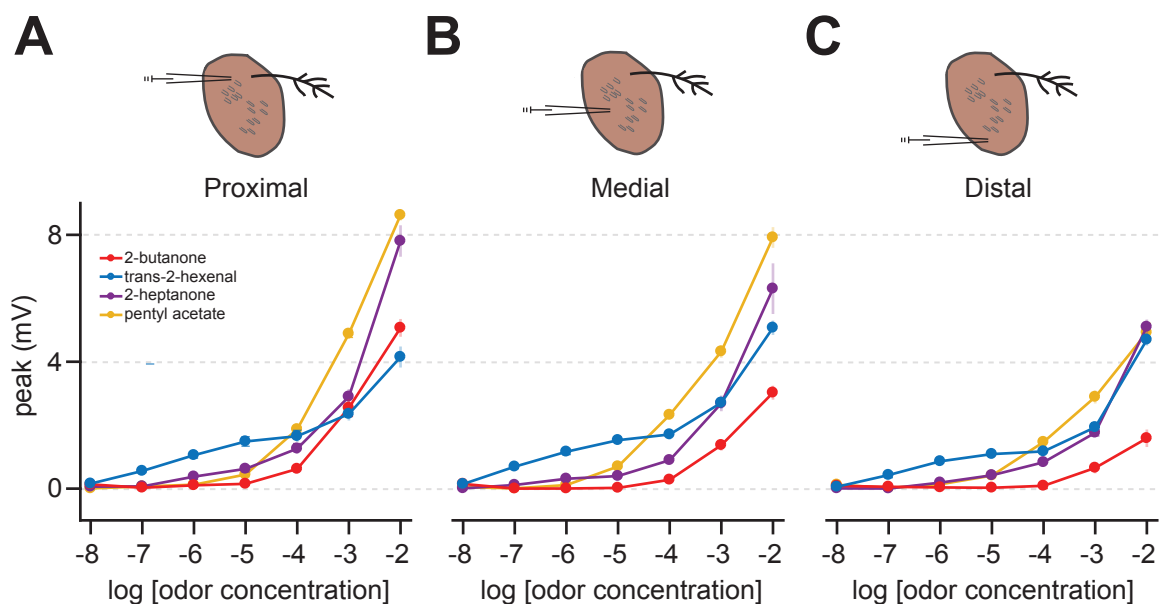


Figure 6.2: Peak LFP vs. odor concentration across different recording locations

LFP was recorded in the third antennal segment across (a) proximal, (b) medial and (c) distal recording locations relative to the second antennal segment of the fly. Peak LFP was quantified from the raw LFP amplitude and averaged across flies for each recording location. Plotted is average peak LFP +/- SEM computed across flies.

We combined data by averaging across all recording locations and plotted concentration curves for each odor. We extracted both the peak deflection (Figure 6.3A) and the average LFP (Figure 6.3B). The peak LFP was calculated as done previously for Figure 6.2, and the average LFP was computed across the 500ms stimulus window as well. Our goal with this analysis was to determine whether the results differed depending on which metric was used to quantify total LFP activity. Overall, we find that both analysis methods capture the same trends in LFP activity across odor concentrations. For instance, pentyl acetate recruits the most LFP at high concentrations including 10^{-3} and 10^{-2} . Interestingly, 2-butanone, 2-heptanone and pentyl acetate all recruit nearly zero mV of LFP activity from concentrations of 10^{-8} to 10^{-4} (Figure 6.3). In contrast, trans-2-hexenal recruits around 1-2mV of LFP activity at concentrations as low as 10^{-7} (Figure 6.3). The peak LFP metric tends to capture higher voltage values (Figure 6.3 A) than average LFP (Figure 6.3 B) partly due to the observation that LFP tapers across the stimulus-evoked window (Figure 6.1). Either value is an accurate and sound metric to use when assessing odor-evoked LFP responses.

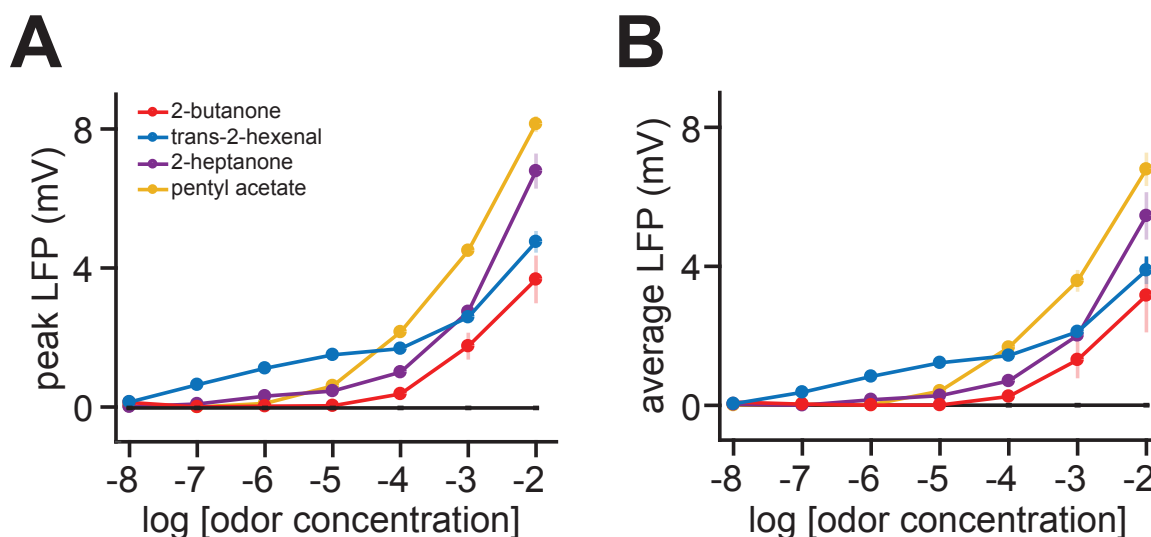


Figure 6.3: Isointense odor tuning curves averaged across locations

(a) Peak and (b) average LFP deflection computed across recording locations for 2-butanone (red), trans-2-hexenal (blue), 2-heptanone (purple) and pentyl acetate (dark yellow). Solvent (paraffin oil) responses are plotted in black. Mean \pm SEM.

In summary, data from this chapter is intended to serve as a reference for future work seeking isointense odors. We find that proximal and medial recording locations capture most of the signal, and we suggest that future LFP measurements can include just these two locations while maintaining accuracy. Trans-2-hexenal appears to activate the most activity at low odor concentrations, while pentyl acetate activates the greatest activity of all stimuli tested. As expected, odors tend to increase exponentially with odor concentration, and most odors recruit noticeable LFP at concentrations of 10^{-5} . Future work may focus on obtaining similar measurements from the maxillary palp for a complete view of combined (antennal + maxillary palp) peripheral LFP.

References

- Couto, A., Alenius, M., and Dickson, B.J. (2005). Molecular, anatomical, and functional organization of the *Drosophila* olfactory system. *Curr. Biol.* *15*, 1535-1547.
- de Bruyne, M., Clyne, P.J., and Carlson, J.R. (1999). Odor coding in a model olfactory organ: the *Drosophila* maxillary palp. *J Neurosci.* *19*, 4520-32.
- de Bruyne, M., Foster, K., and Carlson, J.R. (2001). Odor coding in the *Drosophila* antenna. *Neuron* *30*, 537-52.
- Hallem, E.A. and Carlson, J.R. (2006). Coding of odors by a receptor repertoire. *Cell* *125*, 143-60.

Appendix

LED Barrel

Figures A.1 - A.2

I provide a detailed circuit diagram and overview of the LED barrel I built. I used this barrel to evoke light responses in Or7a>Chrimson and Or42a>Chrimson flies in Chapter 5. The barrel can be used for chronic light exposure, behavior, and fictive odor rearing, to name a few. Currently, there is one barrel in the Hong lab, but all parts are affordable and readily accessible. I list part numbers where I can should anyone be interested in replicating the LED barrel.

Physiology, data acquisition and analysis

Figures A.3 - A.10

I show a sample of my GUIs for data collection and analysis. I provide sample raw data to highlight how spikes were quantified for ORNs and PNs and cell identity was determined. I show pictures of the recording setup used and fly preps.

References cited

Fisek, M. and Wilson, R.I. (2014). Stereotyped connectivity and computations in higher-order olfactory neurons. *Nat Neurosci.* 17, 280-8.

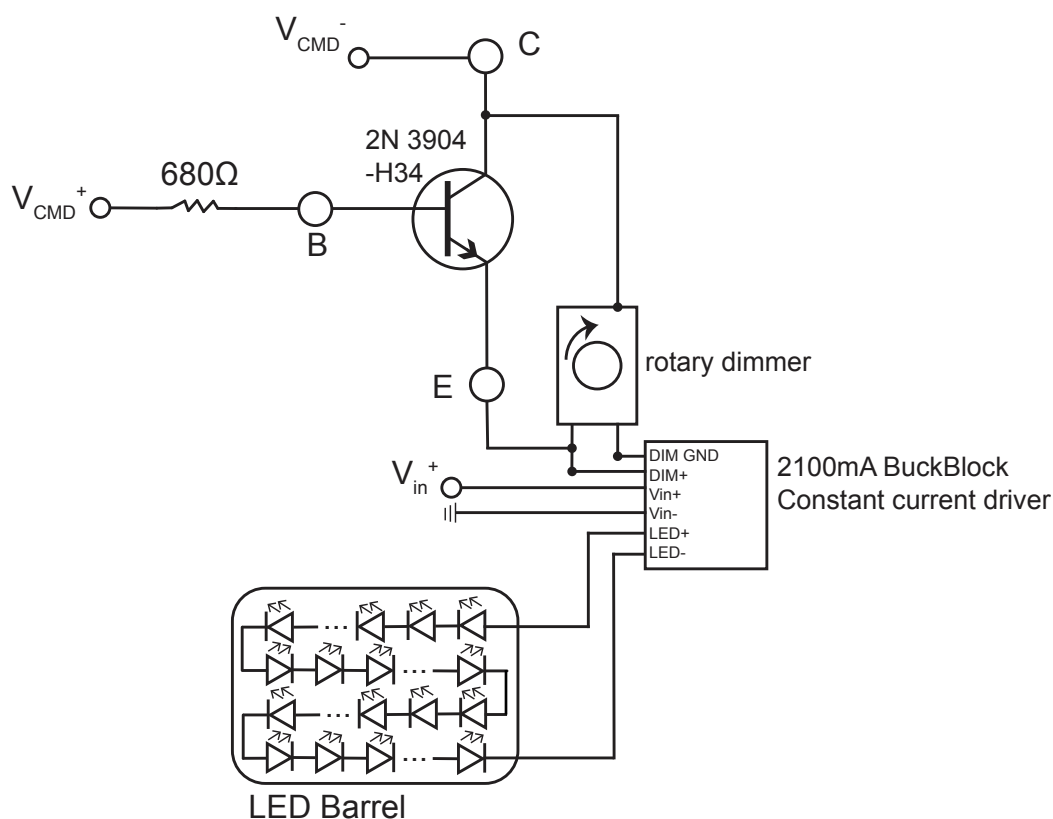


Figure A.1: LED barrel circuit diagram

Circuit diagram of LED rearing barrel with intensity dimmer and constant current drive. Input voltage from a command source is used to drive LED stimulation. The command voltage required is 5V, and this input can arise from an Arduino or MATLAB program. The stimulation can be continuous or pulse on and off. The 'off' stage of a stimulation paradigm can be programmed such that the LEDs become dimmer or completely shut off by varying the amount of voltage set into the circuit from 0V (completely off) to 5V (brightest). Additionally, the rotary dimmer can be used to pre-set a fixed stimulation voltage during the 'on' stage of stimulation. A transistor is used to drive the stimulation protocol. A constant current driver is used to increase the amount of current driving the circuit (LuxDrive by LEDdynamics, A009-D-V-2100) and this was essential to ensure the LEDs were performing near the factory ratings. V_{in}^+ is a 12V DC power source. The

LEDs used are quad-row flexible, stick-on LEDs (SuperBright LEDs, 4NFLS-R24-24V-CL). Each strip is connected in series along the inner perimeter of the barrel. The barrel is a custom-cut aluminum pipe (Metals Depot; 6 inch long, 6 inch outer diameter, 0.125 inch thickness). The material was chosen to function as a layman's heatsink.

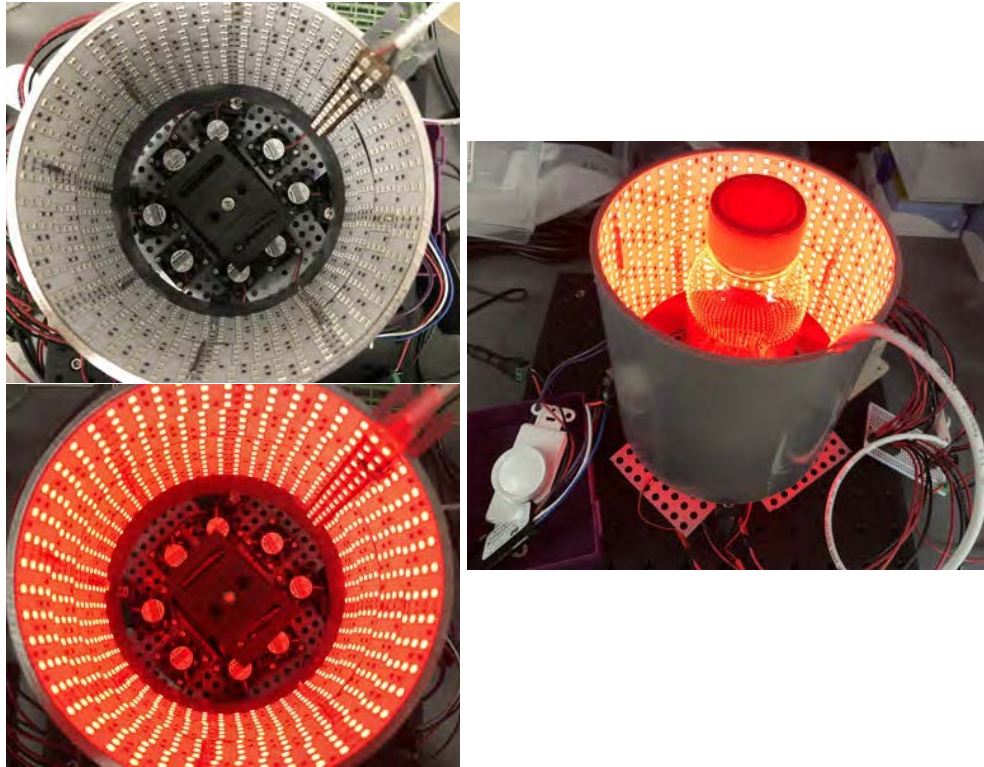


Figure A.2: Photos of LED barrel for rearing and behavior

The LED barrel is positioned on a platform and bread-board from Thorlabs. A clear plastic bottle is suggested to be used to prevent filtering light. A bird's eye view of the inside of the rearing barrel is shown with LEDs off (top left) and LEDs on at an intermediate setting (bottom left). Below the barrel are miniature fans connected in series to a 12V voltage source and dimmer switch (not shown) to provide additional cooling if necessary. An example of a clear bottle positioned in the center of the rearing barrel is shown (right). The rotary dimmer controlling the intensity of the LEDs is visible in the bottom left corner. The final arrangement of the LED rearing set-up should be placed in a light-proof, well-ventilated box. The LEDs are highly efficient and should not over-heat over extended use. Precautions should be taken if this set-up is to be used for long-term light-rearing or behavior.

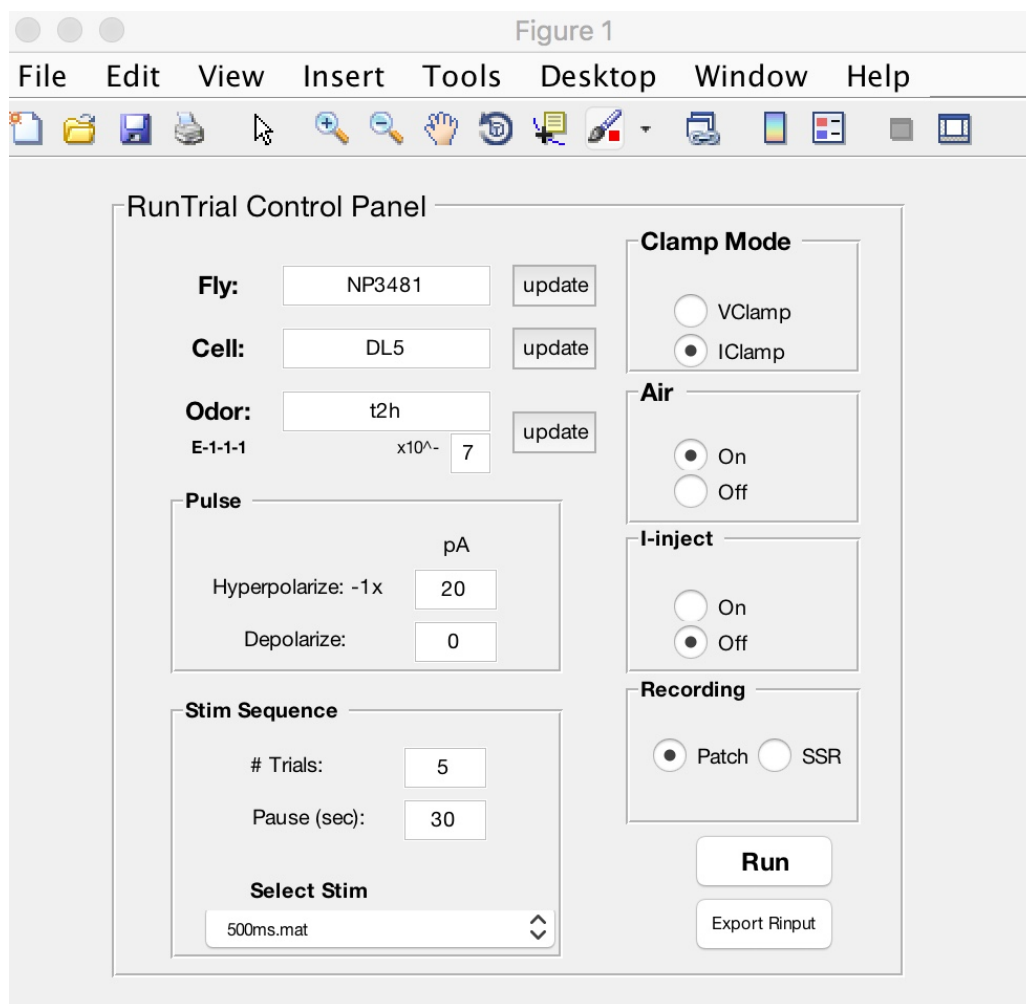


Figure A.3: MATLAB GUI interface for physiological data acquisition

Throughout my experiments, I used a very convenient interface to trigger stimuli, acquire data, and visualize data. I built the GUI around the conventional data acquisition code used in the Hong lab on the electrophysiology computers. I found the GUI helped me stay organized and keep track of my experiments. E-1-1-1: Fly 1, cell 1, trial 1. t2h: trans-2-hexenal.

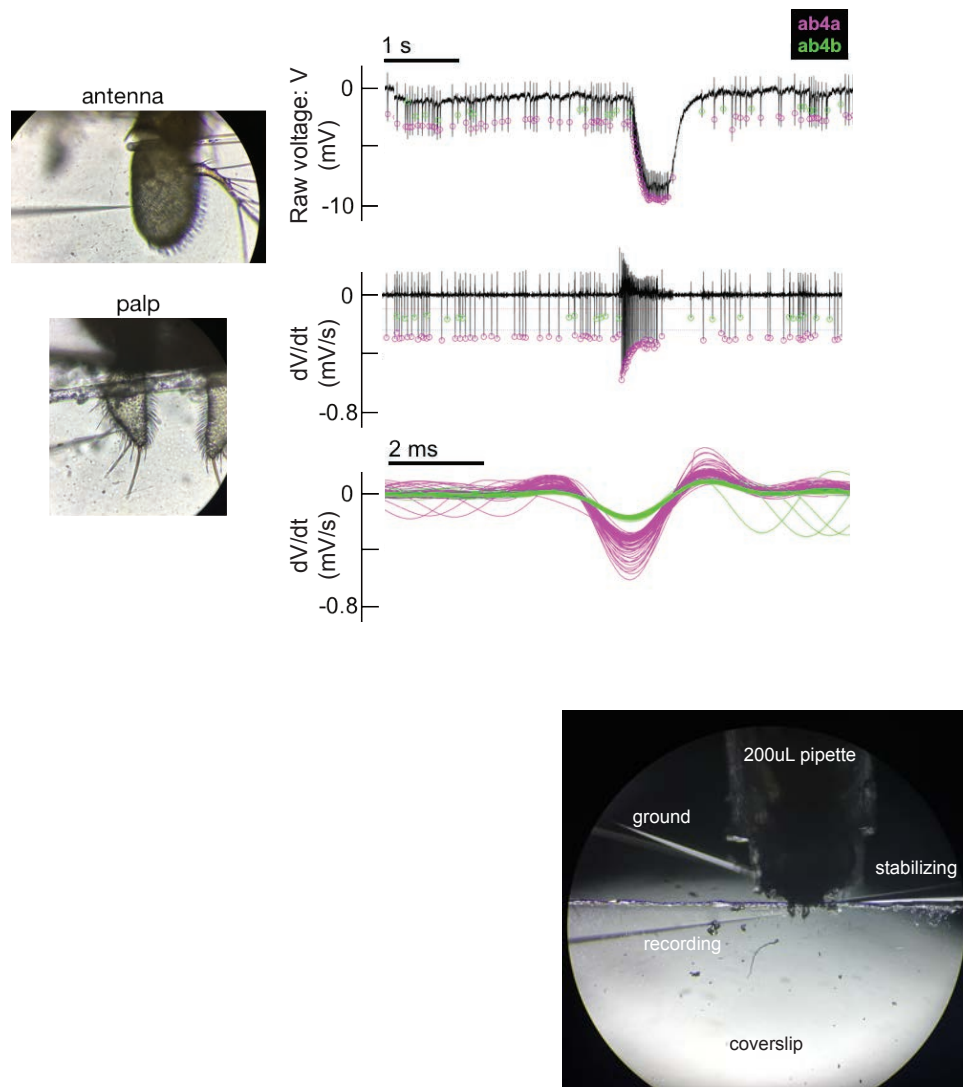


Figure A.4: ORN spike quantification and recording setup

The GUI I built for spike quantification uses essentially the same methods as shown in Fisek, M., and Wilson, R.I., 2013). *Left*: Two different ORNs are shown (magenta and green). Raw voltage, first derivative of voltage, and extracted waveforms are plotted. I include features to manually remove and add missed spikes. The individual spike waveforms are overlaid to aid in distinguishing between different cell types in ORN recordings. *Right top to bottom*: Picture of mounted antenna (top) and palp (middle) with recording electrode under 50X objective. Picture of fly in 200uL pipette, coverslip is positioned below fly, ground electrode is inserted into the eye, stabilizing pipette is holding the palp, and recording pipette is inside a sensilla.

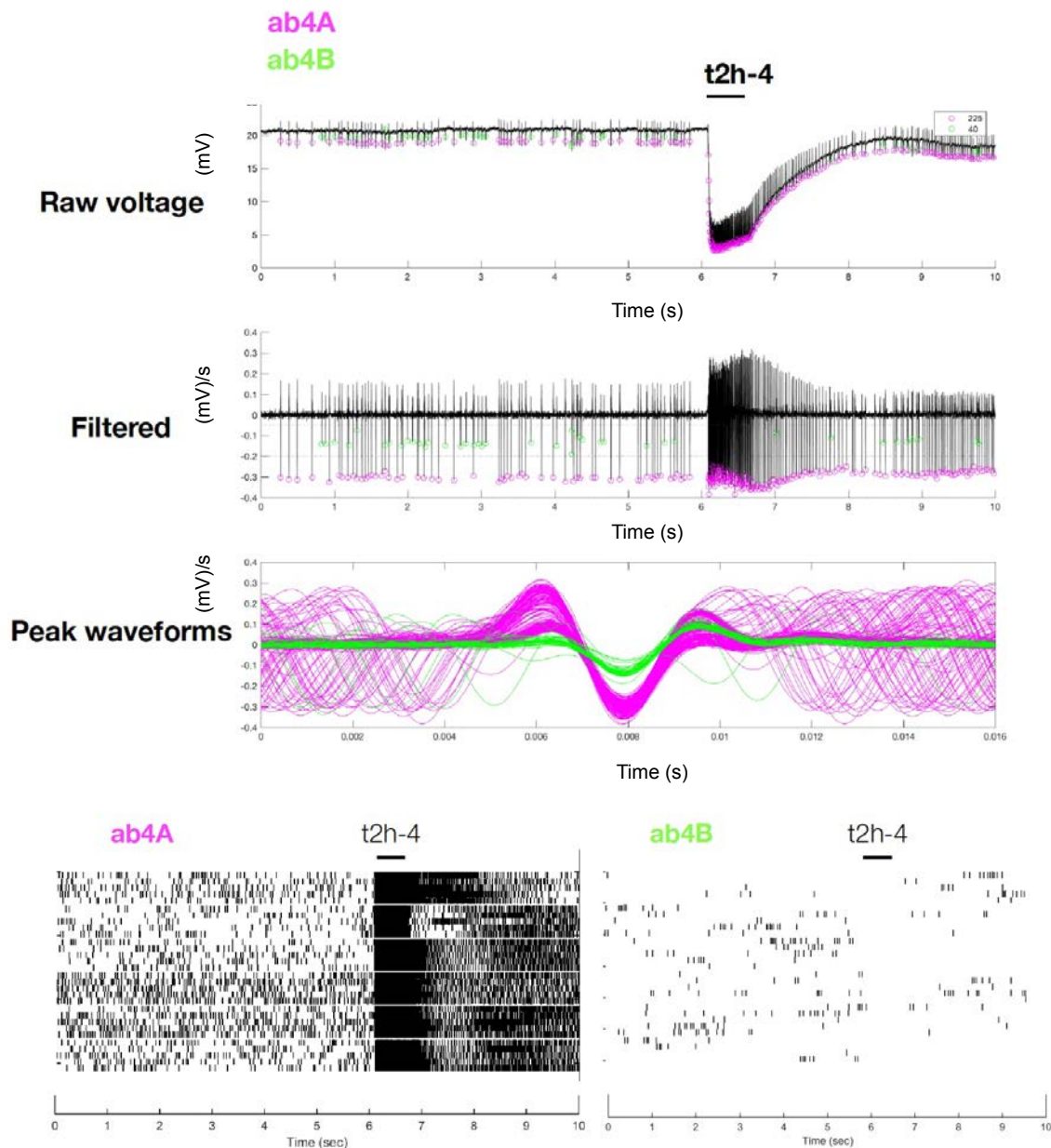


Figure A.5: Sample ab4 spike quantification with trans-2-hexenal stimulation

Raw voltage: Raw voltage (mV) vs. time (seconds) of ab4 single-sensillar recording to trans-2-hexenal 10^{-4} (t2h-4). Magenta = ab4a spikes. Green = ab4b spikes. Legend shows total # of spikes detected per cell. Filtered: First derivative of voltage (mV/sec) vs. time (sec). Peak waveforms: Extracted ab4a and ab4b waveforms. Bottom: Spike rasters from ab4a (left) and ab4b (right) ORNs. Trans-2-hexenal is selective to ab4a (Or7a).

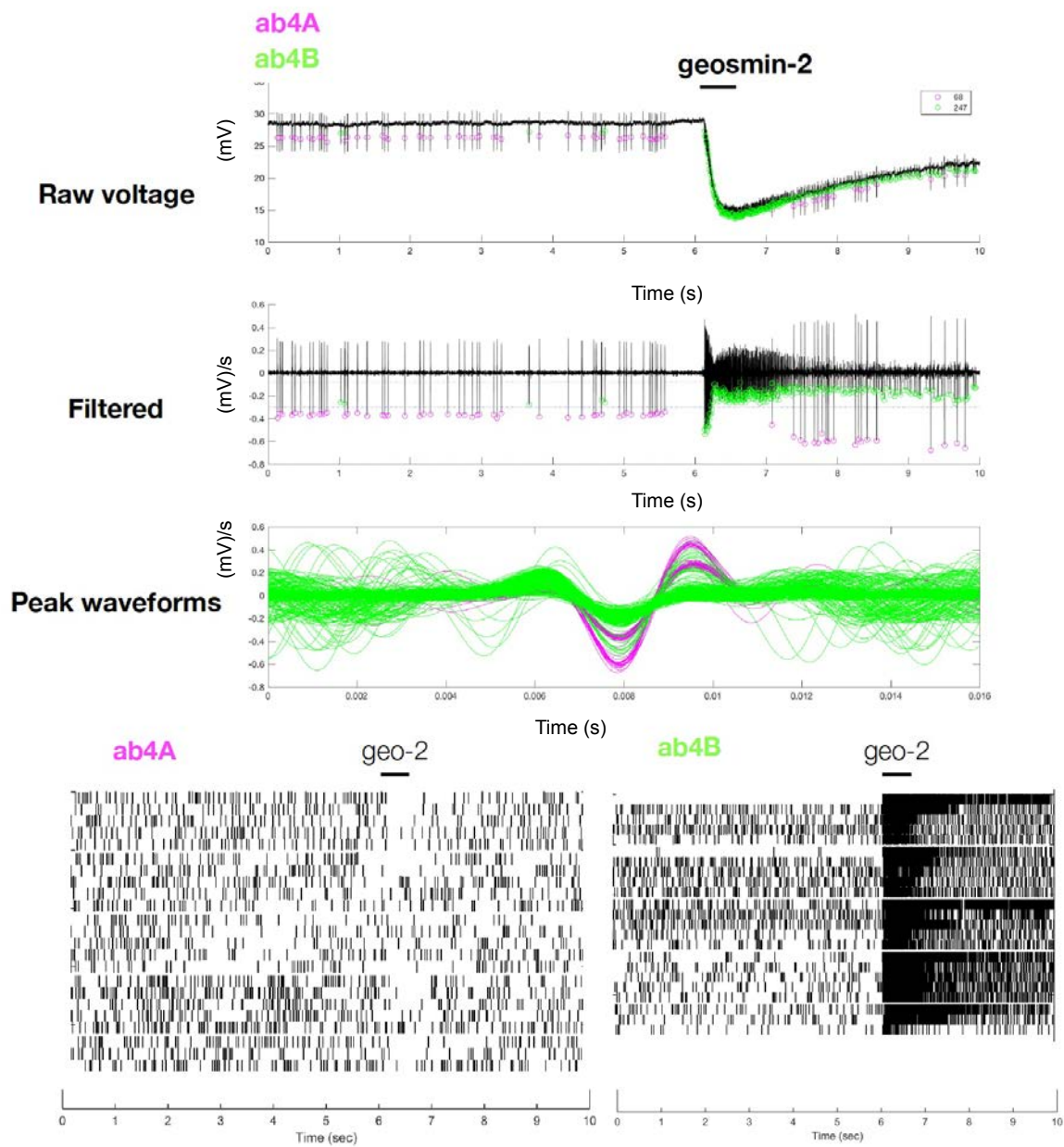


Figure A.6: Sample ab4 spike quantification with geosmin stimulation

Same as in Figure A.5, but in response to geosmin 10^{-2} (geo; the smell of wet soil) to activate ab4b (Or56a) selectively.

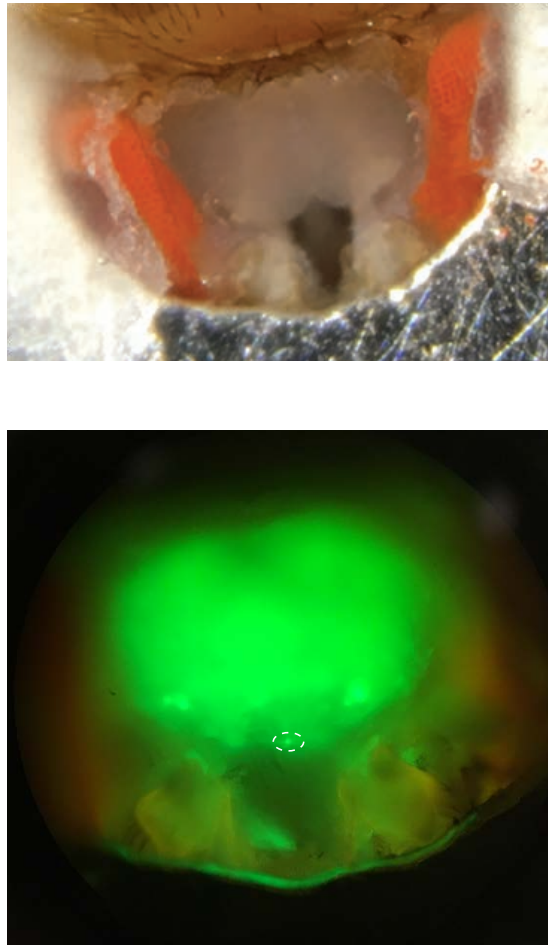


Figure A.7: Sample antennal lobe dissection and view of patch-clamp recording on a GFP⁺ PN

Top: View through a dissecting microscope objective of a typical antennal lobe prep for PN recordings. I removed the cuicle and exposed the brain. The antennae are tucked under a stainless steel foil and the antennal nerves can be seen extending towards the brain. Most of my PhD work involved GFP-targeted patch-clamp recordings of individual cells in the fruit fly brain. The cells are around 5-10 micrometers in diameter, and the recording pipette has roughly a one micrometer diameter. Bottom: The same view as above, but with GFP visible on the electrophysiology rig. I carefully targeted my recordings towards PNs that express GFP. An individual PN is shown in the dotted white circle.

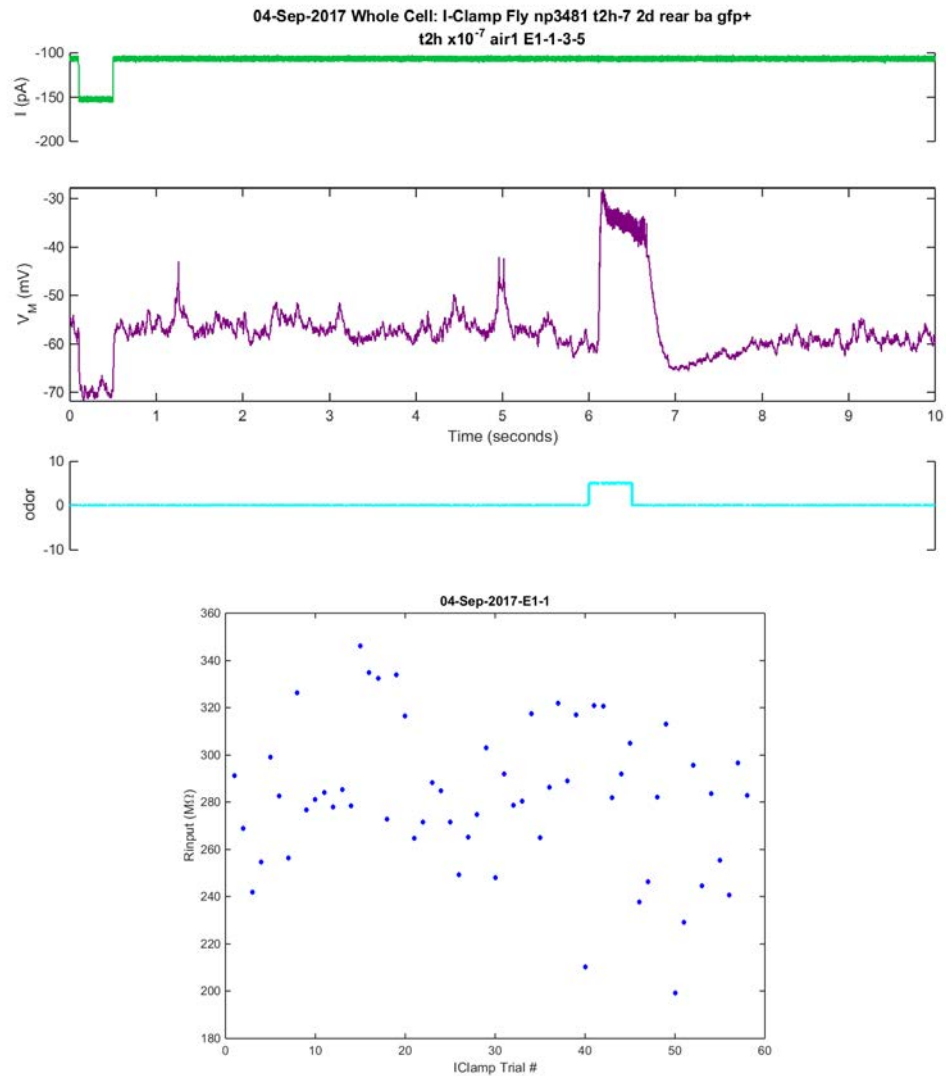


Figure A.8: Sample recording from a DL5 PN

Top: Output figure after a data acquisition trial of a current clamp recording showing current injected (green), raw voltage traces (purple) and odor pulse (cyan). Bottom: Cell input resistance is plotted in real-time following every trial to monitor recording quality. Trans-2-hexenal is used as one of the diagnostic odors to determine cell identity during an experiment.

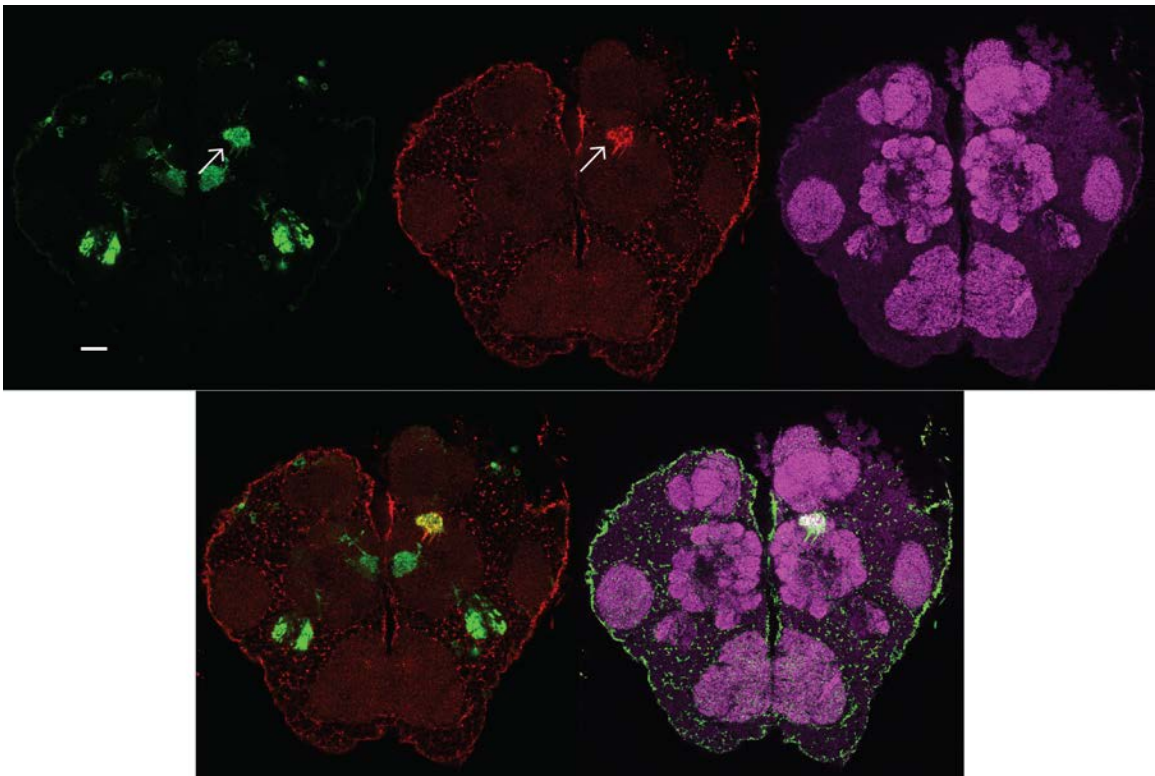


Figure A.9: Validating PN identity using biocytin

The cell in Figure A.8 was confirmed after experimentation using histology. Our internal pipette solution contains biocytin, and this dye permeates into the cell during a recording. We confirm cell identity by staining biocytin with a conjugated Streptavidin secondary antibody. We then visualize fluorescence signal in the targeted glomerulus. Top: CD8-GFP is in green, biocytin is in red, and nc82 neuropil is in magenta. While our fly line labels a few PNs, we see biocytin expression in only one glomerulus from our recording. We use existing maps of the antennal lobe to identify the glomerulus. In this case, it is DL5 (white arrow). Bottom left to right: Overlay of CD8-GFP (green) with biocytin (red). DL5 glomerulus is the overlay of green and red, which becomes yellow in the merged stack. Overlay of biocytin (green) with nc82 (magenta) shows the DL5 glomerulus overlaid in white. Scale bar 20 μ m.

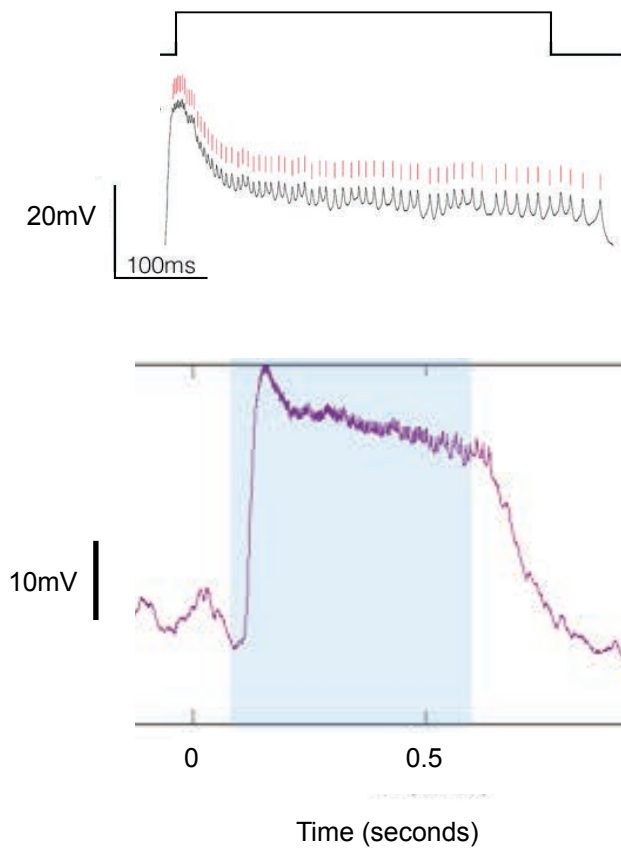


Figure A.10: Quantifying odor-evoked spikes in PNs

Top: Expanded scale of voltage response showing that spikes can be quantified in PNs. A red line is plotted above each identified spike. Bottom: Raw trace on a standard time scale used for the example above.